Curriculum Vitae

James Stephen Lyons Jr.

University of Maryland School of Medicine
Department of Orthopaedics

100 Penn Street • Baltimore, MD 21201 • U.S.A.
Email: jslyons@umaryland.edu

Education:

University of Maryland School of Medicine, Baltimore, MD — Dec 2017
Ph.D. – Program in Molecular Medicine, Molecular Physiology
Mentor: Joseph P. Stains, PhD.
Thesis Topic: Molecular mechanisms of osteocyte mechanotransduction

Harrisburg University of Science and Technology, Harrisburg, PA — May 2013
B.S. – Biotechnology, *Summa Cum Laude*

Relevant Experience:

Senior Toxicologist,
Eurofins Medical Device Testing, Lancaster, PA — May 2017 – Current

Graduate Research Assistant,
University of Maryland, Baltimore, MD — July 2014 – Dec 2017

Business Manager,
Aptagen LLC, York, PA — June 2016 – Jan 2017

Research Technologist,
Penn State College of Medicine, Hershey, PA — May 2013 – July 2014

Research Tech/Business Assistant,
Melanovus Oncology Inc., Hummelstown, PA — Jan 2013 – Aug 2013

Internship,
Penn State College of Medicine, Hershey, PA — May 2012 – Mar 2013

Fellowships and Support:

Current:

T32 Training Program in Integrative Membrane Biology — Nov 2015 – May 2017
NIH/NIGMS – 5T32GM008181-28

Completed:

Graduate Research Assistantship — July 2014 – Nov 2015
Graduate Program in Life Sciences, University of Maryland Baltimore

Professional Membership:

American Society for Bone and Mineral Research April 2016 – Current

Publications:

- **Lyons, J.S.**, Joca, H.C., Law, R., Khairallah, R.J., Kerr, J.P., Konstantopoulos, K., Ward, C.W., Stains, J.P. "Microtubules tune mechanotransduction through Nox2 and TRPV4 to down regulate sclerostin in osteocytes" Science Signaling, 2017
- **Lyons J.S.**, Iyer S.R., Lovering R.L.., Ward C.W., Stains J.P., "Novel multi-functional fluid flow device for studying cellular mechanotransduction" Journal of Biomechanics, 2016
- **Lyons J.**, Bhati A., Trivedi J., Sharma A. "Chapter 25: Nanoparticle based drug delivery systems: Associated toxicological concerns and solutions." Special Topics in Genomics and Drug Discovery. River Publishers, 2013

Patents:

- **James S. Lyons**, Joseph P. Stains, Christopher W. Ward. "Multifunctional Fluid Flow Device" U.S. Patent Application Number: 15/466,255 filed on March 22, 2017
- Joseph. P Stains, **James S. Lyons**, Christopher W. Ward, "Modulation of the Microtubule-Dependent Mechanotransduction as a Therapeutic Intervention in Osteoporosis". US Provisional Patent Application Number: 62/422,717 filed on November 16, 2016

Presentations and Posters:

- **Lyons, J.S.**, Joca, H.C., Law, R., Khairallah, R.J., Kerr, J.P., Konstantopoulos, K., Ward, C.W., Stains, J.P. "Microtubules-dependent regulation of a signaling relay that tunes the osteocyte mechanical load response" Oral, *Physiology Student Seminar Series,* University of Maryland School of Medicine, 2017
- **Lyons, J.S.**, Joca, H.C., Law, R., Khairallah, R.J., Kerr, J.P., Konstantopoulos, K., Ward, C.W., Stains, J.P. "Microtubules-dependent regulation of a signaling relay that tunes the osteocyte mechanical load response" Oral, *Annual Muscle and Membrane Biology Retreat,* University of Maryland School of Medicine, 2017
- **Lyons, J.S.**, Joca, H.C., Law, R., Khairallah, R.J., Kerr, J.P., Konstantopoulos, K., Ward, C.W., Stains, J.P. "Microtubules-dependent regulation of a signaling relay that tunes the osteocyte mechanical load response" Oral, *Graduate Research Conference,* University of Maryland School of Medicine, 2017
- **Lyons, J.S.**, Stains, J.P., Ward, C.W. "Novel multi-functional fluid flow device for studying cellular mechanotransduction" Oral, *Office of Technology Transfer Scientific Review Committee Meeting*, University of Maryland School of Medicine, 2017
- **Lyons, J.S.**, Joca H.C. Kerr, J.P., Ward, C.W., Stains, J.P. "Microtubules, TRPV4, and Sclerostin: Novel insights into Bone Mechanotransduction" Oral, *Molecular Medicine Seminar Series,* University of Maryland School of Medicine, 2016
- **Lyons, J.S.**, Joca H.C. Kerr, J.P., Ward, C.W., Stains, J.P. "Microtubules, TRPV4, and Sclerostin: Novel insights into Bone Mechanotransduction" Poster, *1st Annual Molecular Medicine Retreat,* University of Maryland School of Medicine, 2016
- **Lyons J.S.**, Joca H.C., Kerr J.P., Ward C.W., Stains J.P., Taxol-induced stabilization of the microtubule network blunts the osteoblast/osteocyte response to fluid flow shear stress, *American Society for Bone and Mineral Research Annual Meeting*, Georgia World Congress Center, Atlanta, 2016
- **Lyons, J.S.**, Kerr, J.P., Ward, C.W., Stains, J.P. "Microtubules, TRPV4, and Sclerostin: Novel insights into Bone Mechanotransduction" Poster, *Annual Muscle and Membrane Biology Retreat,* University of Maryland School of Medicine, 2016
- **Lyons, J.S.**, Kerr, J.P., Ward, C.W., Stains, J.P. "Microtubules, TRPV4, and Sclerostin: Novel insights into Bone Mechanotransduction" Oral Presentation. *Student Seminar Series,* University of Maryland School of Medicine, 2016

- **Lyons, J.S.**, Kerr, J.P., Ward, C.W., Stains, J.P. "Microtubules, TRPV4, and Sclerostin: Novel insights into Bone Mechanotransduction" Poster, *Graduate Research Conference,* University of Maryland School of Medicine, 2016
- **Lyons, J.** "Semiconductor nano-crystals for live cell imaging of breast epithelial cancer cells" Poster. *PA Nanotechnology 2012: Nanotech's Role in Advancing PA's Economy,* 2012
- **Lyons, J.** "Novel cancer drug screening assay using quantum dot nano-crystals" Poster. *Capital Area Biotechnology Partnership's Biotechnology Showcase,* 2012

Achievements:

- Poster Presentation Award, *1st Annual Molecular Medicine Retreat, University of Maryland School of Medicine, 2016*
- 8th Annual Graduate Translational Research Award, *Graduate Research Conference, University of Maryland School of Medicine, 2016*
- Poster Presentation Award, *Graduate Research Conference, University of Maryland School of Medicine, 2016*
- Harrisburg University Student Recognition for Contributions To and Leadership while Attending Harrisburg University of Science and Technology
- Biotechnology Poster Presentation Award, Second Place, *Capital Area Biotechnology Partnership's Biotechnology Showcase, Harrisburg University of Science and Technology, 2012*
- Harrisburg University's Honors List
- Harrisburg Area Community College Dean's List
- Nominated to join Phi Theta Kappa Honor Society

Leadership Experience:

Instructor,
*Capital Area Biotechnology Partnership's Biotechnology Showcase 2013***,** Harrisburg, PA
Instructor,
2013 S.T.E.M. Academy, Harrisburg, PA
Instructor,
2013 S.T.E.M. Academy's Chemistry Week, Harrisburg, PA
Instructor,
Capital Area Biotechnology Partnership's Biotechnology Showcase 2012, Harrisburg, PA
Instructor,
2012 Girls S.T.E.M. Academy, Harrisburg, PA
Volunteer,
PA Nanotech. 2012: Nanotech's Role in Advancing PA's Economy Conference, Harrisburg, PA

Additional Training:

- Certificate in Responsible Conduct of Research
- Certificate in Good Laboratory Practice

Practical Laboratory Expertise:

- Cell culture (Primary, Immortalized)
- Mouse colony management
- Molecular Biology (qPCR, Tranfections, Plasmid prep, cloning, RNA/DNA isolation)
- Biochemistry (Western blotting, gel electrophoresis, Co-IP, ELISA, spectroscopy, ITC, column chromatography)
- Microscopy (Immunofluorescence, Realtime Ca2+ imaging, Co-localization)
- Pharmacology (Viability and growth assay, PK/PD, toxicity studies)
- Skeletal Physiology (μ-Computed Tomography, bone histomorphometry, ulnar loading)

Technical Skills:

- Microsoft Office Suite: Word, Excel, PowerPoint, OneNote
- GraphPad Prism 6
- ImageJ
- PrimerExpress
- EndNote
- OriginPro 9
- Visual Basic
- Adobe Creative Suite: Photoshop, Illustrator, Acrobat, InDesign
- Google SketchUp
- SolidWorks 2015

Abstract

Title of Dissertation: Molecular Mechanisms of Osteocyte Mechanotransduction

James S. Lyons Jr, Doctor of Philosophy, 2017

Dissertation Directed By: Joseph P. Stains, PhD.
Associate Professor
Department of Orthopaedics

Diseases of skeletal fragility affect >200 million people worldwide and contribute to ~9 million factures annually. Preventing bone loss and/or restoring lost bone mass is of vital importance to limiting the personal and economic impact of these diseases. The adaptation of the skeleton to its mechanical environment is orchestrated by mechanosensitive osteocytes, largely through regulating the secretion of sclerostin, an inhibitor of bone formation. Osteocytes sense mechanical load in the form of fluid shear stress (FSS), and respond by reducing expression of sclerostin leading to "de-repression" of osteoblastogenesis and stimulation of *de novo* bone formation. However, key mechanistic details of how osteocytes sense mechanical load, transduce these signals to biologic effectors, the identity of these effectors and how sclerostin bioavailability is regulated remain unclear. A widely accepted technique for mechanically stimulating cells in culture is the introduction of FSS on cell monolayers. Here, we describe a novel, multifunctional fluid flow device for exposing cells to FSS. We validated the device using the biologic response of UMR-106 cells in comparison to a commercially available system of FSS. Utilizing this FSS device we show that the microtubule (MT) network

plays a critical role in how osteocytes sense and respond to FSS. We define a microtubule-dependent mechanotransduction pathway that links FSS to the generation of react ROS and Ca^{2+} signals, leading to reductions in sclerostin in osteocytes. In Ocy454 osteocyte-like cells, we demonstrate that an intact MT network is required for FSS-induced Ca^{2+}-influx, calcium calmodulin-dependent protein kinase II phosphorylation, and reduction in sclerostin. Further, the abundance of detyrosinated Glu-tubulin dictates the cytoskeletal stiffness of these cells. By tuning the abundance of Glu-tubulin/cytoskeletal stiffness, we demonstrate that Glu-tubulin regulates the mechano-responsive range at which FSS elicits a Ca^{2+} response in osteocytes. Further, we determined that the FSS-induced reduction in sclerostin requires activation of a signaling cascade that includes production of Nox2-activated ROS, which stimulates Ca^{2+}-influx through the cation-permeable channel TRPV4 and the subsequent activation of CamKII. By developing a better understanding of this fundamental aspect of skeletal physiology, we will raise the possibility of outlining new drug targets to combat diseases of skeletal fragility.

Molecular Mechanisms of Osteocyte Mechanotransduction

by
James S. Lyons Jr.

Dissertation submitted to the Faculty of the Graduate School of the
University of Maryland, Baltimore in partial fulfillment
of the requirements for the degree of
Doctor of Philosophy
2017

Dedication

To my parents, Fran and Dave Conrad, and Jim and Carol Lyons, without the discipline, confidence, and perseverance that you instilled within me, I would not be the person I grew up to be. Most people are lucky if they have one or two loving parents to guide them through life, I was lucky enough to have four loving parents to show me the way. Thank you for everything.

Most Importantly,

To my beautiful and loving fiancé, Bekki Fesig, I truly owe everything that I am today to you for the love and support that you have provided over the past seven years. I would not have achieved half of what I have without you by my side. Thank you for the encouragement and reassurance that I can accomplish anything I set my mind to. I truly love you with all my heart and cannot wait for what life has in store for us. Forever and always, and then some…

Acknowledgements

I would like to acknowledge the Program in Molecular Medicine and my thesis advisory committee, Dr. Chris Ward, Dr. Rich Lovering, Dr. Stuart Martin, Dr. Abraham Schnieder, Dr. Matt Trudeau. Thank you for the insightful feedback and guidance throughout my dissertation research.

I would like to acknowledge all the co-authors on my published manuscripts as without your help and input, none of this would have been possible. Bobby Law, Dr. Kostas Konstantopolous, Dr. Shama Iyer, Dr. Humberto Joca, Dr. Katrina Williams, Dr. Jaclyn Kerr, Guoli Shi, and Dr. Ramzi Khairallah. Thank you for all your help.

I would also like to acknowledge my mentor, Dr. Joe Stains. I could not have chosen a better lab environment and mentor. You have taught me so much more than how to conduct scientific research, but have left me with an entirely different perspective on life. My time in your lab has been by far the best work environment I have ever had the pleasure to experience. The life lessons and memories that I take with me after my graduate school training are truly invaluable. Thank you for the body of knowledge I have gained from my time working for you, and for not only being a fantastic mentor, but a great friend. I look forward to the next “force-multiplier” night.

The most exciting phrase to hear in science, the one that heralds new discoveries, is not 'Eureka!', but 'That's funny...'

-Isaac Asimov.

Table of Contents

List of Figures

List of Tables

List of Abbreviations

DMP1 – Dentin Matrix Protein 1

FGF23 – fibroblast growth factor 23

FGF – fibroblast growth factor

MEPE – matrix extracellular phosphoglycoprotein

PHEX – phosphate-regulating gene with homologies to endopeptidases on the X chromosome

RANK – receptor activator of NFκB

RANKL – receptor activator of NFκB ligand

M-CSF – macrophage colony stimulating factor

TGF-β – transforming growth factor- β

PDGF – platelet-derived growth factor

IGF-I – Insulin-like growth factor I

IGF-II – Insulin-like growth factor II

OPG – osteoprotegerin

OCIF – osteoclast inhibiting factor

OBF – osteoclast binding factor

TGF-/3 – transforming growth factor- /3

BMP – Bone morphogenetic protein

BSP – Bone sialoprotein

NOS – Nitric oxide synthase

NO – Nitric oxide

PKC – Protein kinase C

TRPV4 - Transient receptor potential vanilloid 4

ATP – adenosine triphosphate

NAD+ – nicotinamide adenine dinucleotide

PGE_2 – prostaglandin E_2

PLC – phospholipase C

IP3 – Inositol-1,4,5-triphosphate

MAPK – mitogen-activated protein kinase

ERK1/2 – extracellular regulated kinases 1/2

JNK – c-jun kinase

AP-1 – activator protein-1

VEGF – vascular endothelial growth factor

LRP5 – Low-density lipoprotein receptor-related protein 5

DKK1 – Dickkopf1-related protein 1

DAN – differential screening–selected gene aberrant in neuroblastoma

OSX – osterix

MEF2 – myocyte enhancer factor-2

PTH – Parathyroid hormone

cAMP – cyclic adenosine monophosphate

PKA – protein kinase A

MTs – microtubules

MTOCs – microtubule organizing centers

GTP – Guanosine triphosphate

TCP – tyrosine carboxypeptidase

TTL – tubulin-tyrosine ligase

CCP – cytosolic carboxypeptidase

TTLL – tubulin tyrosine ligase-like

MAP – microtubule associate protein

TATs – tubulin acetyltransferases

HDAC – histone deacetylase

+TIPs – Plus-end tracking proteins

CLIP170 – Cytoplasmic linker protein 170

ATP – adenosine triphosphate

P_i – phosphate

ABP – actin-binding proteins

IF – Intermediate filament

Nox2 – nicotinamide adenine dinucleotide phosphate-oxidase 2

ROS – reactive oxygen species

X-ROS – nicotinamide adenine dinucleotide phosphate-oxidase 2 (NOX2) dependent reactive oxygen species (ROS)

FFD – Fluid Flow Device

FACS – fluorescence activated cell sorting

FSS – Fluid flow shear stress

BafA1 – Bafilomyocin A1

Chapter 1: Introduction

The Structure and Function of Bone

The skeleton is a highly specialized tissue that serves as the supporting framework of the human body. The skeleton serves a variety of highly important structural and mechanical roles as well as systemic physiologic functions[(1)]. The characteristic rigidity and hardness of the bones serve as mechanical leverage for movement and protection for vital organs. Further, the bones provide an environment for marrow (both blood forming and fat storage), acts as a mineral reservoir for calcium and phosphate homeostasis and a reservoir of growth factors and cytokines, and also takes part in acid–base balance[(1)].

The skeleton is made of four different categories of bone mainly based on their shape. The long bones of the skeleton are typically long slender bones like the femur and humerus[(2)]. The short bones are typically short boxy shaped bones including the carpals and tarsals. Flat bones are thin and broad in shape. While not necessarily flat, they mainly function in providing protection or large surface arear for muscle attachment. Flat bones include the scapula, sternum, and bones of the skull[(2)]. The final type of bones are the irregular bones. These are bones with complex shapes which do not fit into the other three categories including the vertebrae and the sphenoid bone[(2)].

In general, all of these bones are made of two different types of bone tissue, known as osseous tissue[(2)](Figure 1). The first type is cortical bone. Cortical bone is sometimes referred to as compact bone due to its very dense, solid structure. The strength of cortical bone comes from its unique microarchitecture. Cortical bone is made up of osteons[(3)]. Each osteon contains osteocytes arranged in concentric layers. The concentric layers are called lamellae and typically surround a central canal which contains one or

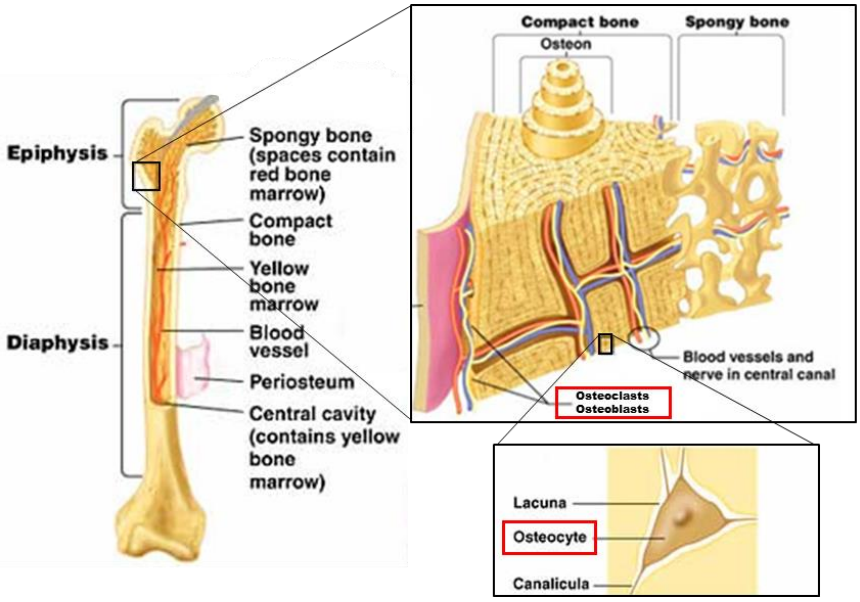

Osteoclast: Macrophage like cells that dissolve and break down bone

Osteoblasts: Form new bone by depositing osteoid (ECM) that subsequently "nucleates" hydroxyapatite crystal formation

Osteocytes: Embedded cells in the calcified matrix

Figure 1. Skeletal Microarchitecture.
Schematic showing the microarchitecture of a human long bone. The different compartments of the long bone are indicated (left). Top inset show the different types of bone, cortical and trabecular, and the osteonal structure of the cortical bone. The location of osteoclasts and osteoblasts are indicated in red. The bottom inset shows the osteocyte, indicated in red, embedded within the lacunar canalicular network within bone. Figure modified from www.humananatomy-libs.com.

more blood vessels/nerves[3]. Central canals generally run parallel to the bone surface. Central canals are then linked by perpendicular canals known as perforating canals[3]. The lamellae arranged around the central canals are called concentric lamellae, interstitial lamellae fill in the spaces between the osteons, and circumferential lamellae can be found along the bone surface[3]. Taken together, this tightly packed concentric rings of osteonal structures within the cortical bone provide great strength and resistance to compressive forces[4].

The second type of osseous tissue is the trabecular or cancellous bone[5]. Trabecular bone is sometimes referred to as spongy bone due to its interweaving web like structure which resembles a sponge[5]. The relative amounts of each type of osseous tissue found in a bone is generally related to its function. For example, cortical bone is very dense and strong while the less dense trabecular bone is softer and weaker[4]. Thus, the load bearing regions of long bones are made of higher amount of cortical bone and less amounts of trabecular bone.

There are two ways that bones form during fetal development. The first type of bone formation is intramembranous ossification[6]. This type of formation mainly occurs during formation of the flat bones, but also occurs in other bones such as the clavicles. Intramembranous ossification also plays an important role in the natural healing of bone fractures[6]. Intramembranous ossification is characterized by the formation of bone from connective tissue such as mesenchyme tissue, which is why it is sometimes referred to as mesenchymal ossification. The formation of bone during intramembranous ossification occurs when mesenchymal stem cells differentiate into osteoblasts and initiate the direct mineralization of highly vascular connective tissue[6].

The second way that bone is formed during development is endochondral ossification[6]. This type of bone formation occurs in the long bones and most other types of bone in the body. In this method of bone formation each bone is represented during development by a line of hyaline cartilage which developed from mesenchyme tissue. This cartilage forms a sort of template of each of the bones. This cartilaginous template is then surrounded by a layer of highly vascularized mesenchyme similar to that of which occurs in intramembranous ossification. Then osteoprogenitors will differentiate and being to ossify the cartilage, gradually replacing the cartilaginous template as the bone is formed[6].

Once the bones are formed, there are two different methods of bones to grow, interstitial and appositional growth[6]. Interstitial growth occurs primarily in the long bones. These bones grow in length from the center or diaphysis to the ends or epiphyses[6]. Appositional growth on the other hand occurs in every bone in the body. In appositional growth, the bones grow in all directions by osteoblasts depositing new bone all over the surfaces of the bone[6]. Then local remodeling occurs to achieve ideal bone microarchitecture and peak bone mass.

The surfaces of the bones are wrapped with a special connective tissue made of a fibrous outer layer and a cellular inner layer. The connective tissue wrapping the outer surfaces of the bone is known as the periosteum while the endosteum lines the marrow cavity, trabeculae of the spongy bone, and the inner surfaces of the central canals[7]. These connective tissues serve a number of functions including separating the bone from surrounding tissues, providing a pathway for circulatory and nervous supply, and

assisting in bone growth and repair. The periosteum also is essential in forming joints, as it is contiguous with tendons and ligaments[7].

The bone itself has a cellular component which will be discussed in the next section, however this component makes up very little of the total mass of bone. In general, the bone matrix consists of two main components, the organic component and the inorganic component. The organic component is called osteoid[7]. This is a vast extracellular matrix made of collagen and non-collagenous proteins. This component accounts for roughly 1/3 of the total mass of bone. The inorganic component consists of mainly hydroxyapatite. Most abundant chemical in hydroxyapatite is calcium phosphate. This component of the bone accounts for nearly 2/3 of the mass of bone[8].

The structure of these two components of the bone matrix are analogous to reinforced concrete used in construction. The concrete is poured around steel rebar. The hydroxyapatite is similar to the concrete in providing strength and resistance to compression while the collagen fibers in the osteoid, similar to the rebar, provide resistance to tensile forces.

The Cells of Bone

There are three main types of cells found in bone. First is the osteoclast. Osteoclasts are giant multi-nucleated cells that resorb bone matrix material [9]. Osteoclasts are unique in that fact that they are derived from monocytes rather than osteoprogenitor cells. Osteoclasts attach to the bone surface and secrete acids and enzymes to dissolve the bone matrix and release stored minerals. This process is referred to as osteolysis[9].

The second cell type found in bone is the osteoblast. Osteoblasts are cells that are derived from osteoprogenitor cells and are responsible for bone formation[10]. Osteoblasts

synthesize and secrete components of the osteoid and ultimately nucleate hydroxyapatite crystal formation. This process of new bone formation is known as osteogenesis[10].

Since osteoclasts and osteoblasts are opposing functions, it is vital that there maintain a homeostatic balance between osteoclast and osteoblast activity in order to reach and maintain healthy peak bone mass[6].

The osteoblasts have three potential fates after the rate of matrix deposition begins to slow. They can either undergo programmed cell death, apoptosis, remain on the bone surface as quiescent bone lining cells, or differentiate into the final type of bone cell, the osteocyte[10]. Osteocytes are responsible for maintaining and monitoring the protein and mineral content of the matrix, sensing mechanical load on the bone, and they participate in the repair of damaged bone. The osteocyte ultimately serves as a master regulator of osteolysis and osteogenesis and are regarded as the master orchestrators of the bone remodeling process[11]. The detailed structure and function of osteocytes will be discussed in the next section.

Osteocyte Structure and Function

When osteoblasts form new bone, often they will entrap themselves within the newly secreted osteoid. Once inside the forming matrix of the bone, these osteoblasts differentiate to become osteocytes. Mature osteocytes will live as long as the organism itself; approximately 25+ years. In the adult human, there are roughly 42 million osteocytes accounting for nearly 90 – 95% of the cellular component of the skeleton[11].

The most widely accepted mechanism for osteoblast embedding is the passive "buried alive" model in which a subpopulation of osteoblasts will slow down their osteoid production relative to adjacent cells and become buried by the matrix being deposited by neighboring osteoblasts[12]. However, it is also important to note that there

are a few groups that suggest this process is actually active and invasive, required degradation of the bone matrix for embedding to occur. In general, the process by which osteoblasts differentiate to become osteocytes is not fully understood. In particular the genetic and molecular mechanisms that regulate this process remain elusive. However, a variety of transitional stages between osteoblasts and osteocytes have been reported based mainly on morphological observations[12]. However, there are a few key changes in gene expression that represent the transition from an embedded osteoblast to a terminally differentiated osteocyte (Figure 2). These changes include the down-regulation of type I collagen and alkaline phosphatase (mature osteoblast markers) and the up-regulation of dentin matrix protein 1 (DMP1), E11/GP38/podoplanin, fibroblast growth factor 23 (FGF23), matrix extracellular phosphoglycoprotein (MEPE), and phosphate-regulating gene with homologies to endopeptidases on the X chromosome (PHEX)[11]. The final marker to indicate the differentiation into a mature osteocyte is the induction of *SOST* which encodes the protein sclerostin[13]. Sclerostin is a principal repressor of bone forming osteoblasts and the detailed function and regulation of *SOST* and sclerostin will be discussed in a later section.

Once embedded within the matrix of the bone, osteocytes also undergo a few characteristic morphological changes. As the osteocyte differentiates, it undergoes up to a 70% reduction in cell volume[14]. While osteoblasts are more cuboidal, osteocytes are stellate shaped cells which are approximately 5 – 20 micrometer in diameter. The cell body of osteocytes reside in small opening within the solid matrix of the bone known as lacunae[15]. Once inside the matrix, osteocytes grow cytoplasmic projections to neighboring osteocytes, blood vessels, and surface osteoblasts through small passages

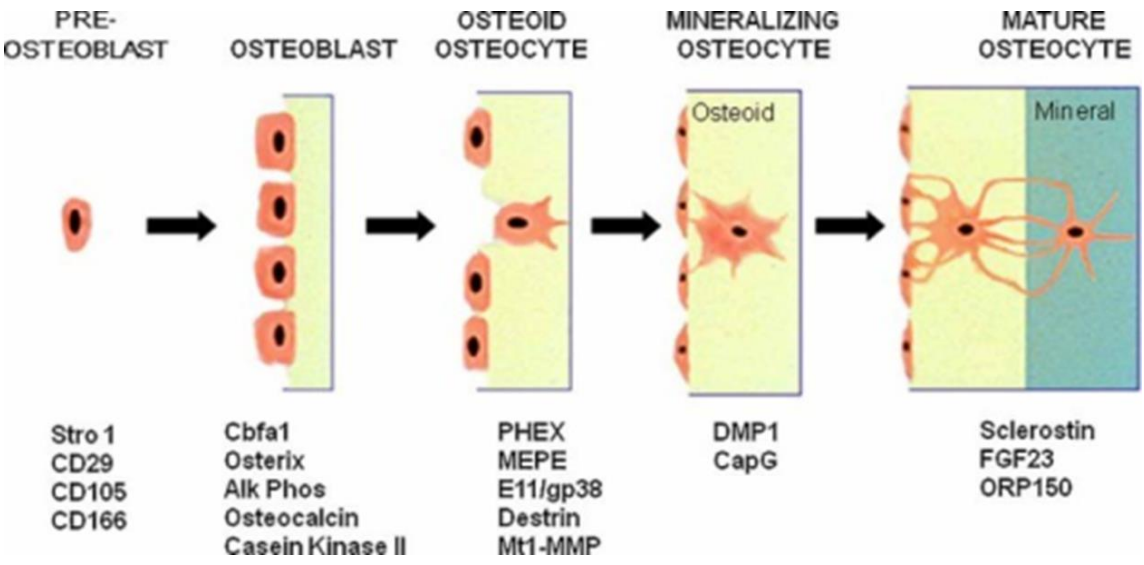

Figure 2. Gene markers of osteoblast to osteocyte differentiation.
Osteocytes are terminally differentiated osteoblasts. As osteoblasts progress through different stages of differentiation, there exhibit significant changes in expression in the indicated proteins. Figure source: (11)

known as canaliculi which can be anywhere from 250 – 300 micrometers in diameter. Each osteocyte cell body can grow 40 – 60 cell processes per cell and this vast interconnected system of cells and processes is referred to as the lacunocanalicular network[15].

Osteocytes also undergo a reduction in their endoplasmic reticulum and Golgi apparatus which to the misconception that osteocytes have reduced protein synthesis and metabolic activity[16]. Osteocytes were originally thought to be passive inactive cells, however as the understanding of osteocytes has developed, it is now understood that osteocytes are in fact highly active cells that play major roles in many key physiological processes both within and beyond the bone microenvironment[17].

Many osteocyte specific genes and proteins have been shown to play a major role in systemic mineral homeostasis. A widely studied example of this is that Dmp1 and PHEX downregulate FGF-23 expression allowing reabsorption of phosphate by the kidney[18]. This essentially maintains sufficient circulating phosphate to conserve normal bone mineral density. Further, excess FGF-23 levels have been shown to decrease the abundance of 1-α hydroxylase which is required for the conversion of 25-hydroxyvitamin D to the active vitamin D metabolite, 1,25 dihydroxyvitamin D[19]. Reduced levels of 1,25 dihydroxyvitamin D results in decreases in the sodium/phosphate cotransporter NaPi-IIb in the intestines, reducing phosphate absorption and leading to hypophosphatemia[20]. While these are just a few well-known examples of the osteocytes role in regulation of systemic mineral homeostasis, many more examples have been described or are currently being explored[17].

One of the first ascribed functions of the osteocyte was as the master orchestrator of the bone remodeling process. Osteocytes possess a key ability to regulate both osteoblast and osteoclast activity through a variety of mechanisms[21]. Mainly, the osteocytes pass messages through the lacunocanalicular system either via secretion of active signaling molecules or through cell to cell communication via gap junctions located at the tips of the osteocyte processes[22]. This communication can interdigitate both mechanical and hormonal signals to regulate bone mass[23]. The unique position of the osteocytes interspersed throughout the bone matrix makes the perfectly situated to sense and respond to various stimuli in order to not only the demands of the bone's mechanical environment but also its other demands in relation to calcium and phosphate homeostasis[11].

While many of the mechanisms of osteocyte regulation of bone remodeling have yet to be described, great strides have been made in understanding some of the factors produced by osteocytes in order to stimulate or inhibit osteoblast and osteoclast activity[17]. The detailed role of the osteocyte during the remodeling process and the osteocyte responses to mechanical loading will be discussed in further detail in upcoming sections.

Bone Remodeling

While the skeleton appears to be a static organ, bone is in fact continually being removed and replaced though a process referred to as remodeling. Remodeling happens at a rate of about 10% per year, meaning that the entirety of your skeleton could be replaced roughly every 10 years[24].

The normal bone remodeling process occurs at randomly dispersed areas of bone throughout the skeleton in which small discrete packets of bone material are removed,

new bone matrix deposited and ultimately new bone mineralized[24]. These processes are essential for maintaining bone strength and mineral homeostasis. Further, more specifically dispersed areas of remodeling control reshaping and replacement of bone during growth and following injury[25]. While remodeling occurs in response to specific mineral or mechanical demands on the skeleton, it is the osteocytes which sense these demands and orchestrate the subsequent response.

The bone remodeling process can be broken down into six phases. The first phase is the quiescent phase[6]. In this phase the bone is at rest (Figure 3).

The second phase of the remolding process is the activation phase. This is the first phenomenon to be described in preparation of the bone surface for resorption to begin[6] (Figure 3). During this phase, mature osteoblasts that have become bone lining cells retract and begin to digest the endosteal membrane though collagenase activity[26]. While remodeling does occur on the periosteal surface it is much less abundant and typically only occurs during injury healing. Further, during this phase, there is local recruitment and activation of mononucleated monocyte-macrophage osteoclast precursor cells[26]. The recruitment and activation of osteoclast precursors relies heavily on receptor activator of NFκB (RANK) and macrophage colony stimulating factor (M-CSF) [27]. These two cytokines are critical for the formation of active multinucleated osteoclasts and are produced and secreted by osteoblasts and osteocytes. Bone marrow stromal cells also play an important role in the activation of osteoclasts by providing further RANK and M-CSF stimulation[27]. Once active multinucleated osteoclasts have formed, they attach to the mineralized bone surface and initiate bone resorption. The osteoclasts actually create a tight seal to the bone surface created a localized environment for which they can safely

dissolve bone matrix material in a very controlled space[27]. Once a seal is made, the osteoclasts secrete hydrogen ions and lysosomal enzymes, particularly cathepsin K. These factors can effectively degrade all of the components of bone matrix, including collagen, at low pH[27].

The third phase of the remodeling process is the resorption phase[6]. During this phase he osteoclasts resorb bone matrix and create irregularly scalloped cavities in the bone (Figure 3). In the trabecular bone, these cavities are referred to as Howship's lacunae, while cylindrical Haversian canals are made in the cortical bone[6]. This phase allows for the release of important minerals within the bone matrix including transforming growth factor- b (TGF- b) , platelet-derived growth factor (PDGF), and insulin-like growth factor I and II (IGF- I and II)[6]. During each remodeling cycle, osteoclast resorption can last approximately 2-4 weeks.

The fourth phase of bone remodeling is known as the reversal phase[6]. In this phase, bone resorption transitions to bone formation (Figure 3). One of the main factors credited to reducing osteoclast activity and playing a role in inhibiting phase three of the remodeling process is osteoprotegerin (OPG), also known as osteoclast inhibiting factor (OCIF) or osteoclast binding factor (OBF). OPG is a decoy receptor to RANKL, thus, plays an important role in reducing or inhibiting the interaction of RANK with RANKL[28]. A tightly controlled balance of OPG/RANK/RANKL is very important in maintaining a homeostatic balance between osteoclast and osteoblast activity. Abnormalities in this balance have been attributed to numerous bone specific disorders including osteoporosis and Paget's disease[29]. The coupling link between the end of bone resorption and bone formation have not been fully elucidated however, a number of

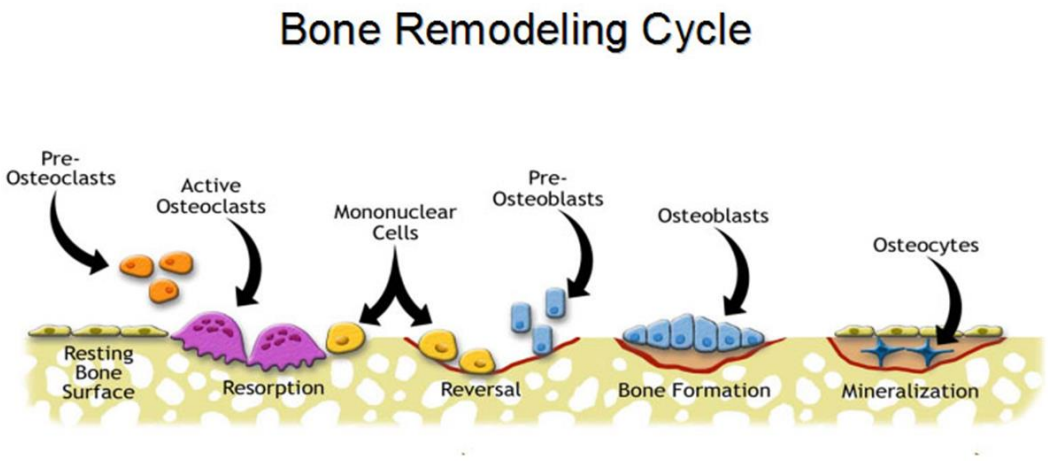

Figure 3. The bone remodeling process.
Bone remodeling is a cycle that includes osteoclastic bone resorption, followed by osteoblastic bone formation. This process is inherently coupled, thus whenever bone is resorbed, new bone must be formed in its place. Figure from: www.orthopaedicsone.com.

groups have proposed potential mechanisms for this process. For example, osteocyte apoptosis occurring when osteocytes are released form the bone matrix has been shown to be a key factor in recruiting osteoblast precursors[30]. Further, a variety of bone matrix derived factors released during resorption have been proposed to be important signaling links which activate bone formation including transforming growth factor -/3 (TGF-/3), IGF-I, IGF-II, bone morphogenetic proteins (BMPs), PDGF, or fibroblast growth factor (FGF)[31].

The fifth phase of the bone remodeling process is the formation phase[6] (Figure 3). Once bone resorption has ceased, the osteoclasts release from the bone surface and recruitment of osteoblast precursor cells takes place. It is fairly well accepted that this recruitment occurs from the growth factors released from the bone matrix as it is resorbed[32]. These growth factors act as chemoattractants in recruiting osteoblast precursors to the site of remodeling as well as being important for their differentiation into mature matrix secreting osteoblasts[32]. Preosteoblasts begin to generate an attachment substance to which the newly formed bone tissue will be attached. Further, they begin to express BMPs responsible for their further differentiation. Then within only a few days the newly formed osteoblasts synthesize and secrete new osteoid matrix and fill the cavities left by the osteoclastic resorption[6]. This occurs until the osteoblasts are inhibited by factors such as sclerostin. The osteoblasts then continue to one of their three ultimate fates as mentioned before.

The sixth and final phase of the bone remodeling process is the mineralization phase[6]. This is the longest phase in the remodeling process. Mineralization begins approximately 30 days after the osteoid is deposited on the bone surface. Mineralization

takes approximately 90 days in the trabecular bone and approximately 130 days in the cortical bone[6]. Important factors which promote mineralization are DMP-1 and bone sialoprotein (BSP). These are matrix protein produced by osteoblasts which are essential for proper mineralization. However, the most important factors made by osteoblasts which regulate mineralization are phosphoprotein kinases and alkaline phosphatase[33]. Bone alkaline phosphatase increases local phosphorus concentrations, removes phosphate-containing inhibitors of hydroxyapatite crystal growth, and modifies phosphoproteins to control their ability to act as nucleators or mineral growth[33]. These proteins along with a sufficient supply of extracellular inorganic pyrophosphate are all required for matrix mineralization[33]. Once the mineralization process is complete and the newly formed cavities in the bone have been filled in, the amount of bone resorbed should be roughly equal to the amount of bone formed. Then, the quiescent or "at rest" phase begins again and the cycle is repeated[6].

Regulation of the bone remodeling process as a whole is very complex. As mentioned above, a number of local factors including growth factors, matrix proteins, and cytokines can regulate the bone remodeling process[34]. However, there are also a variety of systemic factors that can regulate bone remodeling. Genetic factors play a role in bone remodeling and this is highlighted by differences in bone mass among different races and ethnicities[35,36]. Further, vascular and nerve factors play a role in regulating bone remodeling[37]. The bone is innervated by the autonomous nervous system and by sensorial nerve fibers and is highly vascularized. In fact, vascularization constitutes the first phase in ossification and the first event in the repair of fractures or bone regeneration. Thus, vascularization and nerve innervation are important regulators of bone

remodeling[38]. As hinted at in earlier sections, systemic nutritional factors also constitute a major regulator in bone remodeling as circulating calcium and phosphate levels are highly maintained by calcium and phosphate stores in the skeleton[39].

While all of these factors play an important role in regulating bone remodeling, the two main elements which control this process are hormonal factors and mechanical influences. Both of which are mainly sensed by the osteocytes[6]. This allows the osteocytes to orchestrate and regulate osteolysis and osteogenesis in a more controlled fashion utilizing their unique positioning throughout the matrix of the bone. The hormonal regulation of bone remodeling has been extensively studied and even been exploited for therapeutic intervention to such diseases as osteoporosis[40-43]. Since this field is so widely studied and well understood, hormonal regulation of bone remodeling could be an entire section on its own. However, these mechanistic details are outside of the scope of this thesis. Therefore, just as a quick overview, such hormones as calcitonin and estrogens tend to decrease bone resorption while parathyroid hormone (PTH), glucocorticoids, thyroid hormones, and high doses of 1,25 dihydroxyvitamin D have been shown to increase bone resorption[44-46]. Further, growth hormones, vitamin D metabolites, androgens, insulin, progestogens and low doses of PTH tend to increase bone formation while glucocorticoids have been shown to decrease bone formation[47-51]. The osteocyte response to mechanical cues however, is a far less understood field of bone biology. The mechanistic details of how osteocytes sense and respond to mechanical load is the main focus of this thesis and what is already known about and have been previously published regarding osteocyte mechanotransduction will be discussed in great detail in the next section.

Osteocyte Mechanotransduction

Two of the earliest functions ascribed to the osteocyte was mechanosensation and mechanotransduction. As early as the 19th century, a German anatomist names Julius Wolff postulated that the bones of the skeleton can adapt to mechanical forces by adding or removing bones mass[52]. Today, this is known as Wolff's Law and is widely accepted in bone biology. Wolff's Law explains why tennis players display increased bone mass in their dominant racket arm when compared to their non-dominant arm. It also explains why astronauts who spend extended time in zero gravity experience significant bone loss. The major orchestrator of these phenomenon are the embedded osteocytes which sense and respond to mechanical cues (loading and unloading) and then regulate the subsequent bone remodeling response[53]. The osteocyte was originally hypothesized to be the controller of this response to mechanical stimuli due to its position throughout the entire matrix of the bone. This hypothesis was confirmed when targeted deletion of osteocytes in mice expressing the diphtheria toxin receptor showed that these mice no longer experienced unloading induced bone loss[54].

When the skeleton undergoes mechanical loading there are several potential stimuli which could be sensed by the osteocyte. These possible stimuli include physical deformation of the bone matrix itself[53], the load-induced flow of canalicular fluid through the lacunocanalicular network[55], which results in fluid flow shear stress, or electrical streaming potentials that are generated from the flow of the canalicular fluid (which is an ionic solution) past the charged surfaces of the lacunocanalicular walls and/or cell membrane[56]. However the exact mechanism of the stimuli being sensed is impossible to distinguish *in vivo* and is still debated among the field. It is most likely that

there is actually some combination of these being sensed simultaneously which all contribute to the osteocyte response to mechanical loading[57].

However, much of the field has accepted the notion that fluid flow shear stress through the lacunocanalicular network is the main driver of osteocyte mechanotransduction[58]. It is important to note that osteocyte and osteocyte processes are constantly exposed to a basal level of fluid flow shear stress. It has been proposed that this is due to extravascular pressure. This constant low level basal fluid flow shear stress does not actually stimulate an osteocyte mechano-response, but rapid alterations in this fluid flow shear stress generated when the bone undergoes mechanical loading that triggers an osteocyte mechano-response[59].

While almost every cell responds to mechanical stimuli in some form or another, osteocytes seem to be exquisitely sensitive to mechanical cues[60]. Osteocytes have been shown to be more sensitive to fluid flow shear stress than osteoblasts and fibroblasts[61]. Further, it has been observed that osteocytes are more sensitive to fluid flow shear stress than to substrate stretching[62]. There has been many attempts to measure the *in* vivo fluid shear stress experienced by osteocyte *in situ*[63]. However, the most success has been achieved through mathematical modeling of forces within the lacunocanalicular network[64]. These models have predicted a physiologic fluid shear stress experienced by osteocytes of between 3 dynes/cm^2 and 30 dynes/cm^2[65]. Indirect measures of fluid flow shear stress have been performed by real-time measurement of load-induced solute transport. These studies suggested a peak shear stress of 5 Pa (approximately 30 dynes/cm^2)[58]. Most *in vitro* work has been done using fluid flow shear stress levels between 4 dynes/cm^2 and 20 dynes/cm^2[66,67]. However, there have been a few studies

which looked at supra-physiologic fluid flow shear stress levels as high as 40 dynes/cm^2[68].

One of the most debated aspects of osteocyte mechano-biology in the field is what part of the osteocyte is responsible for sensing the fluid flow shear stress. Some groups have suggested that the osteocyte only sense mechanical stimuli through the osteocyte processes and that the osteocyte cell body is essentially insensitive to mechanical cues[69]. Others have suggested that both the osteocyte cell body and processes contribute to sensing mechanical strain[70]. Further, it has been suggested that the putative mechanosensor of osteocytes is the primary cilium; the small hair like projection found on every cell[71-73]. However, there is evidence that all three of these hypotheses are correct, suggesting that in some sense, all three of these structures contributes to the osteocyte's ability to sense mechanical strain. Although, this evidence is in fact striking in all three cases, it remains unclear whether the osteocytes cell body, cell processes, or primary cilium sense mechanical strain independent or in fact work in conjunction to sense mechanical cues[57].

As a mechanotransducer, osteocytes must be able to convert mechanical cues into a biochemical output. In the case of the osteocyte, the ultimate biochemical output is the regulation of osteoblast and osteoclast activity[57]. This intracellular communication required to regulate this bone remodeling process is achieved by the production of a range of biomolecules including nitric oxide (NO), prostaglandins, BMPs, Wnts, and many others[66,74-78]. However, an important early response to mechanical stimuli is an increase in intracellular calcium[79]. It has been shown by many groups that a combination of calcium store release and calcium influx across the plasma membrane both contribute

to this increase in intracellular calcium[80]. This calcium increase activates many downstream signaling cascades including protein kinase C (PKC) and phospholipase A_2[74]. Further, this calcium is required for activation of calcium/calmodulin dependent proteins such as the constitutive forms of nitric oxide synthase (NOS)[76]. Further, other genes that have been shown to be modified by mechanical loading in osteocytes include c-fos, MEPE, and IGF-I[57]. However, these are just a subset of the numerous pathways shown to be involved in the osteocyte mechanical load response.

It is widely accepted in the field that the very first response mediated by mechanical stimuli is the increase in intracellular calcium. It has been shown that voltage operated potassium channels are expressed in osteocytes and it has been suggested that alterations in potassium currents could be involved in the earliest initiation of the mechanical response in osteocytes[81]. However, there is relatively high expression of T-type calcium channels in osteocytes. Thus, early reports suggested a role for T-type calcium channels including CaV3.1 and CaV3.2. It has been postulated that these T-type calcium channels may be responsible for the unique kinetics of the calcium signaling in osteocytes[82]. However more recently it has become clear that while T-type channels may in fact be involved, they only contribute to a portion of the response.

Immediately following the rapid change in calcium concentration, NO, adenosine triphosphate (ATP), and prostaglandin are released by the osteocyte[83,84]. These molecules have been shown to be extremely important, as deleting any one of these three early molecules or inhibiting their release, blocks bone's anabolic response to mechanical loading[85]. NO and prostaglandin E_2 (PGE_2) release tends to correlate and these molecules promote bone formation while inhibiting bone resorption in response to

mechanical strain[86]. PGE_2 may be one of the most important molecules released by osteocytes in response to mechanical cues. It has been shown that treatment with endogenous PGE_2 enhances the bone anabolic response to mechanical loading and blocking PGE_2 inhibits the bone anabolic response to mechanical loading[87]. Further, PGE_2 has been implicated in a feed forward mechanism in which PGE_2 release causing an increase in connexin 43 expression which would promote more NO and PGE_2 release[88]. However, this has yet to be confirmed *in vivo*. ATP release also happens very rapidly in response to mechanical strain[89]. There is evidence that suggests this occurs through connexin 43 hemichannels[90]. Further, these hemichannels may provide a mechanism for Nicotinamide adenine dinucleotide (NAD+) release which has been observed in response to fluid flow shear stress[91]. This release of ATP has been shown to efficiently activate the purinergic nucleotide receptor (P2X7), an ATP-gated ion channel, in osteocytes[92]. It has recently been suggested that this is the main mechanism of osteocyte calcium influx in response to fluid flow shear stress[93]. However, deletion of P2X7 in mice only resulted in about a 70% reduction in the anabolic response to mechanical loading, suggesting that while a major contributor to the osteocyte mechanically induced calcium influx, it is not the only contributor[94] . Many groups have explored the role of stretch activated calcium channels as a potential source of calcium influx in response to mechanical stimuli in osteocytes as well[95]. One group has made a case for transient receptor potential vanilloid 4 (TRPV4) as a major contributor to calcium influx[73]. However, it was shown to only play a role in the primary cilia and other studies have suggested that the primary cilium is not involved in the initial calcium increase observed in osteocytes.

At the heart of all of these potential mechanisms contributing to the increase in intracellular calcium in osteocytes following fluid flow shear stress is the gap junctional protein connexin 43. Not only does connexin 43 play a vital role in the release of all of these biomolecules in response to mechanical stimuli, but also is important for communication the anabolic load response throughout the osteocytic network within the bone matrix[96]. Connexin 43 also allow for signals to be passed from the osteocytes to surface osteoblasts and bone lining cells as well. In all, it is clear that connexin 43 plays a very important role in the osteocyte response to mechanical loading[97].

It has been shown that mechanical stimulation of osteocytes causing an increase in the expression of integrin β1 subunit and activate αvβ3 integrins in response to fluid flow shear stress[98]. Further, there is evidence of enhanced cytoskeletal anchorage to integrins in response to fluid flow shear stress[99]. Recently, a mechanosome model has been proposed in which a multiprotein complex comprised of adhesion proteins and nucleocytoplasmic shuttling DNA-binding proteins can move between the adhesion complexes and the nucleus to regulate gene expression. Also present in these complexes are connexin 43 hemichannels, P2X7 channels, and T-type calcium channels, creating a large nexus of signaling and ion transport that could in fact constitute the entirety of the osteocyte mechanical load response[100].

While the majority of the early calcium response exhibited by osteocytes in response to mechanical load comes in the form of calcium influx, calcium store release has also been implicated in downstream potentiation of the response[80]. The initial calcium bolus observed following mechanical stimulation has been shown to activate phospholipase C (PLC) which lead to inositol-1,4,5-triphosphate (IP3) signaling[101]. IP3

then binds its receptor on the endoplasmic reticulum causing release of intracellular calcium into the cytoplasm[102].

Increased intracellular calcium then activates a number of downstream signaling pathways in osteocytes that lead to regulation of mechanosensitive genes. The calcium dependent kinases PKC and Ras activate the mitogen-activated protein kinase (MAPK) pathway[103]. This activates transcription factors such as extracellular regulated kinases ½ (ERK1/2), c-jun kinase (JNK), and p38, resulting in the upregulation of c-fos and c-jun expression. The gene products of c-fos and c-jun form the activator protein-1 (AP-1) transcription factor which has been implicated in regulation of mechanosensitive genes in osteocytes[103].

In addition to calcium dependent signaling pathways activated by mechanical load in osteocytes, there are reports of a number of growth factors being upregulated as well which lead to downstream signaling events[57]. IGF I and II, vascular endothelial growth factor (VEGF), TGFβ1, BMP 2 and 4, all are upregulated in response to mechanical stimuli and act in both autocrine and paracrine mechanisms on osteocytes[75,101,104,105]. These growth factors then stimulate their corresponding tyrosine and serine/threonine kinase receptors to activate phosphatidylinositol 3-kinase-Akt, MAPK, and SMAD signaling pathways. Further, activation of G-protein-coupled receptors activate adenylate cyclase and subsequent cyclic adenosine monophosphate (cAMP) and protein kinase A (PKA) signaling[106-108].

While all of these pathways contribute to the osteocyte mechanical load response in various ways, it is widely accepted that the most important pathway involved in the osteocyte mechanical load response appears to the Wnt/β-catenin pathway[87]. This

pathway is important for the transmission of mechanical load signals to the bone cells on the surface. It has been shown that the mechanism for PGE_2 mediated enhancement of connexin 43 expression could be through the β-catenin pathway[88]. Deletion of the Wnt co-receptor, low-density lipoprotein receptor-related protein 5 (LRP5), resulted in an impaired osteogenic response to mechanical loading *in vivo*[109]. Negative regulators of the Wnt/β-catenin pathway such as sclerostin and Dickkopf1-related protein 1 (DKK1) are highly expressed in osteocytes and have been shown to be regulated by mechanical loading[110]. Sclerostin is one of the most important bone regulatory factors expressed by osteocytes and it is well accepted that sclerostin and DKK1 must be downregulated in order for the anabolic response to mechanical loading to occur in bone[110]. It is likely that the decreases in sclerostin and DKK1 bioavailability create a permissive environment in which Wnt proteins that are already present can activate the Wnt/β-catenin pathway[111].

The complexity of the signaling pathways activated by mechanical loading in osteocytes highlights the vast coordinated response that is necessary for the proper anabolic or catabolic response orchestrated by the osteocytes[112]. All of these studies taken together provide considerable evidence that osteocytes play key roles in the skeletal response to mechanical loading. However, there is still much to be elucidated in terms of osteocyte mechanotransduction. For example, our knowledge of sclerostin and sclerostin regulation is severely lacking[113]. This is due mainly to a lack a sufficient tools for studying sclerostin. Many of the studies mentioned above have been performed in the only available osteocyte-like cell line MLO-Y4[114]. However, this cell line was determined to be osteocyte like mainly by its morphology. It unfortunately does not express detectable levels of sclerostin protein[115]. Further, many of the mechanisms of

the early calcium bolus in response to fluid flow shear stress are still remaining to be fully understood.

Sclerostin

Sclerostin is widely accepted as one of the most important regulators of bone formation. It has even been targeted for potential therapeutic use to combat diseases of skeletal fragility[116]. However, our knowledge of sclerostin and its role in the skeletal response to mechanical load is still lacking. As mentioned before, the major hurdle in our knowledge has been the lack of the appropriate *in vitro* model to study sclerostin [115].

Sclerostin is an approximately 23kD secreted glycoprotein expressed by osteocytes[117]. However it has been reported that sclerostin can dimerize and trimerize and is rarely detectable in a monomer form[118]. The main function of sclerostin has been shown to repress osteogenesis[119]. In fact, humans with sclerostin deficiency mutations develop two diseases characterized by uncontrolled bone growth called sclerosteosis and van Buchem Disease[120,121]. These diseases are caused by mutations in the *SOST* gene, which encodes the protein sclerostin. While sclerosteosis has been shown to be cause by the insertion of premature termination codons in the *SOST* gene, van Buchem Disease has been shown to be caused by a deletion just downstream of the *SOST* gene[120,121]. This region was later realized to be an important regulatory site for sclerostin expression. Sclerostin is expressed in many tissues during embryogenesis, however postnatally, sclerostin is primarily expressed in the osteocytes with some expression to a less extent in mineralized hypertrophic chondrocytes, and cementocytes[122]. Interestingly, *SOST* mRNA expression has been detected in the heart, aorta, and liver, with high levels in the kidney. However, no sclerostin protein is detectable in these tissues[123].

The structure of sclerostin has been identified to contain a cysteine knot structure[124]. Originally, sclerostin was suggested to be a member of the differential screening–selected gene aberrant in neuroblastoma (DAN) family of glycoproteins which have the ability to antagonize BMP activity. However, the available data provides evidence that sclerostin does not act as a typically BMP antagonist[125]. Further investigation into the structure of sclerostin revealed that the most closely related DAN family member to sclerostin is a protein called Wise which can also antagonize the canonical Wnt/β-catenin pathway[126]. Further, the characterization of the structure of sclerostin revealed 3 loops present along with the cysteine knot structure. One of these loops is high in positively charged residues, showing a possible site of interaction with the predicted binding site on the first β-propeller of LRP5, which is negatively charged[127]. Therefore, the hypothesis that sclerostin was also an antagonist of the Wnt/β-catenin pathway was explored. Indeed, sclerostin has been shown to bind LRP5 and its closely related co-receptor LRP6 and, thereby, inhibit the canonical Wnt signaling[128]. Interestingly, there have been conflicting reports about how sclerostin exhibits its effects on the Wnt/β-catenin pathway. There seems to be evidence that sclerostin does not actually compete for binding with Wnts to the co-receptor. Instead it is possible that sclerostin binding to LRP5/6 induces internalization of the co-receptor[128]. The Wnt/ β-catenin signaling pathway is recognized as an important regulator of bone mass and bone cell functions[129]. This pathway has been shown to be important in osteoblasts for differentiation, proliferation and the synthesis bone matrix. Further, recent work has demonstrated that LRP5 and the Wnt/β-catenin signaling pathway are absolutely required for bone formation in response to mechanical loading, highlighting the importance of not

only LRP5 and the Wnt/β-catenin signaling pathway but also the antagonists of this pathway[130].

There have been a variety of local and systemic factors that have been suggested to regulate *SOST* expression. *SOST* transcript has been shown to be regulated by the *SOST* proximal promoter as well as a distal enhancer region, ECR5[131].

Two essential transcription factors for osteoblast differentiation, RUNX2 and osterix (OSX) bind to the *SOST* proximal promoter and contribute to *SOST* expression[122,132]. There is evidence that both of these factors play a role in activation of *SOST* expression. Since the Wnt/β-catenin signaling pathway plays an important role in osteoblast differentiation, it is likely that sclerostin plays a role in regulating this process. The proximal promoter of *SOST* is also subject to epigenetic regulation[133]. This region is hyper methylated in osteoblasts and then transitions to become hypomethylated in osteocytes. It has been shown that methylation of this site in osteocytes reduces *SOST* expression[133]. It is hypothesized that this methylation plays a role in the regulation of transcription binding to the region. Further, the de-methylating agent AzadC increased the responsiveness of the *SOST* proximal promoter to BMPs[134]. However, the exact mechanism of BMP regulation of the *SOST* proximal promoter is still unclear. In fact, there are conflicting reports of BMP regulation of *SOST*. In MLO-A5 immature osteocytes, *SOST* expression was increased by treatment with BMPs while in MLO-Y4 mature osteocytes, BMPs do not seem to influence *SOST* expression [135].

The ECR5 distal enhancer region is region deleted in van Buchem Disease[120]. Deletion of just the ECR5 enhancer is sufficient to drive significant decreases in *SOST* gene expression independent of changes in the proximal promoter.

The ECR5 enhancer contains a myocyte enhancer factor-2 (MEF2) response element. This response element is responsible for binding to the MEF2 family of transcription factors[136]. Deletion of just the MEF2 response element is sufficient to drive reductions in *SOST* gene expression similar to what is observed when the entire ECR5 region is deleted. Interestingly, there seems to be some level or regulations of *SOST* gene expression by multiple MEF2 transcription factors including MEF2A, C, and D[136]. siRNA knockdown of any of these transcription factors significantly impairs *SOST* gene expression. However, the MEF2C knockout mice pheno-copy the ECR5 knockout mice suggesting that MEF2C is in fact the main transcription factor responsible for ECR5-dependent *SOST* expression[136]. Further, TGFβ-1, -2, and -3, and ActivinA increase *SOST* expression in an ECR5-dependent manner[131]. This is likely through a SMAD2/3 response element also found within the ECR5 region. While the exact mechanism of this regulation is still unclear, there is evidence that the SMAD proteins could be acting as co-modulators for MEF2 transcription factors[131].

Additionally, PTH suppresses *SOST* expression through the ECR5 enhancer. PTH binding to its receptor activates cAMP/PKA signaling which results in a decrease is *SOST* expression[136]. However, the exact mechanism of cAMP/PKA regulation of *SOST* expression has yet to be fully detailed. Interestingly, PGE_2 also seems to suppress *SOST* expression via cAMP/PKA signaling[137]. However, the suppression of *SOST* expression by PGE_2 is independent of MEF2C or MEF2D, supporting diverse mechanisms by which the cAMP/PKA pathway regulates *SOST* expression[137].

As mentioned above, mechanical loading is a major regulator of sclerostin (Figure 4). It has been shown in several models that mechanical loading reduces *SOST*/sclerostin

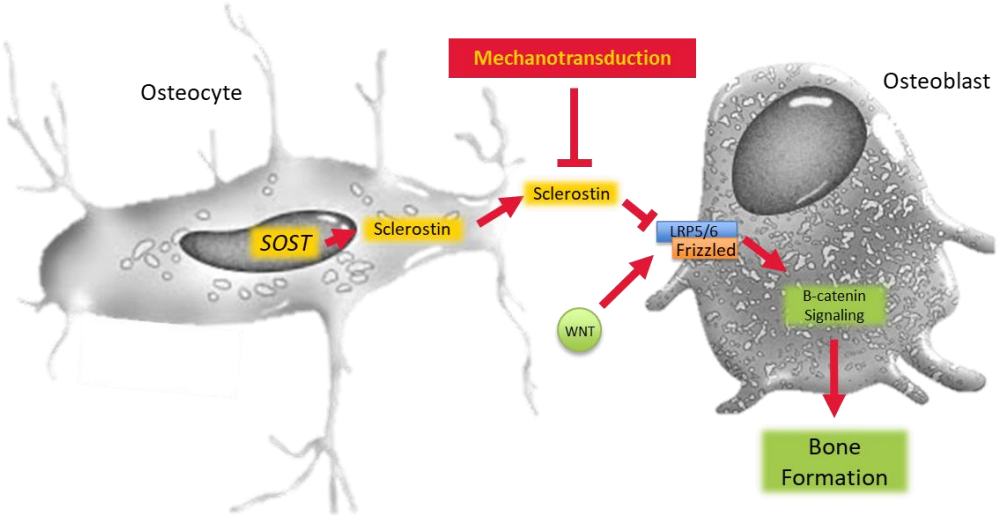

Figure 4. Schematic of the sclerostin dependent regulation of bone formation.
Sclerostin is produced and secreted by osteocytes where it can then act by competing with Wnt for binding to LRP5/6 and antagonize the canonical Wnt/β-catenin signaling cascade. Mechanotransduction in osteocytes blocks the secretion of sclerostin and "de-represses" osteoblastogensis, allowing for de novo bone formation to occur.

both *in vitro* and *in vivo*[138]. However, the exact mechanisms by which mechanical loading regulates *SOST* expression has not been fully detailed. It is likely that there is a combination of any number of the above mentioned signaling pathways that are activated by mechanical loading in osteocytes. For example, the IGF-1 and cAMP/PKA pathways have both been implicated to be involved[139].

Unfortunately, the precise mechanisms of sclerostin secretion have yet to be elucidated. In fact, there is very little known in regards to post-translational control of sclerostin protein. However, advances in *in vitro* models for studying sclerostin should help to advance our knowledge of sclerostin protein[115].

The Cytoskeleton

Every cell has a complex interconnected network of actin microfilaments, microtubules (MTs), and intermediate filaments which constitute its cytoskeleton[140]. The cytoskeleton of the cell is responsible for maintaining cellular shape and integrity, as well as various other important functions including cell motility, vesicular movement, and cellular attachment. Each of the different structures involved in the cytoskeleton have different unique rolls which all work together in a coordinated and complex fashion[140]. Since the cytoskeleton is vital to the integrity of the cell, it is easy to see how the cytoskeleton could in fact play important roles in cellular mechanotransduction. Additionally, there is mounting evidence of a more functional role of the cytoskeleton in regulating cellular mechanotransduction beyond the simple structural role traditionally played by these structures[141]. The structures and functions of each of these cytoskeletal elements and a general background of cytoskeletal mechanotransduction will be discussed in this section.

The first structure of the cytoskeleton is the MT network. MTs are cylindrical tubes about 20-25nm in diameter[140]. MTs are comprised of repeating α-tubulin and β-tubulin dimers[142]. The α-tubulin and β-tubulin monomers are very similar is structure and are both about 50kDa[143]. These dimers polymerize end-to-end into linear protofilaments that associate laterally to form a single microtubule, which can then be extended by the addition of more α/β-tubulin dimers. MTs have a distinct polarity which plays an important role in their function. Since the filament polymerizes in a linear fashion, one end will have α-tubulin exposed, while the other end will have β-tubulin exposed[144]. The α-tubulin exposed end is designated the (-) end, while the β-tubulin exposed end is designated the (+) end. While microtubule elongation is significantly more rapid at the (+) end, it can occur at both ends with the addition of more α-tubulin and β-tubulin dimers[145].

MTs are nucleated and organized by microtubule organizing centers (MTOCs), such as the centrosome found in the center of many cells or the basal bodies found in cilia and flagella[143]. Contained within these nucleating cites is another type of tubulin, γ-tubulin. γ-tubulin is distinct form α-tubulin and β-tubulin. γ-tubulin specifically functions as a nucleator of MT polymerization. γ-tubulin associates with several proteins to form a large protein complex known as the γ-tubulin ring complex which serves template for α-tubulin and β-tubulin to being polymerization[143]. It then acts as a cap on the (-) end of the MT as the polymer grows in the (+) direction. Polymerization of the MT filament depends highly on the concentration of α-tubulin and β-tubulin dimers free in the cytoplasm[143]. The steady state concentration of the dimers at which there is no longer any net assembly or disassembly at the end of the microtubule, is referred to as the

critical concentration. If the dimer concentration is greater than the critical concentration, the microtubule will polymerize and grow. If the concentration is less than the critical concentration, the length of the microtubule will decrease[143].

A unique feature of the MT network is ability of the polymers to simultaneously assemble and disassemble at opposite ends. This is referred to as dynamic instability. MTs can dynamically switch between growing and shrinking. The driving force of this dynamic instability is inherent Guanosine triphosphatase (GTPase) activity of the α-tubulin and β-tubulin dimers[146]. The dimers bind two molecules of GTP, one of which can by hydrolyzed. During MT assembly, the tubulin dimers are in the GTP bound state. This GTP bound state provides stability and plays a structural function to the MT polymer. Shortly after polymerization, the GTP is hydrolyzed to GDP. GDP bound tubulin exhibit very different properties and develop an instable structure that is prone to disassembly. When a GDP bound dimer is at the tip of a polymer, it tends to fall off, however a GDP bound dimer in the center of a polymer tends to remain stable[146]. Therefore, this creates a sort of race between GTP hydrolysis and MT polymer assembly. As the dimer assemble into a polymer, they quickly hydrolyze their GTP to GDP[146]. As long as the assembly process if adding new GTP bound dimers to the end of the polymer continues faster than the hydrolysis of the already added dimers, the MT polymer will remain stable and assembles[147]. The GTP bound dimers at the end of the MT provide stability and are referred to as the GTP cap. However, if the hydrolysis catches up to the end of the polymer, and the dimers at the end of the MT hydrolyze their GTP to GDP before new GTP bound dimers can be added, the entire polymer will undergo rapid disassembly known as catastrophe[147]. Still, as mentioned above, the MT polymer can

dynamically switch between growing and shrinking. Therefore, at any time during catastrophe, new GTP bound dimers can begin being added to the end of the polymer again providing a new GTP bound cap and protecting the polymer from disassembly. This is referred to as rescue[147].

The MT network plays important roles beyond just cell structure maintenance. The dynamic instability of MTs is vital for cell migration of most cells[148]. Dynamic microtubules regulate the levels of key proteins involved in cell contractility and spreading such as RhoA and Rac1[149,150]. The MT network and the actin filament network work together in terms of cell migration. The MT network will push out toward the direction the cell moves, while actin pulls inward the trailing end. However, the MT network has been found to act as "struts" that counteract the contractile forces of the actin[148]. Dynamic MTs are actually required to allow for the retraction of the leading edge of the cell. Further, dynamic MTs are required for the disassembly of focal adhesions, which are areas of attachment for the cell. In addition, MTs also play a role in cilium and flagella, as it has been shown that the major structural component of cilia and flagella. These structures are also used for cell motility as they bend and generate force for swimming, moving extracellular material, and other roles[151].

MTs also play an important role in vesicle trafficking. MTs act as substrates for motor proteins that literally walk along the MT polymer in order to transport vesicles around the cytoplasm of the cell as well as along axons and dendrites in neurons[152]. MTs also play a vital role in cell division as they are required for the segregation of the chromosomes during division[153]. The mitotic spindle is comprised of a complex of MTs, MT associate proteins, and the MTOC. Likewise, this gives the MT network an important

role during development. For example, polarized MTs are required during embryogenesis in order to establish the axis of the egg[154]. Further, the MT are essential for the development of the nervous system[155]. Finally, there have been reports of the MT network affecting gene expression, however the signal transduction mechanisms involved in this are not well understood[156].

More recently, there has been significant evidence implicating a role for the MT network in mechanotransduction in various tissues[141,157]. While the MT polymer does not handle tensile forces very well, it is uniquely resistant to compressive forces when compared to other cytoskeletal elements. This makes the MT network an ideal candidate for transducing mechanical signals to effector molecules and enzymes[158].

With such diverse and plentiful functions, it makes sense that a variety of proteins would interaction with the MT network. The first type of protein that interactions with the MT polymer is a large class of proteins terms microtubule associated proteins (MAPs)[159]. MAPs play a major role in regulating MT dynamics. The abundance and combination of MAPs present significantly affects MT polymerization, depolymerization, catastrophe, and rescue. There are two main classes of MAPs based mainly on their molecular weight[159]. The first class is about 55-62kDa and are called tau proteins[160]. Tau proteins have been shown to directly bind MTs and promote nucleation, prevent disassembly, and induce the formation of parallel arrays. Further, tau proteins have been shown to stabilize MT polymers[160]. The second class of MAPs have a molecular weight of 200-1000kDa and is comprised of MAP1, MAP2, MAP3, and MAP4. Each of these MAPs have different functions[159]. For example, MAP1 plays a role in vesicle transport, while MAP2 crosslinks the MT network to other cytoskeletal elements. MAP4 has been

found to mainly stabilize MT polymers. However, while many MAPs tend to have MT stabilizing functions, other MAPs have been shown to have destabilizing effects by either cleaving or inducing depolymerization of MTs. In fact, proteins such as katanin, spastin, and fidgetin have been observed to regulate the number and length of microtubules via their destabilizing activities[159].

Another type of protein that plays an important role in MT dynamics is plus-end tracking proteins (+TIPs)[161]. The first +TIP to be identified was cytoplasmic linker protein 170 (CLIP170). CLIP170 plays a role in MT rescue from depolymerization. Other +TIPs include EB1, EB2, EB3, p150Glued, Dynamitin, Lis1, CLIP115, CLASP1, and CLASP2. Each of these have differing functions, however some +TIPs have been shown to participate in the interactions of microtubules with chromosomes during mitosis[161].

The final type of MAPs are the motor proteins[162]. Motor proteins are important for trafficking vesicles around the cytoplasm of the cell along the MT polymers. Unlike other MAPs, motor proteins hydrolyze ATP to generate mechanical work in order to move along the MT polymer. There are two major motor proteins which interact with MTs. The first is dynein[162]. Dynein mediated transport takes place from the (+) end towards the (-) end of the MT. Dynein has two large globular head domains where ATP hydrolysis takes place which share structural similarity with the ATPase associated with various cellular activities protein family. In order to traffic vesicles, dynein interacts with an organelle membrane protein complex which includes such elements as dynactin[162]. The second motor protein is kinesin. Kinesin has a very similar structure to dynein and functions in much of the same way. However, kinesin can transport a variety of intracellular cargoes including vesicles, organelles, protein complexes, and mRNAs. The

major difference between Dynein and kinesin is that kinesin transports cargo from the (-) end of the MT polymer towards the (+) end[162].

Since the MT network imparts so many important and divers functions, and is so dynamic and continually changing, it is important that MT dynamics and function remain under strict regulatory control. In fact, although most MT polymers have a half-life of 5 to 10 minutes, some MTs can remain stable for hours[163]. There are several mechanisms in which MT polymer dynamics and function are regulated. These include post-translational modification of α-tubulin and β-tubulin, proteins which interact with the MT polymers, as well as tubulin binding drugs and environmental effects[163](Figure 4). For example, the MT network is extremely sensitive to changes in temperature. A drop of only a few degree Celsius is enough to trigger complete catastrophe and disassembly of all MT polymers.

Most MT post-translational modifications tend to occur on the c-terminal region of α-tubulin, however there are also similar modifications that can take place in β-tubulin[164]. Many of these modifications take place once the dimers are integrated into the completed MT polymer, by enzymes bound to the filament. The c-terminal regions of α-tubulin is rich in negatively charged glutamate residues and forms relatively unstructured tails that project out from the microtubule[164]. However, once the microtubule depolymerizes, most of these modifications are rapidly reversed by soluble enzymes[164].

Detyrosination was one of the first modification identified to preferentially occur in MT polymers rather than tubulin dimers or monomers[165]. MT detyrosination is the enzymatic removal of the c-terminal tyrosine residue from α-tubulin by a yet unidentified

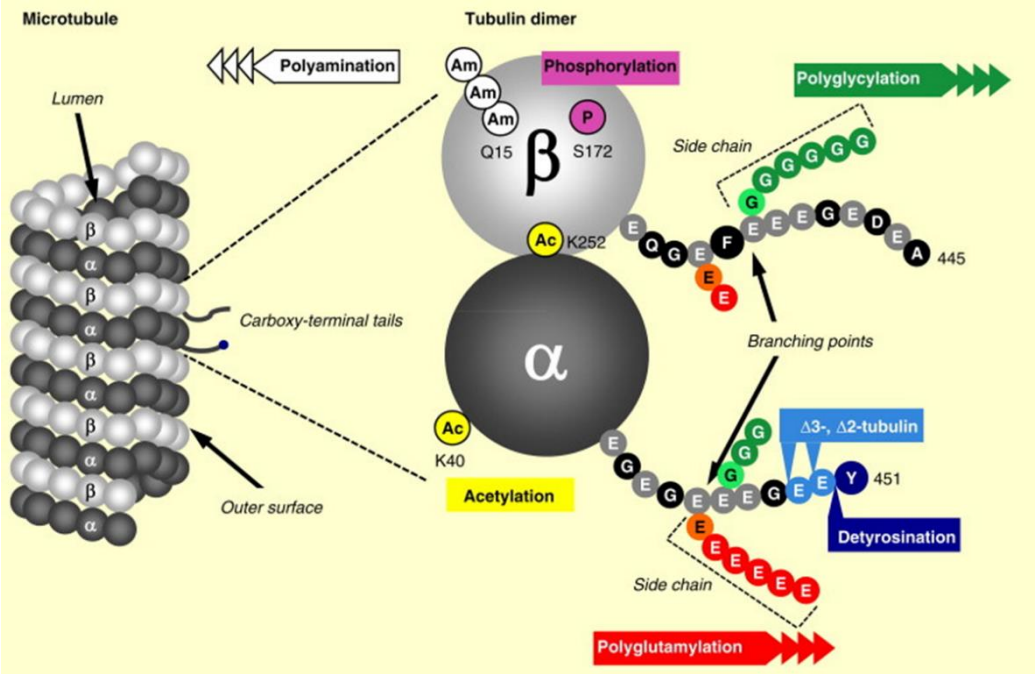

Figure 5. Microtubule post-translational modifications.
Microtubules are long tubular structures comprised of repeating α and ß tubulin dimers. These two proteins are highly susceptible to post translational modifications on both the exposed c-terminal tail and within the lumen of the microtubule. Here is a schematic showing some of these modifications and their locations. Many of these modifications have profound effects on microtubules stability and dynamics. Figure source: (166)

tyrosine carboxypeptidase (TCP). This reaction exposes a glutamate residue and is sometimes referred to as Glu-tubulin to reflect this new c-terminal residue[165]. The lack of the identity of this enzyme has left many questions regarding the reaction, including but not limited to cellular regulation of this modification. The reverse reaction is catalyzed by the better characterized enzyme, tubulin-tyrosine ligase (TTL)[167]. TTL has been shown to have numerous interactions with both of α-tubulin and β-tubulin in the dimer. In fact, TTL can actually interfere with MT polymerization to the point where TTL overexpression inhibits MT polymerization[167]. There is not much known about TTL regulation either, however it is suggested that stathmin, a protein that plays a role in sequestering tubulin dimers therefore promoting MT polymer disassembly, could in part regulate TTL activity by competing for binding with TTL to tubulin dimers[168].

Detyrosination has been associated with MT longevity because many detyrosinated MTs turn over more slowly than tyrosinated MTs. However, detyrosinated MT polymers are not intrinsically more stable to tyrosinated MTs. Instead, detyrosination tends to accumulate in stabilized MTs as the actions of TCP are preferential to that of TTL[169].

Detyrosinated MTs and tyrosinated MTs have differential interactions with various MT binding proteins. For example, MT cap proteins such as CLIP170 or P150 Glued required tyrosinated MTs to localize to the (+) end of the MT polymer, while the MT severing protein spastin preferentially cleave detyrosinated MT polymers. Thus, detyrosination provides the platform for the MT network to partake in a variety of differential functions unique to detyrosinated MT polymers[170]. Further, MT detyrosination and tyrosination may play a role in motor protein function. Kinesin-13 was

shown to bind preferentially to tyrosinated MT polymers, whereas kinesin-1 appears to prefer to bind to detyrosinated MTs[171]. Additionally, there is evidence that kinesin-1 bound to detyrosinated MTs seemed to move at a slower rate whereas detyrosination was observed to increase both processivity and velocity of kinesin-2[172]. Further, alterations in the abundance and locations of detyrosinated MTs caused changes in localization of some motor proteins. This has led some group to hypothesize that MT detyrosination not only can effect which motor proteins interact with the MT polymer but also play a dynamic role in regulation of speed and location of motor protein movement and vesicle trafficking[173]. In addition, it has more recently been observed that detyrosinated MTs and tyrosinated MTs preferentially interact with intermediate filaments and actin microfilaments. Detyrosinated MTs tend to exhibit enhanced crosslinking interactions between other cytoskeletal elements stabilizing and stiffening the cytoskeleton as a whole, whereas inhibition of MT detyrosination disrupted these crosslinks and weakened the cytoskeleton as a whole[141,174].

Δ2-tubulin is a further modification of detyrosinated tubulin. The newly revealed glutamate on the c-terminus of detyrosinated MTs is also removed in Δ2-tubulin[175]. There are a family of cytosolic carboxypeptidases (CCP) that have been shown to remove this c-terminal glutamate residue including CCP1, CCP2, CCP3, CCP4, CCP5, and CCP6[176-178]. Δ2-tubulin is preferentially found in mature neurons and like detyrosinated tubulin, tends to accumulate in long-lived MT polymers. However, unlike detyrosination, the Δ2-tubulin modification cannot be reversed[179]. Overall, the general function of Δ2-tubulin is still unknown, however it is estimated that Δ2-tubulin may represent more than 35% of the tubulin found in the brain[164] .

Two more MT post-translational modifications that are mainly found in neurons is polyglutamylation and polyglycylation[164]. Polyglutamylation is found throughout neurons[180], however in contrast, polyglycylation is restricted to ciliary tubulins[181,182]. These modifications involve the addition of glutamate or glycine chains to the c-terminal domains of both α-tubulin and β-tubulin by a class of enzymes called tubulin tyrosine ligase-like (TTLL) proteins[183]. TTLLs belong to a large protein family of ligases each with its own specificity. Likewise, some TTLL proteins preferentially modify β-tubulin while others prefer α-tubulin. For example, TTLL7 preferentially modifies β-tubulin, while TTLL5 and 6 prefer α-tubulin as a substrate[184]. The potential combination of modifications in polyglutamylated MTs varies wildly. The chain length and which residues in the α-tubulin and β-tubulin c-terminal region are modified allow for many unique modification each with its own unique function[184]. However, due to the shear variability of this modification, it has made elucidating the exact function of each combination very difficult. However, one common element among all the possible combinations seems to be the requirement for the adapter protein PGs1, which localizes the polyglutamylase complex to the MTs[185].

As with other MT post-translational modifications, polyglutamylation may alter protein interactions with the MTs. However, while it has been shown that microtubule associate protein (MAP) 1 and MAP 2, differentially bind to MTs depending on their polyglutamylation state, the effects this modification has on motor proteins is less clear[186]. There have been studies showing correlations between MT polyglutamylation and kinesin function, however a cause and effect relationship is yet to be defined[185,187].

Since polyglutamylation and polyglycylation target the same glutamate residues in the c-termini of α-tubulin and β-tubulin, it has been suggested that polyglycylation could in fact modulate MT polyglutamylation[188]. However, the function of polyglycylation is unclear. TTLL3 and TTLL8 add a single glycine to the MT, which is then extended by TTLL10[189]. Oddly, in humans, TTLL10 is not active. Thus, almost all MTs in humans are monoglycylated. Unfortunately, these differences among organisms has made determining exact functions of this modification difficult to interpret[189].

Acetylation is a very abundant MT post translational modification[190]. However, unlike detyrosination, polyglutamylation, and polyglycylation, the site of MT acetylation is on the lysine 40 residue of α-tubulin[191]. Uniquely, this residue is located on the MT luminal surface, inside of the hollow opening of the tubule[192]. The major class of enzymes responsible for this modification is tubulin acetyltransferases (TATs)[190]. However, how TATs achieves tubulin binding inside of the lumen of the tubule is still unclear. There are currently two working models. One of which involves TATs bidirectionally scanning the MT within the lumen using surface diffusion. This results in stochastic acetylation of lysine 40 residues along the MT[193]. The second hypothesis is that TATs acetylates the MT as it grows by modifying α-tubulin at the (+) end of the tubule, again resulting in acetyl groups distributed along the MT polymer[194]. While it has been shown that many TATs can acetylate tubulin, including ELP3, ARD1-NAT1 and GCN5, the major tubulin acetylase is αTAT1[195]. Eliminating αTAT1 nearly completely abolishes MT acetylation. αTAT1 is regulated by an auto-acetylation site, which when blocked does not affect MT binding of αTAT1, but does significantly

decrease MT acetylation[196]. Once MT disassemble, tubulin dimers are very rapidly deacetylated, similar to tyrosination of tubulin.

The major enzyme catalyzing this reverse reaction is histone deacetylase (HDAC) 6[197]. However, manipulation of HDAC6 effects many pathways as HDAC6 also has a number of other substrates including Hsp90, cortactin, and β-catenin. Interestingly, HDAC6 knockout mice exhibit a very mild phenotype, suggesting that there are in fact compensatory pathways for HDAC6, possibly HDAC5[197]. There are also non-classical deacetylases which can modify tubulin. For example, sirtuin2 has been shown to deacetylate α-tubulin. Accordingly, sirtuin2 knockout also increases MT acetylation, just not as effectively at HDAC6 knockout[198].

Although acetylation is considered a major MT post translation modification, there is little consensus regarding its function[164]. Acetylation has traditionally been associated with long lived MTs, suggesting a role in MT stability. However, there is no evidence that MT acetylation has any effect on MT dynamics[188]. One consensus is that MT acetylation does affect protein interactions with MTs. For example, binding of Hsp90 to MTs is enhanced by acetylation, and acetylation sites are the preferred site of action for the severing protein katanin[199,200]. Further, MT acetylation has been reported to enhance kinesin based vesicle transport[201,202].

While these MT post translational modifications discussed so far are the most common and ubiquitous, there are also many other post translational modifications that have been reported[164]. These include, polyamination, phosphorylation, glycosylation, glycation, palmitoylation, ubiquitylation, sumoylation, however these tend to be far less abundant and less common. In some cases, certain modifications can even be limited to

specific cell types. Yet, much of the detailed functions of these modifications is still being worked out[164].

The second structure that the cytoskeleton is comprised of are actin microfilaments. Actin is a family of multi-functional proteins which can form microfilaments[203]. Actin is a 42 kDa protein which can be found in two forms[204]. The first form is a monomer of actin, referred to a G-actin where the G means globular. The second is a linear polymer microfilament, referred to as F-actin where the F means filamentous[205]. These polymerized microfilaments measure roughly 4-7nm in diameter and perform a number of very important functions. In fact, actin is among the most abundant proteins in eukaryotes and has possibly as many as 30 different isoforms[204].

The monomeric form of actin, G-actin, is a globular protein which consists of two lobes separated by a cleft[206]. The center of this cleft is known as the "ATPase fold" which is the site of the catalytic activity giving actin the ability to hydrolyze adenosine triphosphate (ATP). G-actin is only functional when it contains a molecular of either ADP or ATP in this cleft, however the free globular actin tends to contain ATP[205]. Interestingly, this structure is tightly regulated. A group II cytosolic molecular chaperone protein called CCT is required to make sure that G-actin adopts the correct tertiary structure[207]. While the reasoning for this is still unclear, it is postulated that this is due to the profound toxic effects that could arise from misfolded G-actin which cannot correctly form F-actin[208]. ATP binding promotes G-actin polymerization to form F-actin and is essential for G-actin to form F-actin[209]. The filamentous F-actin is generally described as two parallel strands which rotate at 166 degrees in order to lie correctly on top of each other to form a double helix structure[209]. This double helix structure is the structure

found throughout the cytoskeletal microfilaments. Similar to MTs, the F-actin polymer is considered to have a distinct polarity[210]. This is due to the fact that the polymer's subunits all point in the same direction. The end that possesses an actin subunit which has its ATP binding site exposed is the (-) end, while the end where the ATP cleft is not exposed, is the (+) end[210].

Similar to MT polymerization, actin polymerization requires nucleating factors necessary to stimulate actin microfilament formation. The Arp2/3 complex is an important nucleation factors for actin polymerization[211]. Arp2/3 mimics a G-actin dimer which acts to stimulate the addition of the first monomeric G-actin. This subsequently triggers rapid addition of further monomers creating the F-actin strand. Further, Arp2/3 also binds to actin filaments at a 70 degree angle to nucleate the formation of new actin branches off of existing actin filaments[212].

Actin filament growth is governed by ATP-ADP hydrolysis[213]. G-actin bound to ATP promotes actin filament growth. However, ATP is rapidly hydrolyzed after the addition of the G-actin monomer to the filament. Whether this hydrolysis occur at random or vectorally is still unclear. However, in either case, the resulting phosphate (P_i) is not immediately released[213]. The amount of this actin-ADP-P_i complex is an indicator of the longevity of the filament. Once this P_i is released, the resulting actin bound to ADP promotes filament disassembly[214]. Once the actin filament disassembles, the ADP is released and the free G-actin is able to bind a new ATP molecule. Similar to MT polymerization, there is a critical concentration of ATP bound G-actin necessary to stimulate filament growth and/or filament disassembly[214]. The growth of actin microfilaments can also be regulated by thymosin and profilin. Thymosin is binds to G-

actin and sequesters it from polymerization. By controlling the amount of free G-actin, thymosin is able to effectively promote polymerization or depolymerization of the actin filaments[215]. Profilin binds to G-actin and facilitates the exchange of ADP for ATP[216]. Another class of proteins which help to regulate the actin cytoskeleton is the Rho family of proteins.

Similar to the MT network, there are also a number of proteins which interact with the actin cytoskeleton; actin-binding proteins (ABP)[217]. These proteins provide a variety of functions including stabilization and crosslinking of the filaments. Thymosin and profilin, responsible for regulating actin filament growth mentioned above, are considered ABPs. There are also ABPs which can alter the length of actin microfilaments by cutting them. Gelsolin and cofilin are major proteins responsible for the severing of actin filaments[218]. Further, CapZ and tropomodulin act as actin microfilament capping proteins. CapZ binds the (+) end while tropomodulin binds the (-) end of actin filaments, both of which stabilizing the polymer[219]. Further, proteins such as filamin, α-actinin, spectrin, dystrophin, and fimbrin, all act to crosslink actin filaments together to create complex networks of polymers[220]. While these protein are all similar in structure such that they are either dimers or have two actin binding domains, they all differ in how the crosslink the filaments. For example, α-actinin binds to parallel filaments to connect them, while filamin crosslinks loose unorganized filaments together[220]. Unlike MT polymers, actin microfilaments have not been studied as extensively in regards to post-translational modifications. However, actin has emerged as a major target for reduction oxidation regulation. It has been shown that a number of residues in actin can be oxidized or reduced to cause significant difference in cellular form and function[221].

Actin filaments play a number of key functions in the cells beyond the maintenance of cell integrity[204]. Actin is thought to be the contractile force of the cytoskeleton. While MT resist compressive forces, actin helps to resist torsional and tensile forces[204]. This is achieved by linking the cell membrane to the rest of the more rigid cytoskeletal elements and by attaching the cell to its surrounding environment. If you were to consider the cell a camping tent, the MT network would be comparable to the tent pole which prop the tent up, while the actin filament network would be comparable to the canvas and the tie downs which provide the necessary tension to keep the pole propped up and also attach the tent to the ground. This contractile property of the actin filament network allows it to perform its major functions. For example, the contractility of the network assists in cell migration[222]. Fist, when a cell migrates, the MT network reaches out from the cell. The actin network facilitates the attachment if the protrusion of the cell. Then using the contractile nature of the actin filaments, the actin cytoskeleton contracts and pull the cell forward towards that new attachment point[223]. Likewise, once the cell moves forward, the actin cytoskeleton in the trailing end contracts, pulling the trailing end up to the cell. As mentioned, actin plays an important role in the attachment of cells to their surrounding environments. Actin does this through the generation of focal adhesions[223]. Focal adhesions are the points of attachment for the cell. Cell surface receptors called integrin bind to the extracellular environment via an extracellular domain[224]. Then they span the plasma membrane and attach to the actin microfilament network via cytosolic domains. Typically the actin filament network binds to integrins through adapter proteins such as α-actinin and talin[224]. When these integrins, adapters, and actin filaments create an attachment point, they cluster together forming

what is referred to as the focal adhesion[224]. These focal adhesions have been implicated in a number of cellular processes including signaling events and even mechanotransduction[225]. Further, during cell division, the actin cytoskeleton creates a ring around the cell between where the two cells will separate. Then the actin ring contracts and pinches the cell in half, generating two daughter cells[226]. In muscle, the actin network contractile properties are the basis for how the muscle cells generate force. It is contraction of the microfilaments which causing the muscle as a whole to contract[204].

Important to note is that unlike tubulin, actin can also be found inside the cell nucleus[227]. Inside the cell nucleus, the actin can form a nuclear actin network which is comprised of unique actin isoforms and ABPs and serves its own unique functions. Similar to the cell as a whole, nuclear actin plays a role in maintaining the architecture of the nucleus, however it can also play a role in transcription and gene activity by influencing chromosome reorganization and translocation, and by regulating the transport and activity of transcription factors within the nucleus[227].

More recently the actin microfilament network has been implicated to play important roles in mechanotransduction[228]. Many recent reports have suggested that mechanical stimuli causes tugging forces on cell attachment sites which is a nexus for mechanically induced signaling events[225]. This is similar to the mechanosome hypothesis proposed in osteocytes. However, it has also been postulated that actin plays an important role in regulating gene expression in response to mechanical stimuli by transducing the mechanical cues to the cell nucleus. It is hypothesized that since the actin filament network is responsible for maintaining the architecture of the cell nucleus, that

mechanical stimuli can cause changes in the actin cytoskeleton which perturb or deform the cell nucleus. This effectively alters nuclear shuttling and subsequent gene expression[229]. However, while there is evidence to support some of these models, the exact mechanisms of the actin cytoskeleton's role in mechanotransduction is still being explored.

The final element that makes up the cell's cytoskeleton are the intermediate filaments (IFs)[140]. Unlike MTs and actin filaments which are mainly made up of a single protein or protein dimer, IFs are made up of a whole family of proteins which have similar structures[230]. They receive their name, intermediate, due to their average diameter. IFs tend to have a diameter in between that of actin and MTs of around 10nm[230]. There are about 70 different genes which encode for different IF proteins which all share similar characteristics[231]. In general IF proteins have a central alpha helical rod domain that is flanked by more variable non-alpha helical N and C termini[230]. IF have a much more complex higher order structure than that of actin and MTs. The complete and function IF is made of several levels of protein association and filament interactions before becoming a complete IF[232]. You can think of IFs as a rope, in which several smaller strands wind together to make a larger strand, and then several of these larger strands wind together to make the rope. IF proteins and filaments tend to assemble in a very similar fashion. This gives the IFs much stronger mechanical properties when compared to actin and MTs[233]. IFs are very deformable and can even be stretched to several times their original length. Unlike MTs which can break very easily, IFs are very resistance to breakage. While MTs are resistant to compressive forces, IFs tend to be more resistant to tension forces[233].

There are about 70 different IF proteins which are categorized into six different types based mainly on their protein sequence and structure[231]. Types I and II are acidic and basic keratins. Keratins are the most divers among the IF proteins. So much so that they are sub categorized into epithelial keratins, found in epithelial cells and trichocytic keratins, found in hair, nails, and etc[231]. Type III IFs are those which can form homo and heteropolymeric proteins. These IFs include desmin in muscle, glial fibrillary acidic protein in astrocytes, peripherin in peripheral neurons, and vimentin the most widely distributed IF found in such cell types as fibroblasts, leukocytes, endothelial, and bone cells[231]. Type IV IFs include α-internexin, neurofilaments, synemin, and syncoilin. Type V IFs are nuclear lamins. These are specialized IFs which have been shown to have specialized structural function within the cell nucleus[231]. Type Vi IFs are nestin which plays a specialized role in the nervous system[231]. While these six categories makes up most of the known IF proteins, there are a few that remain unclassified including filensin and phakinin[231].

Importantly, IFs do not contain any nucleoside triphosphate binding site like actin and tubulin. Therefore, assembly is not as strictly regulated as with other cytoskeletal elements[234]. Further, there are no nucleation factors which trigger IF assembly. Instead IFs laterally associate into full 60nm long unit-length filaments in a process that is complete in seconds[234]. This is a spontaneous association that is so strong, even at extremely high pH levels, the assembly still occurs. Then, in a much slower phase, these unit-length filaments anneal end to end, in order to elongate the filament[234]. In the sense, the unit-length filament serves as both the nucleator and the elongation factor for IF growth. Interestingly, once the IF is completely formed, there tends to be a reduction in

filament diameter. This suggests another level of subunit reorganization, however this "radial compaction" as it is referred to is still not fully understood[234].

IFs tend to assemble in an anti-parallel orientation. Therefore unlike MTs and actin, the full IF does not exhibit any polarity[234]. Due to this, IFs cannot serve as a basis for cell motility or intracellular transport. Instead, the main function of the IFs is to maintain structural integrity of the cell. While MTs and actin are largely cytosolic structure, with the exception of a small subset of actin, IFs are found throughout the entirety of the cell[234]. IFs link the plasma membrane with the nuclear envelope and even inside the cell nucleus. Therefore, it makes the IFs unique suited to stabilize and even determine the shape of the cell. This also gives the IFs a specialized role in cell attachment, working together with actin filaments to anchor the cell to its surrounding environment[234]. Further, it has been shown that IFs play a role in stress-bearing. IFs have been shown to absorb stress on the cell membrane in order to maintain the integrity of the cell and the overall cell structure[235]. It has also been suggested that the IFs may play roles in mechanotransduction as they are an integral part of linking the cell to its environment. It is hypothesized that the tugging effect caused my mechanical strain on the cell, tugging on attachment points, is a nexus for stimulating a mechanically induced response[235]. IFs could in fact play an important role in mediating this tugging effect as the IFs try to absorb this stress and maintain the cell structure. A very important function of IFs is that they also link the elements of the cytoskeleton together[235]. This is extremely important in epithelial cells where IF associated proteins including plakoglobin, desmoplakin, desmogleins, and desmocollins, link the IFs to desmosomes; a

structural node which connects the cytoskeleton together both within a cell and with neighboring cells. IFs in heart muscle cells are connected in a similar fashion[235].

Similar to MTs, many of the IF proteins can be subject to post-translational modifications[236]. The complexity of these modifications and the regulatory control that they can mediate has only recently become apparent. It has been observed that most IF proteins can be phosphorylated or ubiquitinated, however there are also specific modifications that happen to only a few IF proteins[236]. IF phosphorylation tends to be associated with IF reorganization and can be facilitated by a number of kinases and phosphatases. Further, IF phosphorylation could also cause dynamic subunit exchange in which an IF subunit can be incorporated anywhere along the IF rather than at the end. IF phosphorylation has also been shown to play important roles in neuromuscular function, viral egress, and cell growth[236]. Farnesylation is a modification that has only been observed in nuclear lamins. This modification allows nuclear lamins to attach to the inner nuclear membrane and has been shown to play an important role in the structural integrity of the nuclear envelope. These are a few of the most well understood post-translational modifications to IF proteins[236]. However, there is accumulating evidence in regards to sumoylation, glycosylation, transamination, and ribosylation of IF proteins as well. Acetylation of keratins is a very rapidly expanding field and shows significant evidence in modulating IF function. However, the full understanding of these modifications and their impact on IF function is still to be elucidated[236].

Once common feature of all of the elements of the cytoskeleton (MTs, Actin, IFs) is that they are responsible for maintaining the structural integrity of the cell. Thus, the cytoskeleton is extremely important when considering the cellular response to mechanical

signals[237]. Whether the cell is stretched as is the case with skeletal muscle, or subjected to fluid flow shear stress as is the case with osteocytes, it is the role of the cytoskeleton to resist those forces and transduce a cellular response. This combined with growing evidence that the cytoskeleton plays a more functional role in mechanotransduction, makes elucidating the precise molecular mechanisms of the role of the cytoskeleton in these processes vital.

Present Studies

It has been observed that the distribution of cytoskeletal elements seems to changes when osteoblasts differentiate into osteocytes[238]. It has been shown in primary osteocytes grown in 3D culture that the cell processes are dependent on actin[239]. Further it was shown that actin filaments were essential for chicken osteocytes to maintain their cell structure[15]. Fimbrin and α-actinin, actin crosslinking proteins are enriched in the osteocyte processes, with fimbrin being very abundant at the sites of bifurcation of the processes. Further, osteocytes show higher expression of the cytoskeletal proteins villin and spectrin when compared to osteoblasts[238]. These details regarding the actin cytoskeleton have been widely accepted in the field and have grown many to believe that the actin cytoskeleton and not the MT network are important for osteocyte mechanotransduction. Many mathematical models have been introduced which model the stress level on the actin filaments and have even gone so far to suggest that actin filament mediated integrin attachment is a point of amplification of the stresses perceived by the osteocyte which is required in order to stimulate a response[95]. However, disruption of the MT network with the drug colchicine completely abrogated the ability of MLO-Y4 osteocyte-like cells to respond to mechanical signals as indicated by an inhibition of mechanically induced ERK signaling and PGE_2 release[240]. One potential explanation for

this could be that the primary cilium of osteocytes is highly enriched in MTs. Thus, disruption of the MT network could eliminate the function of the osteocyte primary cilium inhibiting the ability of the osteocyte to sense mechanical stimuli[73]. More recently, when osteocytes are subjected to fluid flow shear stress, a dynamic remodeling of the MT network was observed such that the MT polymers orient themselves in the direction of the fluid flow suggesting a more important role for MTs in the osteocyte mechanical load response than previously postulated[72].

Another hypothesis of how the cytoskeleton impact osteocyte mechanotransduction is through the linker of nucleoskeleton and cytoskeleton complex which creates a continuum of cytoskeletal elements all the way from integrin attachment points to the inside of the nucleus[241,242]. The hypothesis is that the cellular response to mechanical cues is caused by nuclear movement within the cytoplasm of the cell. The impact of the cytoskeleton on osteocyte mechanotransduction is an indirect effect of the external force being transmitted to and exerted on the nucleus through the cytoskeleton and the linker of nucleoskeleton and cytoskeleton complex[243]. Some groups have even used this model to hypothesize that the osteocyte response is due to nuclear deformation caused by forces transmitted through the cytoskeleton[244-246].

While there is evidence suggesting that any of the proposed hypotheses regarding the role of the cytoskeleton in osteocyte mechanotransduction could be true, it is also clear that none of these hypotheses is a complete picture of the osteocyte mechanical load response. Many of the current hypothesis give large picture and more broad perspectives on the topic[247]. Thus, we set out to explore some of the more precise molecular

mechanisms of how the osteocyte cytoskeleton modulates osteocyte mechanotransduction.

Recently, a relay of mechanical signaling has been characterized in heart and skeletal muscle. This relay involved the stretch mediated activation of nicotinamide adenine dinucleotide phosphate-oxidase 2 (Nox2) to generate reactive oxygen species (ROS)[248]. This ROS then leads to the calcium sparks that are characteristic of muscle contraction. The nexus of NOX2 dependent ROS generation in response to mechanical cue has been termed X-ROS[249]. This model gained significant attention in a model of Duchenne muscular dystrophy where dense and disorganized MT network accompanies severe muscle dysfunction[157]. It was shown that increased MT density and increased cytoskeletal stiffness correlated with the excessive X-ROS in a mouse model of Duchenne[157]. Not long thereafter, it was determined that the mechanism mediating this excessive X-ROS and increased cytoskeletal stiffness was the MT post-translational modification detyrosination[141]. As mentioned above detyrosination is important for crosslinking the MT network to other cytoskeletal elements. However, stiffening of the cytoskeleton due to the abundance of detyrosinated MTs is a very recent revelation[141]. It was shown in cardiac muscle that when the muscle is compressed, the level of detyrosinated MTs impacts how the MT network absorbs the stress[174]. When detyrosination was abundant, the MT network would have increased crosslinking which would cause the MTs to buckle when the cardiac muscle was compressed. However, when detyrosination was inhibited, the MTs would slide past one another without buckling when they cardiac muscle was compressed. This buckling versus sliding action

of the MT network significantly altered the overall stiffness of the cell, or the cell's resistance to mechanical force[174].

Considering that one of the earliest responses to mechanical signals by osteocytes is calcium mobilization[68], we developed the hypothesis that this mechanism is conserved in osteocytes and may play a role in regulating the osteocyte mechanical load response. First, we developed a novel method for introducing fluid flow shear stress to cells in culture and validated this method against an accepted system for studying fluid flow shear stress[250]. Then, we examined the localization of MTs in a newly developed immortalized primary osteocyte cell line and determined the abundance and localization of MT detyrosination [251]. Then, we determined the effects of alterations to the MT network and MT detyrosination on osteocyte calcium mobilization in response to fluid flow shear stress. Further, we examined potential candidate ion channels which could be contributing to this calcium response [251]. We also observed a novel rapid regulation of sclerostin protein in response to fluid flow shear stress and explored a mechanistic link between calcium mobilization and sclerostin regulation [251]. Finally, we broadly confirmed that these findings were conserved *in vivo*.

Chapter 2: Materials and Methods

Fluid Flow Device Design

The multi-functional Fluid Flow Device (FFD) is designed for applying fluid flow to a single well of a typical 96 well assay plate (Figure 6A). The FFD has an inlet port situated in the center of the well and an outlet port slightly offset to one side (Figure 6B). The FFD is tapered to allow a firm fit in a single well of the multi-well plate (Figure 6C). The FFD is designed to pair with any standard size 96 well assay plate and can be connected to any commercially available fluid flow control system (i.e., peristaltic pump, syringe pump, pressurized or gravity flow system). Furthermore, this device can be scaled up to accommodate larger tissue culture dishes and can be multiplexed to apply fluid flow to multiple wells simultaneously within the 96 well plate.

Fluid Flow Simulation

SolidWorks 2015 Flow Simulation software was used to perform computation fluid dynamics on the FFD and simulate the flow environment inside the well during flow. The FFD was drawn to scale with a fully enclosed geometry. Two boundary conditions were set for the flow simulation, inlet pressure and outlet flow volume. The inlet pressure set to 542.85 dynes/cm^2 (calculated from our flow rate, 35 mL/min and tubing diameter, 1.5 mm) and set to pulsate at 6 Hz to simulate pulsatile flow from our peristaltic pump.

In order to determine the pressure, we used the known inlet diameter and flow rate. The flow velocity (cm/sec) was calculated using the known flow rate set by our pump and area of the inlet (calculated from the known diameter) using the equation:

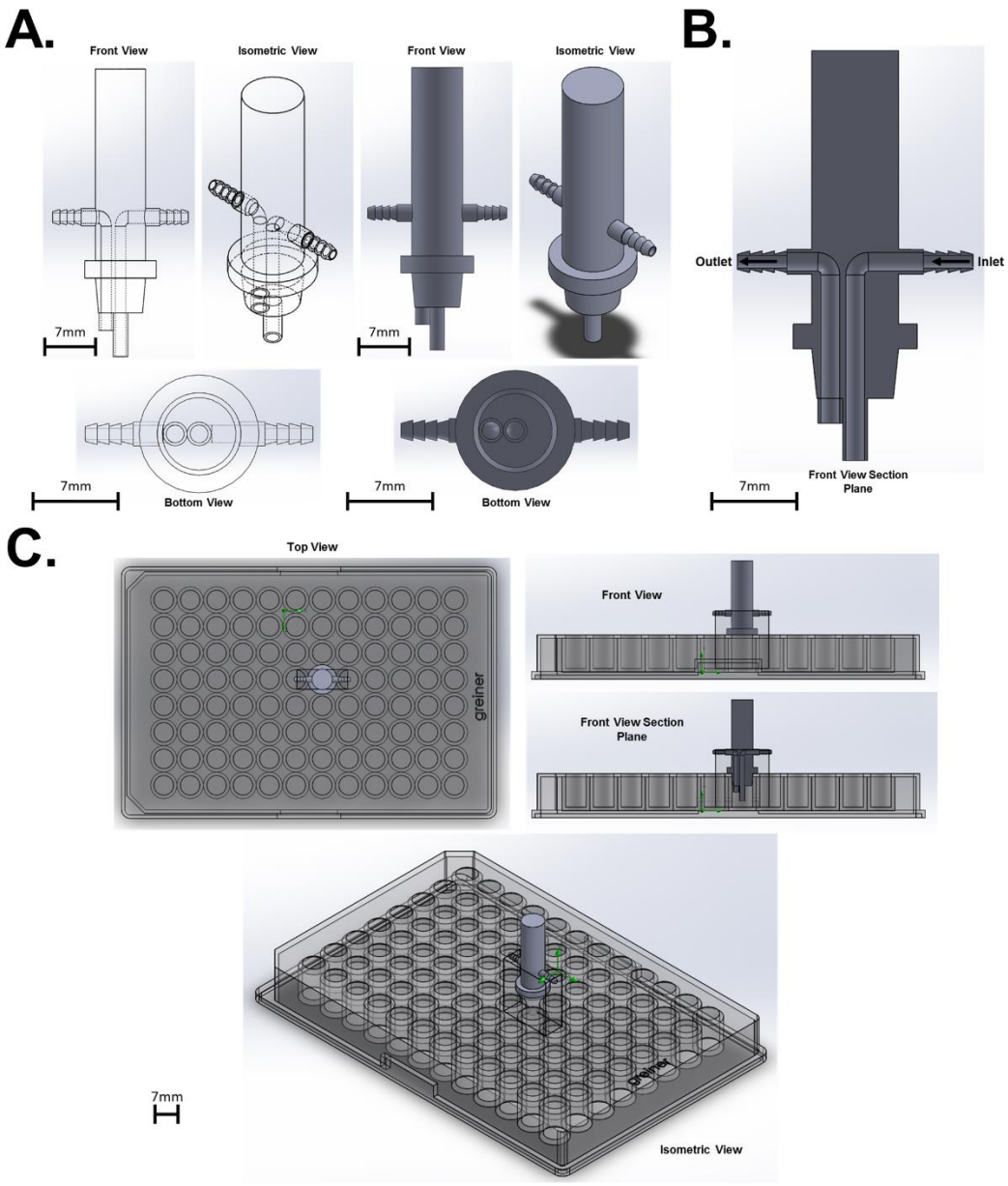

Figure 6. Computer rendering of the novel FFD.
(**A**) Design of the FFD. (**B**) Section cut of the FFD to show the inlet and outlet channels within the device. (**C**) The FFD interfacing with a typical 96 well assay plate.

$$v = \frac{Q}{A}$$

where v = velocity, Q = flow rate, and A = area of the inlet. Using the calculated velocity, we determined the pressure in Pascals using the Navier-Stokes equation simplified to Bernoulli's equation:

$$\frac{1}{2}\rho V^2 + p + \rho g z$$

where ρ = density, V = velocity, p = pressure, g = gravity, and z = height. In order for Bernoulli's principle to hold true for our system, the following assumptions were made: (1) flow buffer is a Newtonian fluid, (2) the flow is incompressible, and (3) there is no friction inside the flow. The outlet flow volume was set to 5.8 x 10-7 m3/s. For all simulations, the flow buffer was assumed to be similar to water (i.e., density = 1 g/cm3).

Chemicals and Reagents

Taxol, colchicine, GSK2193874, GSK-1016790A. N-acetylcysteine, Parthenolide, MG-132, KN-93, Bafilomyocin A1, and Brefeldin A were purchased from Sigma. BAPTA AM ester and Jasplakinolide was from Cayman Chemical. GP91ds-TAT was from Anaspec. siR-tubulin was from Cytoskeleton, Inc.

Cell Culture and Treatments

UMR-106 rat osteoblast-like cells (ATCC) were cultured in DMEM media containing 10% FBS, 1X penicillin/streptomycin, and 2.5mL gentamycin, and cultured at 37ºC, 5% CO_2, as described. Media was changed every two to three days[252].

Osteocyte-like OCY454 cells were provided by Dr. Divieti-Pajevic at Boston University[115]. This is an immortalized primary osteocyte like cell line developed by

breeding DMP-1 GFP mice with mice expressing SV40 large T antigen (Immortomouse, Charles River Laboratories). The double transgenic offspring were euthanized and osteocytes isolated from long bones. The isolated cells were then sorted for DMP1-GFP expression using fluorescence activated cell sorting (FACS) to yield a homogeneous osteocytic population of cells. The cells were then validated for expression of accepted osteocyte gene and protein markers, including *SOST*/sclerostin and *TNFSF11*/RANKL, PTH and PGE_2 responsiveness, and fluid flow shear stress responsiveness[115].

OCY454 cells were cultured on type I rat tail collagen (BD Biosciences) coated dishes in α-MEM supplemented with 10% FBS, 1X penicillin/streptomycin, and 2.5mL gentamycin. Cells were maintained at 33°C and 5% CO_2. Media was changed every two to three days. Prior to experiments cells were seeded into appropriate tissue culture treated vessel and maintained at 37°C and 5% CO_2 overnight[115].

For alteration of the MT network, cells were pretreated with 0.1% DMSO (control), colchicine (2 μM, 20 min), Taxol (1 μM, 2 h), or PTL (25 μM, 2 h). In the case of the combined treatment, cells were dosed with PTL for 30 min before Taxol was added to the same media for an additional 1.5 h for a total incubation time of 2 h. To modulate TRPV4 activity, the cells were treated with the TRPV4 antagonist GSK2193874 (15 μM, 30 min) or TRPV4 agonist GSK-1016790A (15 μM, 30 min) prior to the stimulation of the cells. To modulate reactive oxygen species, the cells were treated with NAC (10 mM, 15 min), H_2O_2 (100 μM, 30 min), or GP91ds-TAT (10 μM, 30 min) prior to the stimulation of the cells. To modulate the actin cytoskeleton, cells were treated with jasplakinolide (10 μM, 2 h). To inhibit CamKII signaling, cells were treated with KN-93 (10 μM, 2 h). To inhibit protein secretion, cells were treated with Brefeldin A (2 μM, 3

h). To inhibit lysosomal degradation, cells were treated with Bafilomyocin A1 (100 nM, 6 h). To inhibit proteasomal degradation, cells were treated with MG-132 (10 μM, 3 h).

Transient Transfections

One day prior to transfection, cells were seeded at 25,000–30,000 cells/cm^2 in the appropriate multiwell tissue culture plate[252]. Ocy454 cells were transfected with JetPrime reagent (Polypus), according to manufacturer's recommendations[252]. ON-TARGETplus mouse TRPV4 siRNA and ON-TARGETplus non-targeting siRNA were purchased from Dharmacon. siRNAs were used at 0.42 μg/cm^2. CamKII T286D and CamKII T286A constructs were purchased from Addgene. pMAX GFP control plasmid was purchased from Lonza. Plasmids were used at 0.27 μg/cm^2. Cell treatments were begun 48 h post-transfection.

Fluid Flow Shear Stress (FSS) Application

Cells in culture were exposed to fluid flow using our custom FFD[250]. Following cell treatments, cells were removed from incubators and cell media was removed. Cells were rinsed in HEPES-buffered Ringer solution containing 140mM NaCl, 4mM KCl, 1mM $MgSO_4$, 5mM $NaHCO_3$, 10mM glucose, 1.8mM $CaCl_2$ and 10mM HEPES (pH 7.3). Ringer solution was also used as fluid flow buffer[250]. For Calcium-free conditions, HEPES-buffered Manganese Ringer solution, containing 140mM NaCl, 4mM KCl, 1mM $MgSO_4$, 5mM $NaHCO_3$, 10mM glucose, 2mM MnCl and 10mM HEPES (pH 7.3), was used and cells were loaded with BAPTA AM ester. FFD was placed into well of tissue culture plate and cells were subjected to 4 dynes/cm^2 or 16 dynes/cm^2 of FSS as indicated

for 1 min. Following application of FSS, cells were immediately lysed for Western blot analysis or RNA isolation.

Calcium and ROS Imaging

Cells were seeded into optically clear 96-well plates (Corning), incubated overnight at 37°C, and 5% CO_2 and treated as indicated. For Ca^{2+} imaging, cells were loaded with Fluo-4 AM ester (ThermoFisher, 5μM) for 30 min, washed, and allowed to rest for 15 min to allow dye de-esterification, as described. For ROS imaging, cells were loaded with CellROX Deep Red Reagenet (ThermFisher, 5μM) for 30min and then washed, according to manufacturer's recommendations. Individual wells were imaged on an inverted fluorescence microscope equipped with a mercury light source, Ludel excitation filter wheel (ex: 485) and a Nikon DS-Qi2 (em: 510-535). All imaging automation was controlled by Nikon NIS-Elements software[141]. For all Ca^{2+} imaging experiments, time lapse images were collected every 500 ms for 30 sec before initiation of fluid flow, then fluid flow was turned on and cells were imaged for 1 min during fluid flow. For ROS imaging experiments, time lapse images were collected every 1 sec for 30 sec before initiation of fluid flow, then fluid flow was turned on and cells were imaged for 1 min during fluid flow. After 1 min, fluid flow was turned off and cells were imaged for another 30 sec post fluid flow. Time-lapse fluorescence intensity measurements were collected using ImageJ Time Series Analyzer plugin and data was analyzed and plotted using Origin Pro software.

Atomic Force Microscopy

Ocy454 cells were plated onto 22 mm x 22 mm glass coverslips and allowed to grow for 16-24 h at 37 °C, 5% CO_2 with αMEM media. Thereafter, cells were washed with PBS before being incubated with pharmacological agents as indicated for 2 h at 37°C, 5% CO_2 in αMEM. After each treatment, cells were transferred to 60 mm culture dishes with pre-warmed HEPES based media containing identical concentrations of the aforementioned agents. The HEPES media is free of phenol red and provides extra buffering capacity during imaging. Cells were probed with an MFP-1D atomic force microscope (Asylum Research) using MLCT cantilevers (Bruker) with a nominal spring constant of k=0.01 N/m[253,254]. The pull distance used was 2 µm with a tip velocity of 4 µm/s to generate ~1-2 nN of force onto the cell corresponding to ~1 µm indentation ensuring that the cytoskeleton was effectively being probed. The elastic moduli (i.e., the stiffness) of the cells were calculated using the Sneddon/Hertz model which has been described previously[255].

Immunofluorescence

Ocy454 cells were seeded on glass coverslips and grown overnight at 37°C, 5% CO_2[256]. After 24 h the cells were washed with pre-warmed PBS twice. The cells were fixed at room temperature with 4% formaldehyde in PBS for 15 min. The cells were then permeabilized with 0.1% triton X-100 in PBS for 8 min. For histological sections of bone, decalcified, paraffin embedded sections were prepared using 3 – 5 min washes in xylene, 2 – 10 min washes in 100% ethanol, 2 – 10 min washes in 90% ethanol and 2 – 5 min washes in MilliQ water[97]. Coverslips or sections were incubated in SuperBlock PBS (Life Technologies) for 1 h before the addition of primary antibodies. Primary antibodies

were diluted in SuperBlock PBS and added to the coverslips or sections for an overnight incubation at 4°C. Secondary antibodies were diluted in SuperBlock PBS and incubated at room temperature for 6 h. Coverslips were mounted using ProLong Diamond with DAPI (Life Technologies). The antibodies used were: α-tubulin (Sigma, T9026), Glu-tubulin (Abcam, ab48389) and TRPV4 (Abcam, ab39260). Goat anti-mouse Alexa 488, 647 and goat anti-rabbit Alexa 488, 568 were purchased from Life Technologies. Actin was stained using phalloidin-TRITC (Molecular Probes). Slides were imaged on the same inverted fluorescence microscope equipped with a mercury light source, Ludel excitation filter wheel (ex: 485) and a Nikon DS-Qi2 (em: 510-535) as used for Ca^{2+} imaging experiments[141].

SiR-tubulin labeling and confocal imaging.

Murine long bones (tibia, fibula) were isolated, flushed of marrow, and placed in 60mm Fluo-dish glass bottom plates. These long bones were then incubated in αMEM containing the live cell tubulin stain, SiR-tubulin (1μM; 37°C and 5% CO_2 for 2 hr). Confocal fluorescent imaging (Nikon A1R; 40x H_2O Obj, 1,4NA) was used to profile the structure of the MT network in the bone embedded osteocytes as previously described[157].

Western Blotting

Western blotting of whole cell extracts isolated from cells in culture following FSS were prepared using modified RIPA buffer containing 50 mM Tris, pH 8.0, 150 mM NaCl, 10 mM sodium pyrophosphate, 10 mM sodium fluoride, 10 mM β-glycerophosphate, 1 mM EGTA, 1 mM EDTA, 1% NP-40, 0.5% sodium deoxycholate, 0.1% SDS and 1 × HALT protease and phosphatase inhibitor cocktail (Thermo

Scientific)[257]. Long bone extracts from murine tibia or ulnar were prepared using same modified RIPA buffer by adding 5-6 1.6mm diameter stainless steel beads (Next Advance) to an Eppendorf tube containing excised bone cleaned of soft tissue and flushed of bone marrow. Samples were then homogenized in a Next Advance Bullet Blender system at 5 min intervals for 15 min total at 4ºC. Protein concentrations were determined used Pierce BCA Protein Assay Kit (Thermo Scientific)[97].

Equal amount of protein were loaded and electrophoresed on 10% SDS-PAGE gels and transferred to polyvinylidene difluoride membranes. Membranes were blocked in 5% non-fat dry milk, except with sclerostin antibody, membranes were blocked in 5% non-fat dry milk with 3% BSA. Membranes were probed with the indicated primary antibodies in blocking buffer overnight at 4ºC. Antibodies were detected with the appropriate horseradish peroxidase–conjugated secondary antibodies (Cell Signaling Technology) and enhanced chemiluminescence detection reagent (BioRad)[258].

The antibodies used were: sclerostin (R&D Systems, AF1589), α-tubulin (Sigma, T9026), Glu-tubulin (Abcam, ab48389), phospho- or total pan-PKC (Cell Signaling Technologies, 9371S, 2058S), phospho- or total ERK1/2 (Cell Signaling Technologies, 9101L, 9102L), phosph- or total CamKII (Cell Signaling Technologies, 12716S, 11945S) and GAPDH (Millipore, MAB374). Blots were acquired using an EpiChem gel documentation system (UVP Bioimaging Systems) and analyzed using ImageJ software[259].

Quantitative RT-PCR

RNA extraction was done by Directzol RNA mini prep (Zymo). RNA was reverse transcribed with either iScript (BioRad) or RevertAid (Fermentas) reverse transcription

master mix, according to the manufacturer directions. Quantitative real time PCR was carried out by SYBR green master mix from Quanta using an Applied Biosystems 7300 sequence detection system. A melting curve was performed to ensure amplification of a single PCR product. For each sample, the relative gene expression was determined by simultaneously normalizing the gene of interest with three housekeeping genes (RPLl13, HPRT and GAPDH) by the $2^{-\Delta\Delta Ct}$ method, using GeNorm v3.5 software (Ghent University Hospital Ghent, Belgium) as described[256]. Primer sequences are shown in Table 1.

Micro Computed Tomography (microCT)

8-week-old male mice were treated with 75mg/kg of Taxol every other day for 3 doses and then sacrificed 30 days later. Femurs were dissected and fixed in 4% PFA for 2–4 days and then transferred to 70% ethanol[97]. Three-dimensional microCT was performed on the femurs using SkyScan 1172 (Bruker, Kontich, Belgium). The skeletal parameters assessed by microCT followed published nomenclature guidelines (Bouxsein et al., 2010). Bone morphology and microstructure were assessed at the mid-diaphysis for cortical parameters, including cortical bone volume (Ct.TV), periosteal perimeter (Ct.Peri.Pm), endosteal perimeter (Ct.Endo.Pm), cortical thickness (Ct.Th), cortical porosity (Ct. Po) and mean polar moment of inertia (MMI). Trabecular parameters were assessed at the distal femoral metaphysis for trabecular parameters, including the trabecular bone volume fraction (BV/TV), trabecular bone thickness (Tb.Th), trabecular number (Tb.N) and trabecular separation (Tb. Sp). Analysis was completed with n=4. Femurs were scanned with 2K resolution, a 10 μm^3 voxel size, and 0.5 mm Al filter at 60 kV and 167 µA. Trabecular bone was delineated manually in a region of interest 0.2 mm

Calcium Channel Primers		
Gene	Forward Primer	Reverse Primer
Cav1.2	CCTTAAGTCAAAGCAACTTTTTTTCC	ACCGCCTTATCTAAACTGACTGTTAAC
Cav1.3	CCCAAAAACCCATACCAGTACAAG	CCAGGCAGAGCGTGTTGAG
Cav1.4	TCCCGCATATCTATCACGTTCTT	TCACCCTTACTGAGCAGCTTCA
Cav3.1	GGCTTAGTTCCCCGCTGTCT	GGTACCATCTGCAAAAGGATCAG
Cav3.2	TGGGTTCCGGAGGTTCTTC	CAGCGCAATGCCCATGA
Cav3.3	TTTCTTCAAGGACCGATGGAA	CGCAGAACACGCATGATACG
Cav1.1	CGAGGGCTTGAACAAAATCATC	GGCACTTCCAGCGGAAGA
TRPC1	TGACCTCCATGCGACAGAAG	GACAGATCTTGGCGCAGTTCA
TRPC2	GATTCCTGTCGGATGTGTATAGGTTAG	CCCTGAAGAGAGGTGATTAAAGTAGGT
TRPC3	GGAAGGCCTCTATGCCATAGCT	GCTCTCGTTTGCAGGGAGAAT
TRPC4	AGCCTCTTTGATTTAACCACTCTGA	TAGGTTATGTCTCTCGGAGGCAAT
TRPC5	TGGCACCTTACCACCTCCTT	GTTGAACCAGTTGCCAAGATAGAGA
TRPC6	CACTGCCTGTCCCCTTCAAT	AGCTCAGACATCCATTTCTTAAATTTC
TRPC7	GGGCACGTGGGCTGATATC	CTTGTCTCTCCCAACAGCCTAGTT
TRPA1	TGAGATCGACGGGAGTGTTTATC	GGTGCTGAAGGCATCTTGGA
TRPV1	TTTCAGGGTGGACGAGGTAAA	AGTTGCCTGGGTCCTCGTT
TRPV2	GATGAGCGCTGGTGCTTCA	ATCCTCAGATAAGGTGGGAAGAGTCT
TRPV3	CATGTCTAGAAGATCTGAGCTAAGTTGATC	TAAGGGTATTCCCATAGCTCATTCC
TRPV4	ACAAGAACTCAGGCACAGATGAAG	GCTGGTGGCCGTCACAGT
TRPV5	TCGAGCTCAGGTTTGACTCATC	GGAAATCTTGCCTGTTACTCTGACA
TRPV6	AATAAGTGGGAGGGCACAGAAC	TCACACGCTTTCCCACAATC

Table 1: Calcium channel primer sequences used for qRT-PCR.

to 2.0 mm proximal to the distal femoral growth plate. For cortical bone parameters, transverse microCT scans were performed at the femoral diaphysis beginning at 56% of the femoral length (measured from the head of the femur) extending 0.6 mm distally[97].

Ulnar Loading

Mice were anesthetized with isoflurane (0.5% - 2%) and forelimb positioned into a modified 305B muscle lever system (Aurora Scientific Inc.) The volar flexed carpus was placed into a small cup on a fixed substrate while the elbow was placed into a small cup on the lever arm of the force transducer. Limbs were preloaded at 0.3 N and then subjected to repeated loading of 2.5 N at a frequency of 2 Hz for 90 secs[260]. This was performed daily for 3 days. Ulnar loading was controlled by an Aurora Scientific Inc. force transducer system. After the third day of loading, the mice were euthanized and ulna were excised for molecular analysis. Contralateral unloaded ulna were used as controls[260].

Dyamic Histomorphometry

Mice were subjected to daily bouts of ulnar loading for 3 days. On day 3 mice were injected with Calcein (i.p. 30μM). After 14 days, mice were injected with alizarin red (i.p., 30μM). 3 days later mice were euthanized and the ulnas isolated and flash frozen. Frozen ulnas were then cut in 100μm transverse sections and imaged on same inverted microscope used for immunofluorescence experiments, equipped with a mercury light source, Ludel excitation filter wheel (ex: 485) and a Nikon DS-Qi2 (em: 510-535).

Statistical Analysis

Experiments were repeated a minimum of 3 times with triplicate samples, unless indicated otherwise. Graphs show averages with error bars indicating standard error. Samples were compared by an ANOVA for unpaired samples with a Dunnet's or Holm-Sidak post-hoc test or a t-test, as appropriate, using GraphPad Prism 6 software. A p-value <0.05 was used as a threshold for statistical significance.

Chapter 3: Design and Validation of Fluid Flow Shear Stress Model

Introduction

Cells respond to their mechanical environment by activating biochemical signaling pathways, a process known as mechanotransduction. Mechanotransduction regulates diverse physiologic function in healthy cells and burgeoning evidence implicates dysregulation of mechanotransduction cascades in disease pathology [261]. Given that these mechanotransduction pathways often integrate multiple signaling events, there is a growing interest to identify key signaling nodes that can be targeted to modulate outputs that drive physiology or disease.

In the skeletal system, osteocytes sense mechanical strain within bone and respond with mechanotransduction signals (e.g., calcium (Ca^{2+}), nitric oxide, extracellular ATP) and the expression of factors (e.g. receptor activator of NFκB ligand (RANKL) and sclerostin) that control the activity of bone resorbing osteoclasts and bone forming osteoblasts [57,112,262-265]. Given that fluid flow through the lacunar-canalicular network generates shear stress driving mechanotransduction in bone [57], fluid flow is most often used to interrogate osteocyte response to mechanical load.

A number of commercially available [72,83,266,267] and do-it-yourself [268-270] systems have been developed to model fluid flow in osteoblast and osteocyte-like cultured cells and each has its own limitations, such as limited throughput and/or functionality. We have designed a multifunctional fluid flow device (FFD) that when paired with standard 96 well culture plates and a commonly used fluid flow apparatus (e.g., peristaltic pump, syringe pump, pressurized or gravity flow system), provides the user a versatile, cost-effective device that can be easily used for both live cell imaging

and molecular biology applications. Further, this device is scalable and can be adapted to medium-to-high throughput application.

Results

Computational Fluid Dynamics

The results of the fluid flow simulation indicate that the fluid flows through the inlet of the FFD, where it impacts the bottom of the well and then spreads radially and evenly (Figure 7A). Then the fluid flows up the walls of the well before being pulled through the outlet of the FFD, without interrupting the flow across the bottom of the well (Figure 7B). In addition to flow trajectories, the computational solver calculated dynamic pressure (Figure 8A), flow velocity (Figure 8B), turbulence intensity (Figure 8C) inside the well, and the average shear stress at the bottom surface of the well (Figure 8D). Under the described conditions, the cell monolayer cultured on the bottom of the tissue culture vessel are subjected to a uniform average 4 dynes/cm^2 of shear stress (Figure 8D). Further, the velocity trajectories indicate that the flow across the bottom surface of the well is uniform such that the entire well of cells will be subjected to the same forces (Figure 7). The turbulence intensity within the system without the addition of cells is extremely low, 0.65% (Figure 8C). These findings show that the FFD mimics physiologic fluid flow reported to be experienced by bone cells *in vivo* [271].

Device Validation

It is well established that osteoblasts, including UMR106 osteoblast-like cells, are mechano-responsive with fluid flow inducing a rapid influx of Ca^{2+} across the plasma membrane [79,112,272-279]. We validated the FFD by comparing fluid flow-induced Ca^{2+} influx with this device to that obtained with the widely used Ibidi chamber; a commercially available device that allows biologically relevant laminar flow derived shear stress on cells cultured within the chambers. Comparing the response of UMR106

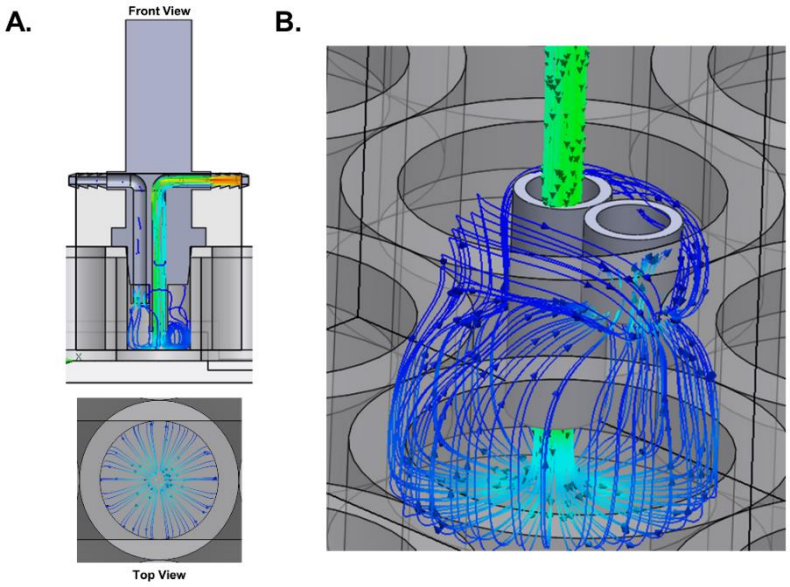

Figure 7. Vector lines indicating fluid flow trajectories.
(**A**) Trajectories of flow from the front section view and a top view. (**B**) Up close view of the inlet and outlet trajectories within the well of the plate. Data were determined using SolidWorks 2015 Flow Simulation software.

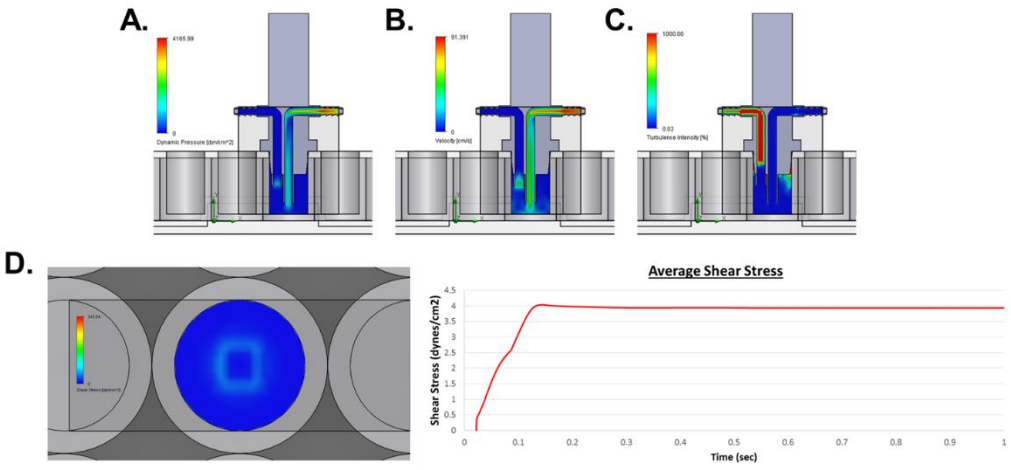

Figure 8. Computational fluid dynamics.
(**A**) Simulated dynamic pressure within the device and well. (**B**) Simulated velocity within the device and well. (**C**) Simulated turbulence intensity within the device and well. (**D**) Simulated shear stress at the bottom surface of the well. Computational trace of the average shear stress at the bottom surface of the well over time. Data were determined using SolidWorks 2015 Flow Simulation software.

cells between both devices yielded virtually indistinguishable peak Ca^{2+} magnitudes and elevation/decay kinetics of Ca^{2+}-dependent fluorescence (Figure 9). The Ca^{2+} traces shown in Figure 9 are the average traces calculated from single cell traces (n>30) from three independent experiments. Single cell traces from a single, representative experiment are shown in Figure 9B. To validate that this Ca^{2+} influx is biologically relevant, western blot analysis was performed for activation of PKC signaling, a ubiquitous Ca^{2+}-dependent signaling pathway. Indeed, a rapid phosphorylation of PKC was observed in response to FSS (Figure 10)

In addition to Ca^{2+} influx, fluid flow initiates ERK signaling in osteoblasts, including UMR106 cells [280-283]. We tested the response of UMR106 cells seeded in a 96 well tissue culture plate and subjected the cells to 4 dynes/cm^2 of shear stress for 1 minute. After flow, the cells were immediately lysed and examined by western blot. Consistent with the literature, fluid flow-induced rapid activation of ERK signaling as indicated by an increase in phosphorylated-ERK (Figure 10). These data support the notion that the FFD generates a physiologic conditions and biological responses comparable to the accepted commercially available methods.

Device Multiplexing

In order to demonstrate the multiplexing capability of the FFD to be used for simultaneous independent replicates, we performed western blot analysis on whole cell extracts from UMR106 cells subjected to fluid flow simultaneously in separate wells. Indeed, we observe similar activation of both ERK and PKC signaling across each well (Figure 11). These data demonstrate the consistent stimulation and biological responses among cells simultaneously exposed to fluid flow conditions across independent wells.

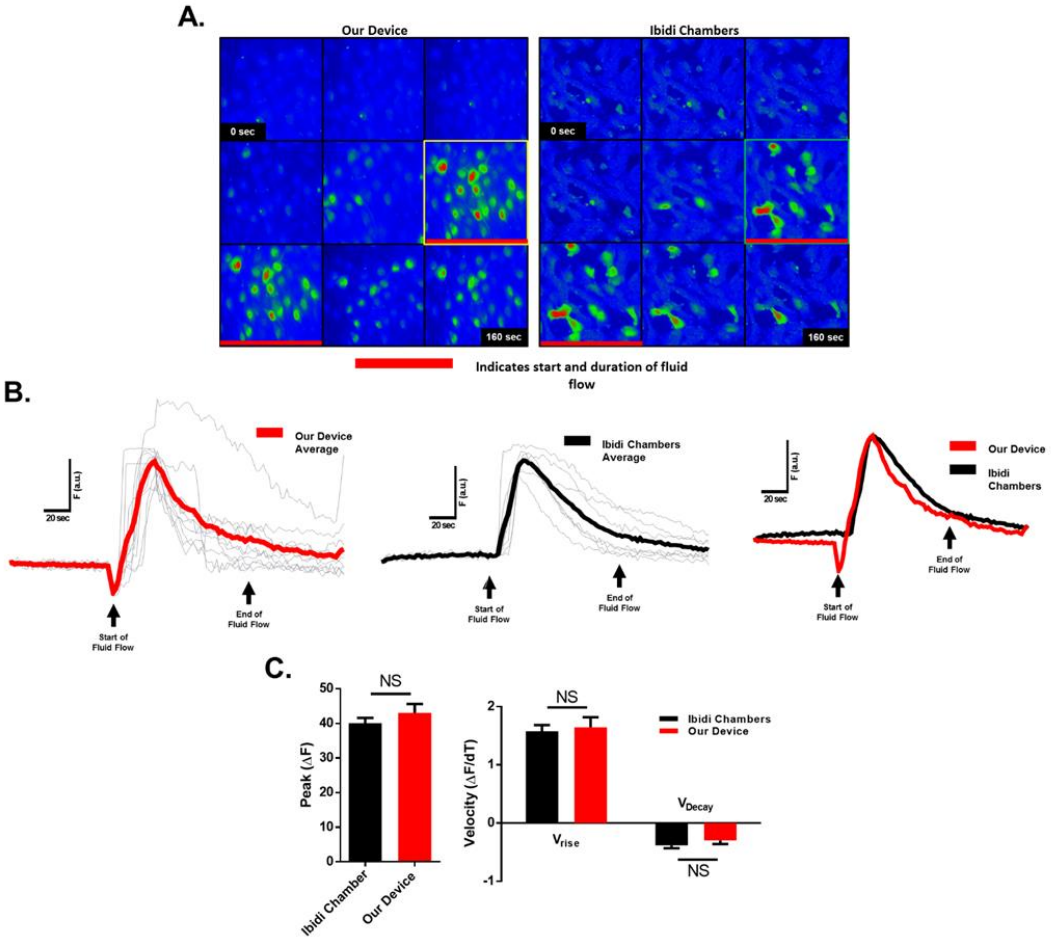

Figure 9. Real-time Ca2+ imaging of UMR106 cells during application of fluid flow.
(**A**) Fluo-4 Ca2+ indicator dye fluorescence before (basal) and during flow (response) of cells seeded in both the Ibidi chambers and a 96 well plate with the FFD. Red line in image sequence indicates start and duration of fluid flow. (**B**) Trace of Ca2+ indicator dye fluorescence intensity over time scaled to same basal level of fluorescence intensity. (**C**) Peak change in Ca2+ indicator dye fluorescence intensity and elevation/decay kinetics of Ca2+-dependent fluorescence. Asterisks indicate statistical significance at $p<0.05$.

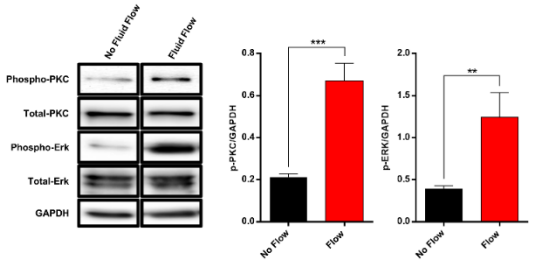

Figure 10. Western blot analysis of UMR106 cells exposed to fluid flow in the FFD.
Fluid flow induced rapid activation of PKC signaling and ERK signaling as indicated by an increase in phosphorylated PKC and phosphorylated ERK. Data are from the same gel and exposure. ImageJ quantification of western blot relative to GAPDH. Asterisks indicate statistical significance at $p<0.05$.

Discussion

We have designed a fluid flow device to enable cell-based assays of fluid flow-dependent mechanotransduction. This FFD addressed the lack of a cost-effective and functionally flexible platform for these measures. Our approach was to design a low-cost flexible perfusion apparatus that, when coupled with commercially available 96 well plates and commonly available perfusion apparatus, yields such a system. Importantly, model simulations revealed that the FFD delivers physiologically relevant fluid flow to cultured cells. We also show that fluid flow with the FFD yielded quantitatively similar results to those reported with a commercially available system [79,284,285]. Together the results support the FFD as a reliable and valid solution to the shortcomings of commercially available fluid flow systems (i.e., cost and functionality).

The design of the FFD yields several important advantages over other fluid flow systems. First, the FFD couples to commercially available 96 well plates. This format supports both imaging as well as molecular and biochemical analyses using the same device. Indeed, we were unable to recover sufficient amounts of protein from the Ibidi chambers to perform analysis of signaling events by western blotting, underscoring the multifunctional applicability of our device. Using the same device for every experiment, rather than a device specifically for imaging and another device specifically for molecular and biochemical analyses, reduces experimental variables [286]. Furthermore, this format also allows expandability to a medium-to-high throughput cell culture platform if multiple FFDs are used in the same plate with a multichannel peristaltic pump, obtaining fully independent replicates for each sample. Supporting this notion, our western blotting data demonstrate the consistent biological response to fluid flow among simultaneously stimulated wells using the multiplex format. Second, the FFD supports various fluid flow

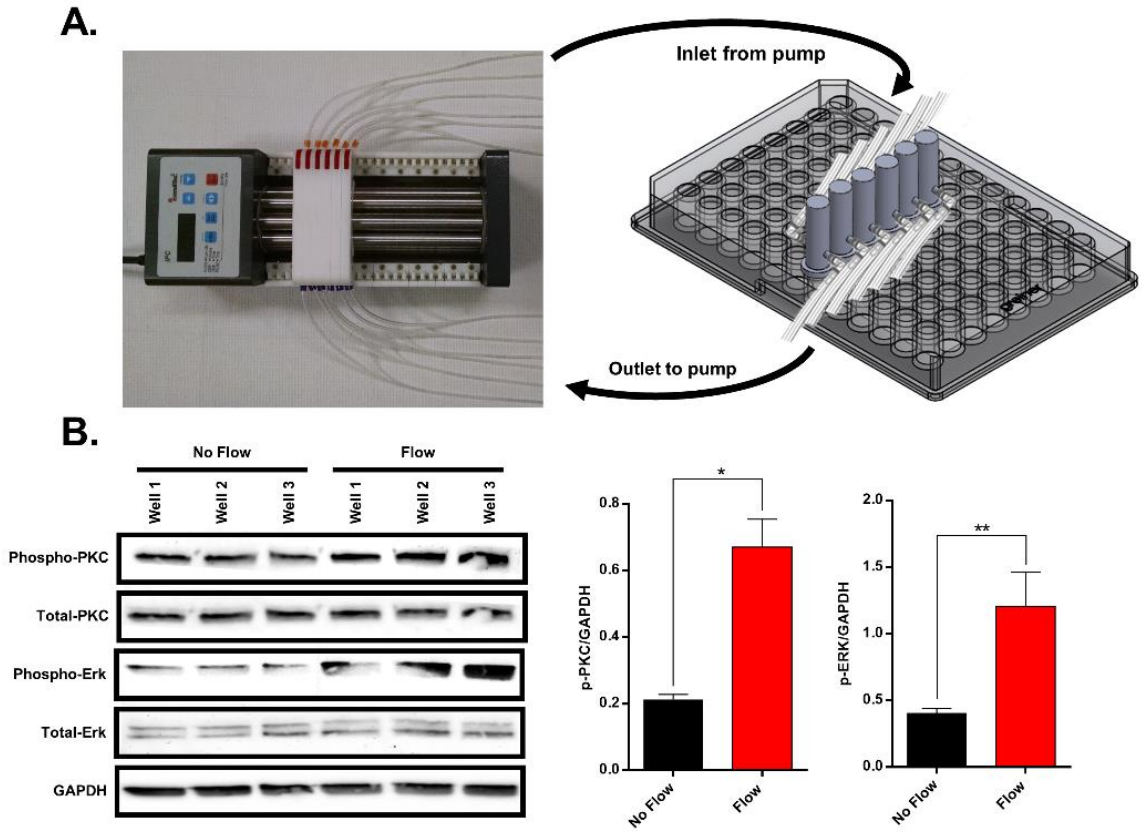

Figure 11. Demonstration of the multiplexing capability of the FFD.
(**A**) Example of the multi-channel peristaltic pumped used when multiplexing the FFD and a computer rendering of the FFD multiplexed in a single 96 well assay plate across 6 independent wells. (**B**) Western blot analysis of UMR106 cells simultaneously exposed to fluid flow in separate wells. ImageJ quantification of western blot analysis relative to GAPDH. Asterisks indicate statistical significance at $p<0.05$.

systems, which expands the flexibility and versatility of this system. Taken together, the FFD design provides a flexibility in function that is unparalleled by any currently available commercial solutions. Third, a significant advantage of the FFD is the cost savings. Current commercial devices that incorporate a culture platform enclosed in a perfusion chamber can be prohibitively expensive. While these chambers are more cost effective than full commercial systems that cost upwards of $30K, the FFD presented here offers a significant cost-savings given the estimated cost of a few dollars per unit plus the cost of a 96 well plate.

In conclusion, the FFD presented here overcomes a variety of drawbacks that are associated with currently available models [287]. This FFD is highly versatile in its functionality and cost substantially less. Also, the device delivers physiologically relevant fluid flow conditions to cells in monolayer culture. The device elicits biological responses in osteoblast-like cells similar to what is reported in the field [79,284,285]. Overall, this device provides an improved method for studying the response of not only bone cells, but also any mechano-responsive cell type *in vitro* and will help advance the study of mechanotransduction.

Chapter 4: Osteocyte response to fluid shear stress is regulated by detyrosinated microtubules dependent cytoskeletal stiffness

Introduction

Bone dynamically remodels to adapt to mechanical loads in order to maintain its structural integrity. Bone-embedded osteocytes, residing in the fluid filled lacunar-canalicular system, are central to skeletal mechano-responsiveness[17]. In response to mechanical load, osteocytes experience fluid shear stress (FSS), which triggers Ca^{2+}, extracellular ATP, nitric oxide, and PGE_2 signals[57,288]and orchestrate bone remodeling through effector molecules, like sclerostin, RANKL and osteoprotegerin [17,57,288]. These effectors act on bone forming osteoblasts and bone resorbing osteoclasts to add, remove and replace bone to accommodate mechanical demands. Sclerostin (gene name: *SOST*) is an osteocyte-specific secreted glycoprotein that suppresses bone formation by antagonizing canonical Wnt/β-catenin signaling, reducing osteoblast differentiation, and bone formation[128,289]. In a fundamentally important response to mechanical load, osteocytes reduce sclerostin expression, leading to "de-repression" of osteoblastogenesis and stimulation of de novo bone formation [138,290].

In humans, *SOST* deficiency leads to the high bone mass disorders sclerosteosis and van Buchem disease [120,121], and genetic ablation of *SOST* in mice results in a profound increase in bone mass [119]. Despite evidence that therapeutically targeting sclerostin is extraordinarily effective at improving bone quality in animal models and in humans [291,292], the mechanotransduction pathways linking FSS to the downregulation of sclerostin remain undefined. Similarly, despite the mechano-responsive nature of osteocytes, the identity of the "mechano-sensor" is controversial. Furthermore, while

integrin-associated mechanosomes, osteocyte cell processes, primary cilia and connexin43 hemichannels have been implicated as mechano-sensors and in mechano-activated Ca^{2+} influx in bone cells [69,71,293-296], they have not been mechanistically linked to sclerostin downregulation.

The cytoskeleton, composed of microtubules (MT), actin and intermediate filaments, is a dynamic structure that forms an interconnected three-dimensional framework of molecular struts and cables within the cell [297]. A growing body of evidence indicates that the cytoskeleton is critical for the cellular response to the mechanical environment, as it integrates and transduces mechanical energy to mechano-sensitive proteins that generate biological signals in a broad range of cell types [228,298]. MTs, composed of polymerized α-and β-tubulin dimers, serve as critical struts that resist compressive forces on the cell [297]. The MT network is a dynamic structure whose density and stability is regulated by post-translational modifications (e.g., detyrosination, acetylation and phosphorylation) and microtubule associated proteins (MAPs) that affect the equilibrium between MT filament growth, disassembly, and association with other cytoskeletal elements [164,299]. When the α-tubulin subunit of MTs is detyrosinated generating Glu-tubulin, this subset of modified MTs forms crosslinks with actin microfilaments and intermediate filaments, stabilizing and stiffening the cytoskeleton as a whole [174,300,301].

In this chapter, we demonstrate a microtubule (MT)-dependent mechanotransduction pathway linking FSS to sclerostin downregulation in osteocytes. Specifically, our data reveal that the MT network defines the mechano-sensitivity of osteocytes to FSS. The subsequent Ca^{2+} influx drives sclerostin downregulation.

Additionally, we show that a subset of post-translationally modified MTs, and more specifically Glu-tubulin, tune cytoskeletal stiffness, which defines the mechano-sensitivity of osteocytes to FSS, leading to regulation of sclerostin bioavailability.

Results

Ocy454 cells respond to FSS with a rapid increase in intracellular Ca^{2+} that is required for the mechanically-induced downregulation of sclerostin.

Unlike some of the commonly used osteocyte cell lines, the recently developed Ocy454 osteocyte line, derived from the Immortomouse, reliably produce detectable sclerostin protein and are sensitive to mechanical stimuli [115]. In Ocy454 cells loaded with the Ca^{2+} indicator dye Fluo-4AM, FSS at 4 dynes/cm^2 elicited a rapid, transient increase in intracellular [Ca^{2+}] in ~84% of cells (Figure 12A,B), resulting in a concomitant 3-fold decrease in sclerostin protein observed within 5 minutes post-FSS (Figure 12 C). This FSS-induced downregulation of sclerostin protein was inhibited by blocking Ca^{2+} signaling, by loading the cells with BAPTA AM and removing Ca^{2+} from the fluid flow buffer (Figure 12C), demonstrating that Ca^{2+} is required for the downregulation of sclerostin.

Microtubules are present in the putative mechano-sensitive cell structures of Ocy454 cells.

The cytoskeleton, comprised of actin, MT and intermediate filament networks, is a dynamic structural and signaling scaffold within all cells. While the cytoskeleton has a multiplicity of cellular functions, its ability to transmit mechanical forces to proteins and enzymes that generate biological signals make it essential for mechanotransduction. In other cell types, MTs have been implicated in mechanotransduction-elicited Ca^{2+}

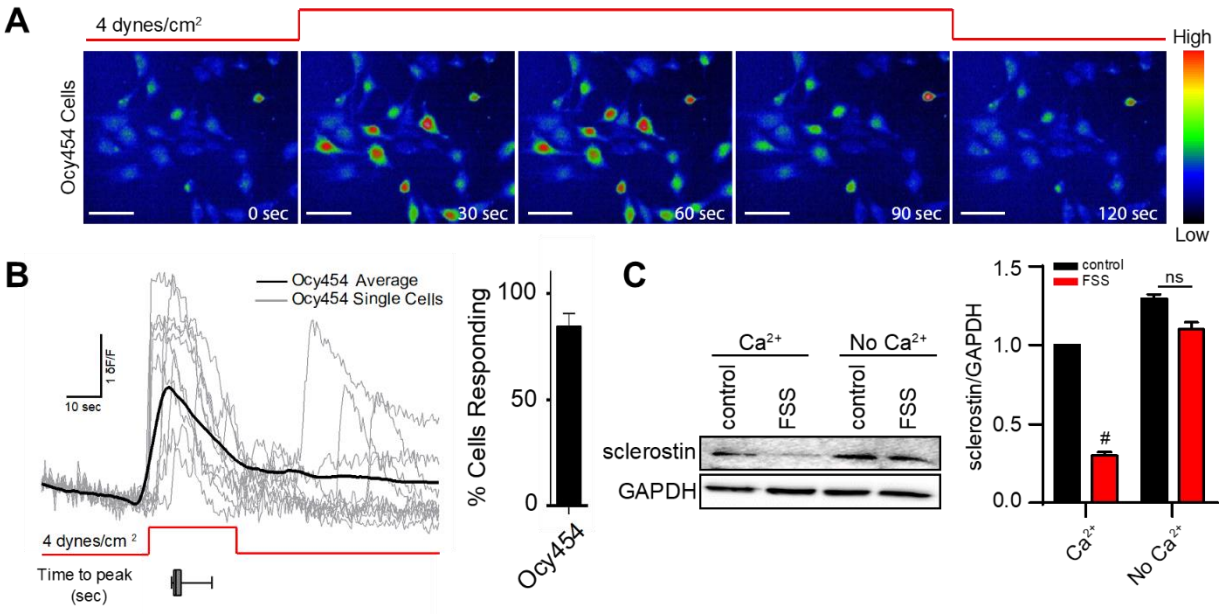

Figure 12. FSS induces a rapid Ca^{2+} response in Ocy454 cells that is required for sclerostin downregulation.

(**A**) Representative images of Ocy454 cells loaded with Fluo-4 Ca^{2+} indicator dye imaged in real-time during exposure to 4 dynes/cm^2 FSS. Pseudocolored images are shown. n=5 independent experiments. Scale bar, 100 μm. (**B**) FSS-induced Ca^{2+} response in Ocy454 cells exposed to 4 dynes/cm^2 FSS. The calcium trace indicates Fluo-4 fluorescence changes over time. The average calcium trace of all cells is shown in a bold line. Representative individual cell Ca^{2+} traces are shown in gray. % Cells Responding indicates number of cells which elicit more than 25% increase in fluorescence (mean ± s.e.m.). (**C**) Untreated Ocy454 cells and BAPTA-AM ester loaded Ocy454 cells were subjected to 4 dynes/cm^2 FSS with Ca^{2+} containing or Ca^{2+} free flow buffer, respectively. Immunoblotting was performed for sclerostin (n=3 independent experiments). GAPDH served as a loading control. Densitometric quantitation of the sclerostin to GAPDH ratio is shown. Statistical significance determined using one-way ANOVA with Dunnet's post hoc test. # indicates $p < .0001$ versus control, ns indicates not statistically significant.

signaling [302-304]. In bone cells, an intact MT network is required for mechano-sensation by osteoblasts or osteocytes in culture [240,305-307], and the MT network of osteocytes remodels and reorients itself in response to FSS [72,307,308]. Additionally, MTs are an important component of the primary cilia, which has been proposed as a mechano-sensor in osteocytes [71,73]. Another putative mechano-sensitive component is the long cellular process, extending from the cell body of the osteocyte, which is extraordinarily sensitive to FSS application [69]. Immunofluorescent labeling of Ocy454 cells revealed significant MT structure within the cell processes and primary cilia of Ocy454 cells (Figure 13A). Similarly, *ex vivo* murine femurs labeled with SiR-tubulin, a live cell MT label, revealed distinct fluorescence within the osteocyte cell processes, indicating the presence of MTs within the proposed mechano-sensitive structures of osteocytes (Figure 13B).

Microtubules are required for the osteocyte response to FSS.

The MT network is dynamically unstable with MT-end binding proteins and post-translational modifications promoting MT filament disassembly or growth. Previous reports in osteoblasts/osteocytes showed that colchicine, a drug that binds tubulin and promotes MT depolymerization, inhibited ERK signaling, cell proliferation, and altered osteoblast gene expression (osteopontin, collagen and matrix metalloproteinases) [240,305-307]. Consistent with these reports, we observed that reduction of the MT network density with colchicine treatment (2μM, 20 min) of Ocy454 cells reduced responses to mechanical cues. In response to either 4 or 16 dynes/cm^2 of FSS, colchicine treatment significantly decreased the number of cells responding (*i.e.*, decreased mechano-sensitivity), while also reducing the magnitude (peak $\Delta F/F$) of the Ca^{2+} response (*i.e.*,

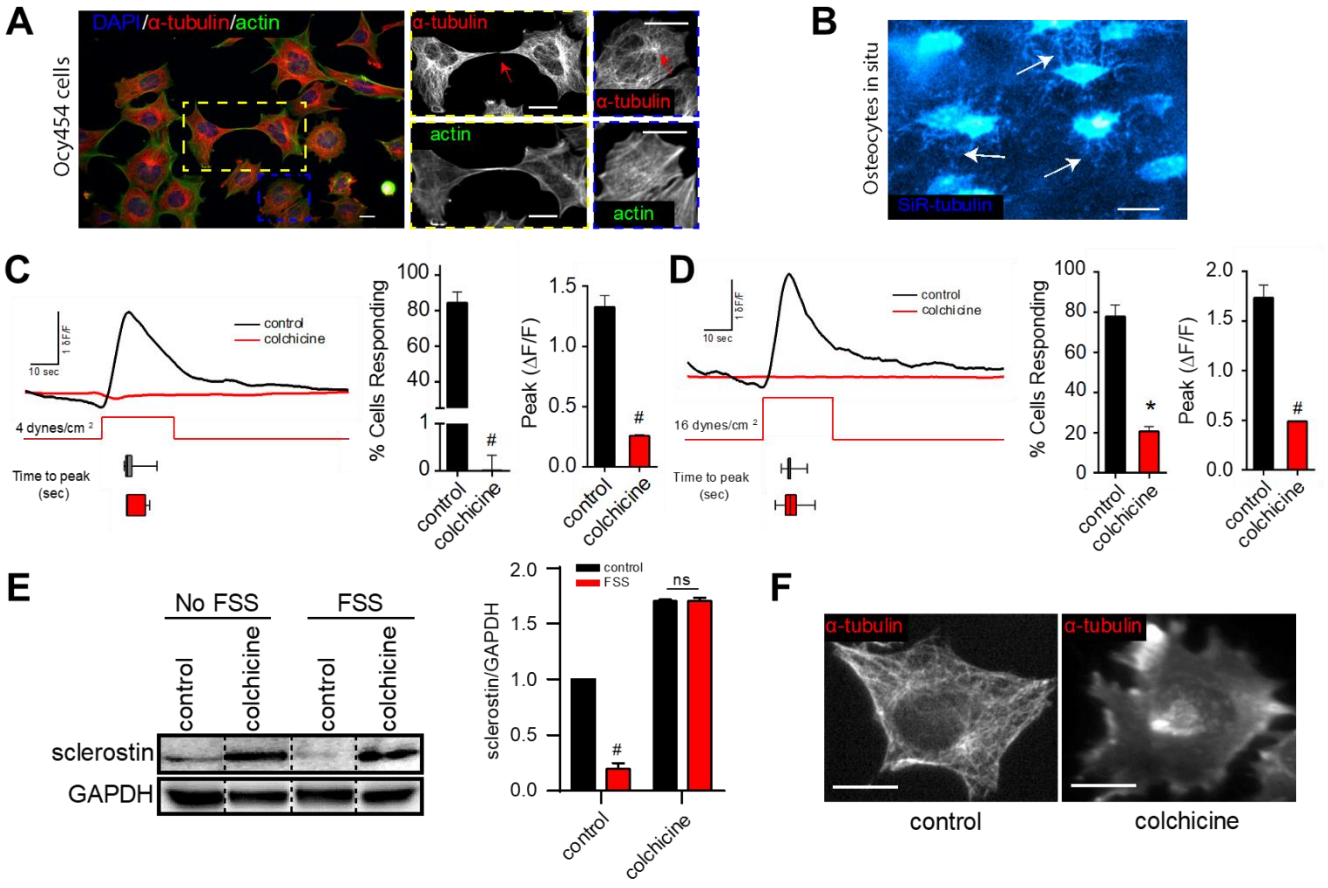

Figure 13. Microtubules are present in the mechanically sensitive areas of osteocytes *in vitro* and *in situ*, and an intact MT network is required for FSS-induced Ca^{2+} influx and sclerostin downregulation.

(**A**) Ocy454 cells were fixed and stained for α-tubulin, phalloidin (actin), and DAPI (nuclei). Insets depict location of α-tubulin in osteocyte cell process and primary cilia, indicated by red arrows. Scale bar, 10 μm. (**B**) Murine femurs stained with SiR-tubulin imaged by confocal microscopy. White arrows indicate the presence of MTs in the osteocyte cell processes *in situ*. Scale bar, 20 μm. (**C**) FSS-induced Ca^{2+} response of Fluo-4 loaded Ocy454 cells treated with colchicine and subjected to 4 dynes/cm^2 FSS. The calcium trace (left) indicates the average Fluo-4 fluorescence changes over time, % Cells Responding (middle) indicates number of cells which elicit more than 25% increase fluorescence, and Peak (ΔF/F) indicates peak magnitude of Ca^{2+} response in those cells that responded (right). Ca^{2+} traces are aggregated data from >200 cells imaged in n=3 independent experiments across all conditions. (**D**) FSS-induced Ca^{2+} response of Fluo-4 loaded Ocy454 cells treated with colchicine and subjected to 16 dynes/cm^2 FSS. Ca^{2+} traces are aggregated data from >200 cells imaged in n=3 independent experiments. (**E**) Ocy454 cells treated with colchicine were subjected to 4 dynes/cm^2 FSS followed by immunoblotting for sclerostin. GAPDH served as a loading control. Sclerostin to GAPDH ratio is indicated (n=3 independent experiments). The image is from a single exposure of a contiguous membrane. The vertical dotted line indicates the removal of irrelevant lanes. (**F**) Immunostaining for α-tubulin in control and colchicine treated Ocy454 cells. Scale bar, 10 μm. Graphs depict mean ± sem. * indicates $p<0.001$ versus control; # indicates $p<0.0001$ versus control by student's unpaired two tailed *t*-test or one-way ANOVA with Dunnet's post hoc test. ns indicates not statistically significant.

decreased mechano-responsiveness) in the responsive cells (Figure 13C,D). Likewise, MT network disruption with colchicine eliminated the FSS-induced decrease in sclerostin protein (Figure 13E). Immunofluorescent labeling validated the disruption of MTs following colchicine treatment (Figure 13F). These data are the first to demonstrate the MT network is required for mechanotransduction-elicited Ca^{2+} influx and sclerostin downregulation in osteocytes.

Microtubule stabilization alters the set point for FSS-induced Ca^{2+} influx.

Having identified the MT network as essential for osteocyte mechano-responsiveness, we sought to determine the broad impact of the MT network on regulating osteocyte mechanotransduction. Taxol is a drug that binds to and stabilizes the MT filament against depolymerization, thereby increasing MT network density. Real time Ca^{2+} imaging of Ocy454 cells treated with Taxol (1μM, 2 h) showed a significant decrease in the percentage of cells responding to 4 dynes/cm^2 FSS, as well as a decrease in the magnitude (peak ΔF/F) of their response (Figure 14A). However, unlike the effect of colchicine-mediated MT depolymerization, the Taxol-induced suppression of both mechano-responsiveness and mechano-sensitivity was restored at 16 dynes/cm^2 FSS (Figure 14B). Consistent with the impact of increased MT density on Ca^{2+} signaling, Taxol treated Ocy454 cells subjected to 4 dynes/cm^2 FSS had a blunted FSS-induced downregulation of sclerostin protein, which was overcome at 16 dynes/cm^2 of FSS (Figure 14C). Immunofluorescent labeling of the MT network validated the increase in MT density following Taxol treatment (Figure 14D). These results imply that the density

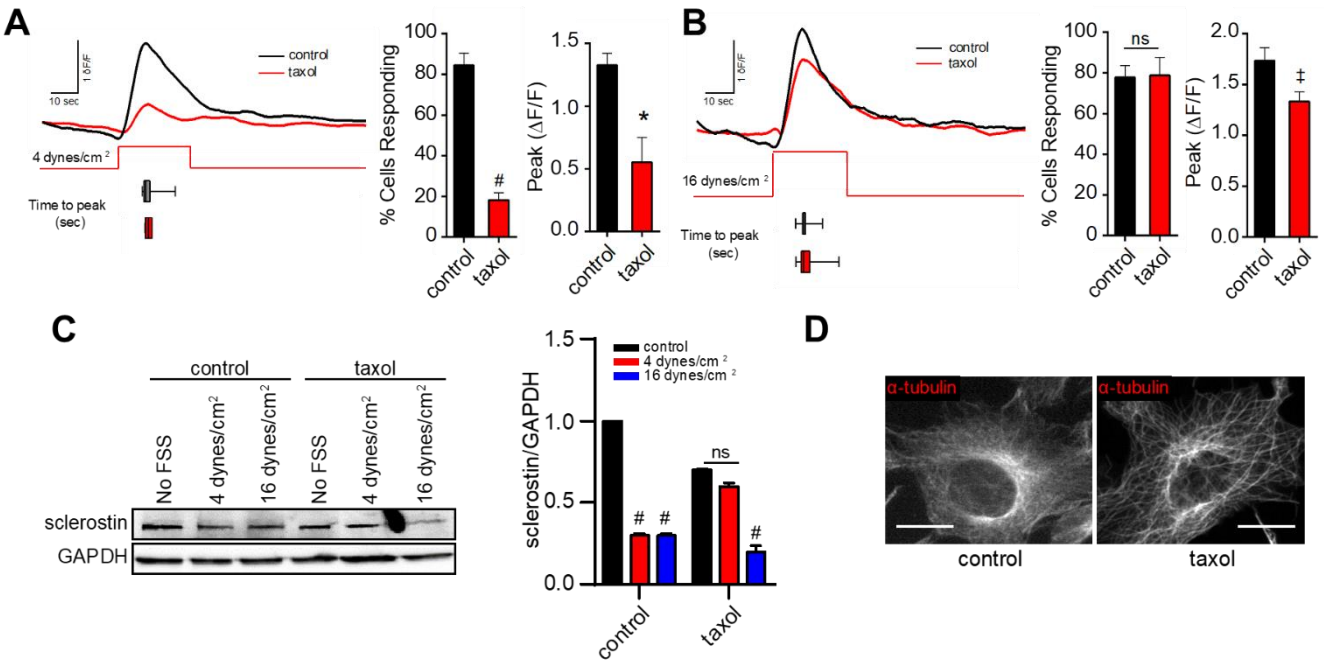

Figure14. Taxol treatment blunts the FSS-induced Ca^{2+} response and sclerostin downregulation but is overcome by increased FSS.

(**A**) FSS-induced Ca^{2+} response of Fluo-4 loaded Ocy454 cells treated with Taxol and subjected to 4 dynes/cm^2 FSS. The calcium trace (left) indicates the average Fluo-4 fluorescence changes over time, % Cells Responding (middle) indicates number of cells which elicit more than 25% increase fluorescence, and Peak (ΔF/F) indicates peak magnitude of Ca^{2+} response in those cells that responded (right). Ca^{2+} traces are aggregated data from >200 cells imaged in n=3 independent experiments. (**B**) FSS-induced Ca^{2+} response of Fluo-4 loaded Ocy454 cells treated with Taxol and subjected to 16 dynes/cm^2 FSS. All Ca^{2+} traces are aggregated data from >200 cells imaged in n=3 independent experiments across all conditions. (**C**) Control or Taxol treated Ocy454 cells were subjected to FSS as indicated followed by immunoblotting for sclerostin. GAPDH served as a loading control. Sclerostin to GAPDH ratio is indicated (n=3 independent experiments). (**D**) Immunostaining for α-tubulin in control and Taxol treated Ocy454 cells. Scale bar, 10 μm. Graphs depict mean ± sem. ‡ indicates $p<0.05$ versus control; * indicates $p<0.001$ versus control; # indicates $p<0.0001$ versus control by student's unpaired two tailed *t*-test or one-way ANOVA with Dunnet's post hoc test. ns indicates not statistically significant.

and/or stability of the MT network impacts the threshold for FSS-induced activation of Ca^{2+} influx and sclerostin downregulation.

The abundance of Glu-tubulin in the MT network regulates the mechano-sensitivity of Ocy454 cells to FSS.

Taxol induced MT stabilization is associated with an increase in the fraction of Glu-modified tubulin in the MT filament. Glu-tubulin arises from detyrosination, the enzymatic cleavage of an COOH-terminal tyrosine residue of α-tubulin by tubulin tyrosine carboxypeptidase (TTCP; identity unknown) leaving a glutamate [309]. This reaction can be reversed by the ligation of tyrosine back to the glutamate by a tubulin tyrosine ligase (TTL). Given recent work implicating Glu-tubulin as a regulator of MT-dependent mechanotransduction in cardiac and skeletal muscle [141], we examined its impact on osteocyte mechanotransduction.

To profile the presence of Glu-tubulin in the osteocyte MT network, Ocy454 cells and murine femurs were examined by western blotting and immunofluorescence. Glu-tubulin was observed in the osteocyte cell process and primary cilia in Ocy454 cells (Figure 15A) and in the cell processes of osteocytes in formaldehyde fixed paraffin embedded sections of murine cortical bone (Figure 15B). As observed in other tissues, Taxol treatment of Ocy454 cells *in vitro* or murine cortical bone *ex vivo* markedly increased the level of Glu-tubulin (Figure 15C,D).

The abundance of Glu-tubulin within the MT network can be effectively reduced by parthenolide (PTL), a sesquiterpene lactone that inhibits the activity of the TTCP enzyme responsible for detyrosination [310]. In striated muscle, the PTL-induced reduction of Glu-tubulin inhibited mechano-signaling [141], suggesting that the abundance of Glu-

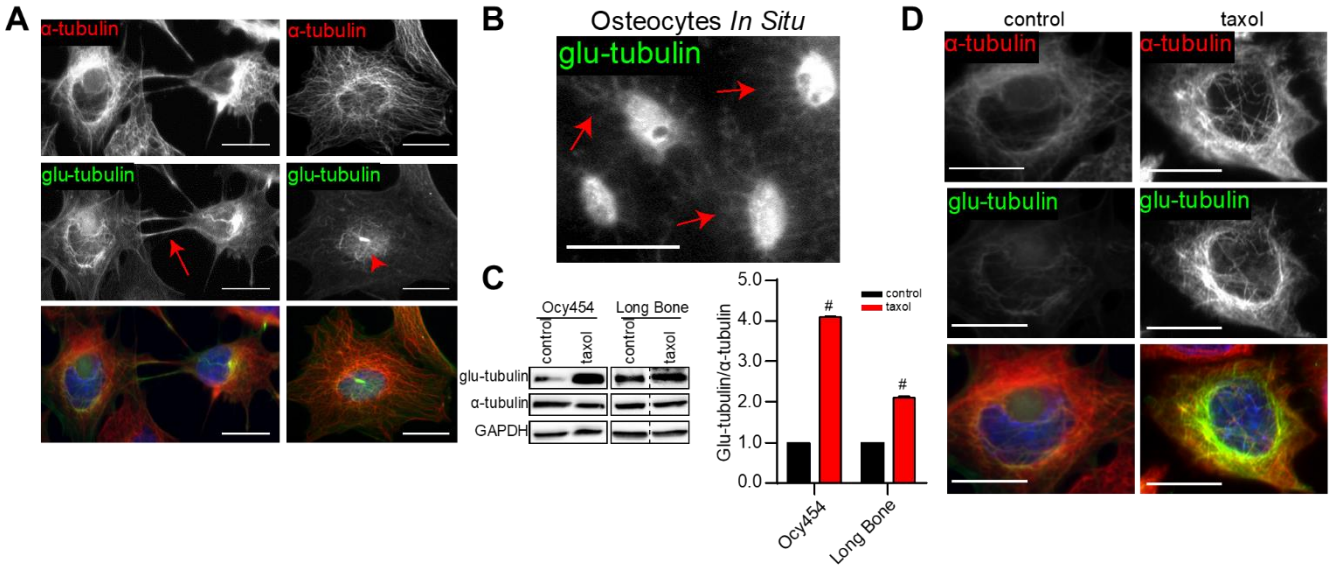

Figure 15. Glu-tubulin is expressed within mechanically sensitive areas of osteocytes and increased by treatment with Taxol.

(**A**) Ocy454 cells were fixed and immunostained for α-tubulin (red) and Glu-tubulin (green). DAPI stained nuclei are shown in blue. Osteocyte cell process and primary cilia are indicated by the red arrow and red arrowhead, respectively. Scale bar, 20 µm. (**B**) Murine long bone sections were immunostained for Glu-tubulin. Osteocyte cell processes are indicated by red arrows. Scale bar, 50 µm. (**C**) Ocy454 cells and *ex vivo* murine long bone were treated with Taxol followed by immunoblotting for indicated proteins. GAPDH served as a loading control. Glu-tubulin to α-tubulin ratios are indicated (n=3 independent experiments). The image is from a single exposure of a contiguous membrane. The vertical dotted line indicates the removal of irrelevant lanes. Statistical significance was determined using a student's unpaired two tailed *t*-test. # indicates p <.0001. (**D**) Immunostaining for α-tubulin (red) and Glu-tubulin (green) in control and Taxol treated Ocy454 cells. DAPI stained nuclei are shown in blue. Scale bar, 10µm.

tubulin was the dominant regulator of mechano-activation. Real time Ca^{2+} imaging of Ocy454 cells treated with PTL (25 μM, 2 h) and exposed to FSS showed a significant reduction in mechano-sensitivity (% cells responding) and mechano-responsiveness (magnitude of the cellular response, peak ΔF/F) at both 4 and 16 dynes/cm^2 of FSS (Figure 16A,B). Additionally, PTL treatment blunted the FSS-induced downregulation of sclerostin at both 4 and 16 dynes/cm^2 of FSS (Figure 16C). Importantly, these effects of PTL on mechano-responsiveness occurred with a reduction in Glu-tubulin, yet no apparent alteration in the overall structure of the MT network (Figure 16D). These data suggest that the level Glu-tubulin plays a key role in modulating osteocyte mechanotransduction.

Given that Taxol increases both the density of the MT network and its level of Glu-tubulin, we sought to determine their respective contributions. To this end, we simultaneously treated cells with PTL and Taxol to promote an increase in MT density while eliminating the concomitant increase in Glu-tubulin. Compared to cells treated with Taxol or PTL individually, their combination restored mechano-responsiveness, as both the FSS-induced Ca^{2+} response and sclerostin downregulation at 4 dynes/cm^2 were rescued (Figure 17A,B,C). Immunofluorescence microscopy of treated Ocy454 cells confirmed that the combination of Taxol and PTL resulted in the expected Taxol-driven increase in MT density, with PTL preventing the concomitant enhancement of Glu-tubulin (Figure 17D). In total, these data strongly support that Glu-tubulin, rather than MT density, is the dominant regulator of the osteocyte response to FSS.

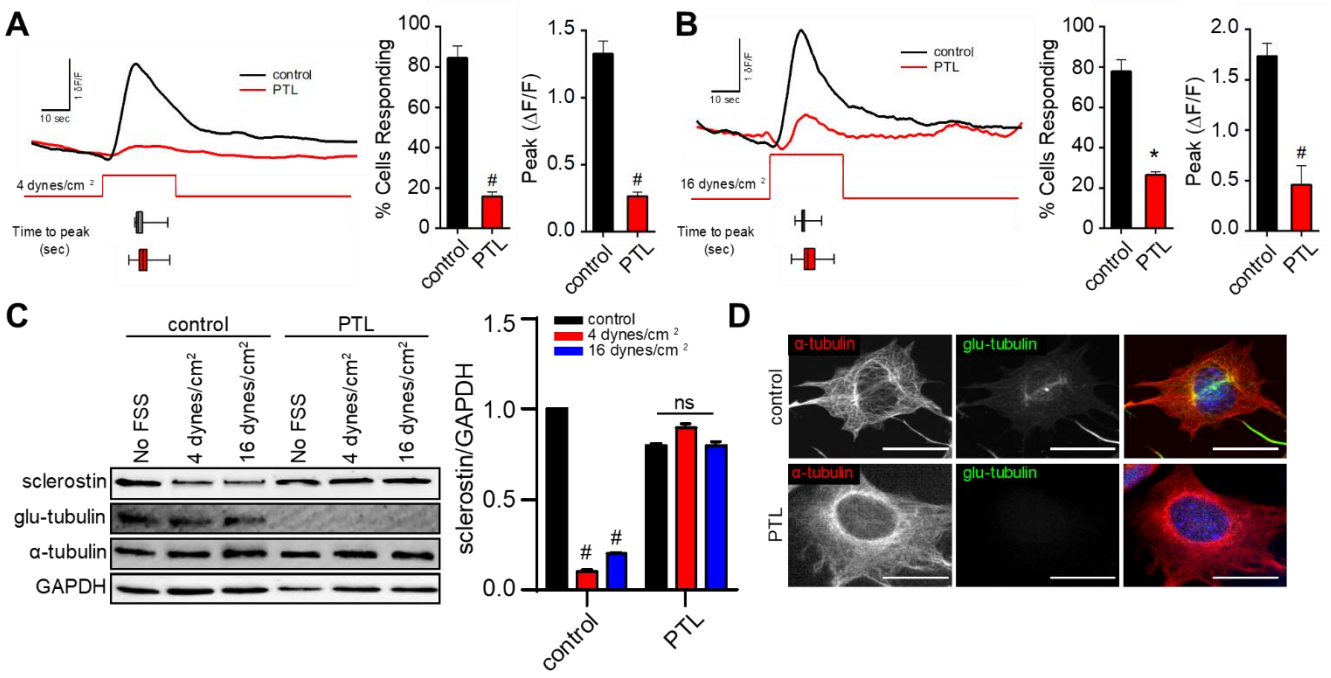

Figure 16. Loss of detyrosinated, Glu-tubulin abrogates the FSS-induced Ca^{2+} response and sclerostin downregulation.

(**A**) FSS-induced Ca^{2+} response of Fluo-4 loaded Ocy454 cells treated with parthenolide (PTL) and subjected to 4 dynes/cm^2 FSS. The calcium trace (left) indicates the average Fluo-4 fluorescence changes over time, % Cells Responding (middle) indicates number of cells which elicit more than 25% increase fluorescence, and Peak (ΔF/F) indicates peak magnitude of Ca^{2+} response in those cells that responded (right). Ca^{2+} traces are aggregated data from >200 cell imaged in n=3 independent experiments. (**B**) FSS-induced Ca^{2+} response of Fluo-4 loaded Ocy454 cells treated with PTL and subjected to 16 dynes/cm^2 FSS. Ca^{2+} traces are aggregated data from >200 cell imaged in n=3 independent experiments across all conditions. (**C**) Control or PTL treated Ocy454 cells were subjected to FSS as indicated followed by immunoblotting for indicated proteins. GAPDH served as a loading control. Sclerostin to GAPDH ratio is indicated (n=3 independent experiments). (**D**) Control Ocy454 cells or Ocy454 cells treated with PTL were fixed and immunostained for α-tubulin (red) and Glu-tubulin (green). DAPI stained nuclei are shown in blue. Scale bar, 10μm. Graphs depict mean ± sem. * indicates p<0.001 versus control; # indicates p<0.0001 versus control by student's unpaired two tailed *t*-test or one-way ANOVA with Dunnet's post hoc. ns indicates not statistically significant.

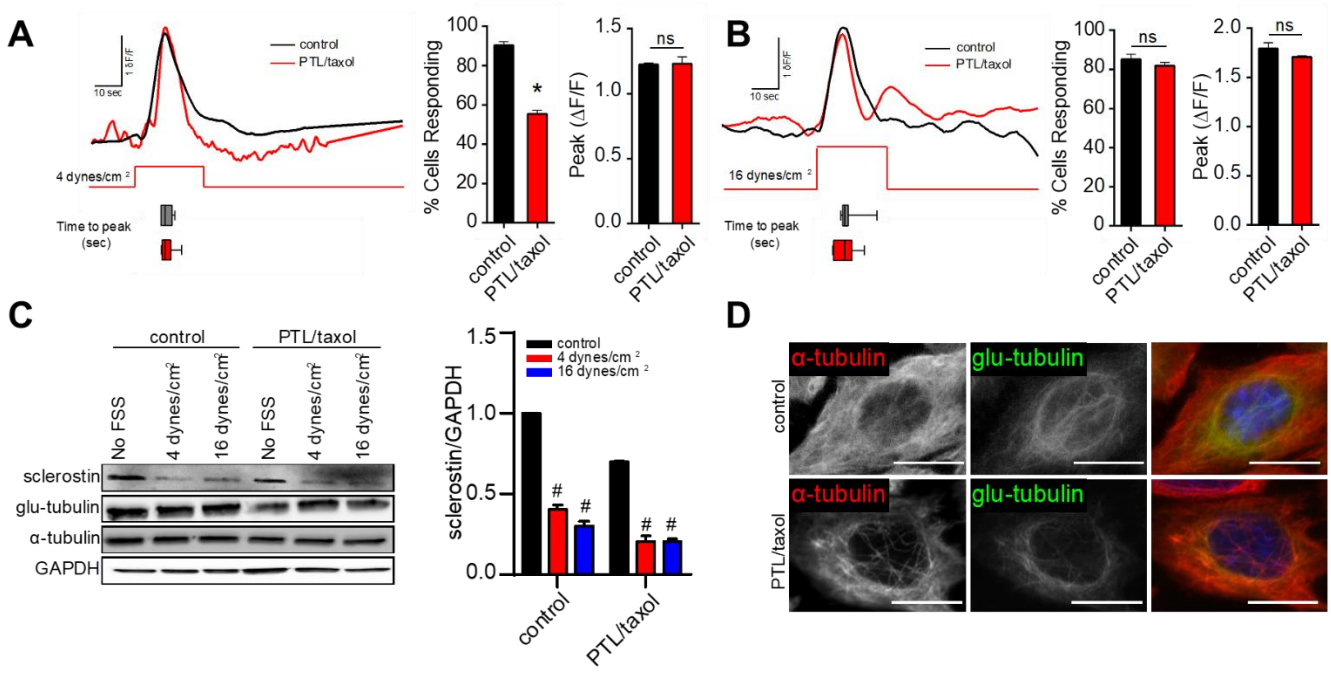

Figure 17. Combination treatment with parthenolide and Taxol restores the FSS-induced Ca^{2+} response and downregulation of sclerostin protein.

(**A**) FSS-induced Ca^{2+} response of Fluo-4 loaded Ocy454 cells treated with combination of parthenolide (PTL) and Taxol and subjected to 4 dynes/cm^2 FSS. The calcium trace (left) indicates the average Fluo-4 fluorescence changes over time, % Cells Responding (middle) indicates number of cells which elicit more than 25% increase fluorescence, and Peak (ΔF/F) indicates peak magnitude of Ca^{2+} response in those cells that responded (right). Ca^{2+} traces are aggregated data from >200 cells imaged in n=3 independent experiments. (**B**) FSS-induced Ca^{2+} response of Fluo-4 loaded Ocy454 cells treated with combination of PTL and Taxol, and subjected to 16 dynes/cm^2 FSS. Ca^{2+} traces are aggregated data from >200 cells imaged in n=3 independent experiments. (**C**) Control Ocy454 cells or Ocy454cells treated with combination of PTL and Taxol were subjected to FSS as indicated followed by immunoblotting for sclerostin. GAPDH served as a loading control. Sclerostin to GAPDH ratio is indicated (n=3 independent experiments). (**D**) Control Ocy454 cells or Ocy454 cells treated with a combination of Taxol and PTL were fixed and immunostained for α-tubulin (red) and Glu-tubulin (green). DAPI stained nuclei are shown in blue. Scale bar, 10μm. Graphs depict mean ± sem. * indicates $p<0.001$ versus control, # indicates $p<0.0001$ by student's unpaired two tailed *t*-test or one-way ANOVA with Dunnet's post hoc test. ns indicates not statistically significant.

The abundance of Glu-tubulin regulates cytoskeletal stiffness in Ocy454 cells.

Glu-tubulin promotes MT interactions with other cytoskeletal elements (e.g., actin, intermediate filaments, and MAPs), which increases the stiffness of the cytoskeleton [141,174,300,301]. Accordingly, we interrogated cytoskeletal stiffness in Ocy454 cells. Nanoindentation atomic force microscopy (AFM) revealed that Taxol treatment significantly increased the elastic modulus, reflecting an increase cytoskeletal stiffness (Figure 18A). Western blotting confirmed a marked increase in the Glu-tubulin in the Taxol treated cells (Figure 18B). In contrast, PTL treated cells showed a significant decrease in cytoskeletal stiffness and nearly undetectable levels of Glu-tubulin (Figure 18). Interestingly, the combination treatment with PTL and Taxol, which increases MT density while maintaining a modest level of Glu-tubulin, resulted in a significant increase in the elastic modulus (increased cytoskeletal stiffness) over PTL treatment alone, returning it to near control levels (Figure 18A) When examined in the context of FSS-stimulated Ca^{2+} influx and sclerostin downregulation, these AFM data support a model in which cytoskeletal stiffness, which is affected by the abundance of Glu-tubulin, defines both the mechano-sensitivity and responsiveness of osteocytes to FSS.

Discussion

Here, we report a novel mechanotransduction pathway in osteocytes that links FSS to the activation of Ca^{2+} influx that drives the mechanically-induced downregulation of sclerostin. Central to our discovery is that the MT network, whose level of Glu-tubulin defines the cytoskeletal stiffness, determines the mechano-sensitivity of osteocytes to FSS.

Our data show that MTs are, at minimum, required for mechano-signaling, consistent with reports on other mechano-signaling events in bone [240,305-307]. We build

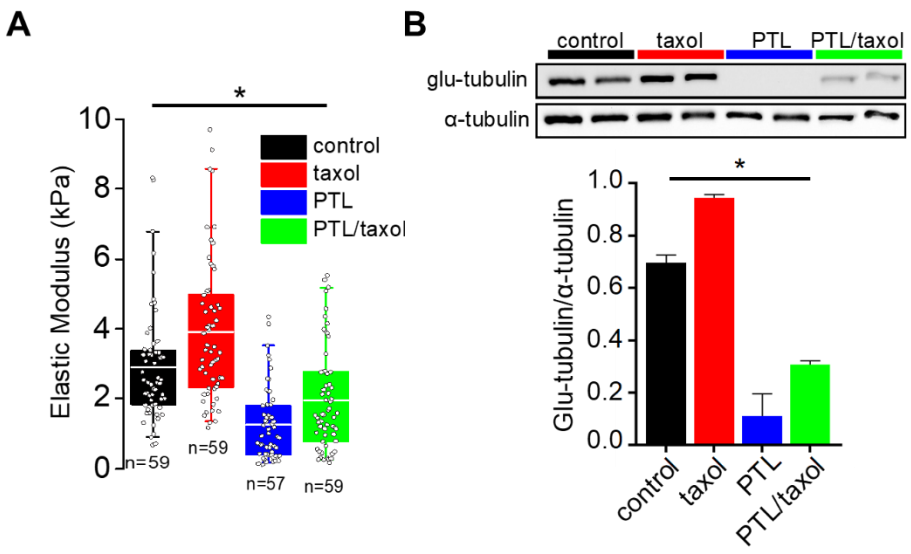

Figure 18. Alterations in the MT network modify cytoskeletal stiffness of Ocy454 cells.
(**A**) Ocy454 cells treated with Taxol, parthenolide (PTL), and a combination of PTL and Taxol were subjected to atomic force microscopy nano-indentation. Statistical significance was determined using one-way ANOVA with Holm-Sidak's multiple comparison test. Box edges denote 25th and 75th percentiles, whiskers denote 10th and 90th percentiles, and white line indicates mean. Data shown are aggregate of 3 independent experiments with number of cells/group indicated. (**B**) Protein extracts from control Ocy454 cells or Ocy454 cells treated with PTL, Taxol or combination of PTL and Taxol were probed for Glu-tubulin and α-tubulin. The Glu-tubulin to α-tubulin ratio is graphed below, indicating the mean ± sem. Statistical significance was determined using one-way ANOVA with Holm-Sidak's multiple comparison test. * denotes statistical significance between all groups. Exact p values for each comparison are shown in Table 2.

Figure 18A

Comparison	P value
control vs. taxol	P=0.0019
control vs. PTL	P<0.0001
control vs. PTL/taxol	P=0.0026
taxol vs. PTL	P<0.0001
taxol vs. PTL/taxol	P<0.0001
PTL vs. PTL/taxol	P=0.0189

Figure 18B

Comparison	P value
control vs. taxol	P=0.0466
control vs. PTL	P=0.0014
control vs. PTL/taxol	P=0.0113
taxol vs. PTL	P=0.0004
taxol vs. PTL/taxol	P=0.0017
PTL vs. PTL/taxol	P=0.0320

Table 2: Exact p-values from Figure 18

upon this fundamental concept by demonstrating that the MT network, and specifically its level of Glu-tubulin, are critical regulators of cytoskeletal stiffness, which tunes the mechano-responsive range at which osteocytes are activated by FSS. We reveal that a targeted reduction in Glu-tubulin levels (*e.g.*, PTL treated) decreases MT-dependent cytoskeletal stiffness, impairing the osteocytes ability to sense and transduce mechanical cues . In contrast, driving up the abundance of Glu-tubulin increases cytoskeletal stiffness, which increases the level of FSS needed to activate the mechanotransduction pathway. Thus, the cytoskeleton becomes a dynamic integrator of mechanical cues, affecting the mechanical set point at which an osteocyte can respond to a given mechanical load. Our discovery that MTs are central to this mechanotransduction pathway may unify several models of osteocyte mechano-sensing. The primary cilia hypothesis [71,73,293], the integrin-based mechanosome [69,295] and perhaps even Cx43 hemichannels opening in response to mechanical activation of integrins [294] are all based on structures linked to the MT network.

Our data, not only align with the reports that implicate MTs in mechanotransduction, they also interdigitate well with the observations that the MT network of osteocytes remodels and reorients itself in response to FSS [72,307,308]. It is reasonable to speculate that the FSS-dependent remodeling of MTs is itself a mechano-adaptation event that adjusts the homeostatic set point for mechanotransduction. As mentioned above, our data also create a unifying basis for how various known mechano-sensitive elements, (e.g., primary cilia, cell processes, integrin-mediated mechanosomes, and connexin43 hemichannels) may integrate mechanical signals into biological

responses via the cytoskeleton. Further, our data are the first to mechanistically link the mechano-activated Ca^{2+} influx to sclerostin downregulation.

In summary, we have defined the MT-dependent mechanotransduction pathway linking FSS Ca^{2+} influx signals that downregulate sclerostin protein in osteocytes. Given the fundamental nature of osteocyte mechano-responsiveness to bone turnover throughout the life span, these new mechanistic insights may provide a new perspective for understanding diseases and conditions that manifest through altered skeletal structure and properties. Furthermore, given the impact of the MT network on the fundamental regulation of Ca^{2+} signaling and sclerostin production in osteocytes, we propose the MT network as a novel target for manipulating the osteocyte response to mechanical cues for therapeutic interventions in bone.

Chapter 5: TRPV4 as a major contributor to osteocyte fluid shear stress induced calcium influx

Introduction

It is widely accepted in the field that the very first response mediated by mechanical stimuli is the increase in intracellular calcium[68]. It has been shown that voltage operated potassium channels are expressed in osteocytes and it has been suggested that alterations in potassium currents could be involved in the earliest initiation of the mechanical response in osteocytes[81]. However, there is relatively high expression of T-type calcium channels in osteocytes. Thus, early reports suggested a role for T-type calcium channels including CaV3.1 and CaV3.2. It has been postulated that these T-type calcium channels may be responsible for the unique kinetics of the calcium signaling in osteocytes[311]. However more recently it has become clear that while T-type channels may in fact be involved, they only contribute to a portion of the response.

Immediately following the rapid change in calcium concentration, NO, adenosine triphosphate (ATP), and prostaglandin are released by the osteocyte[57]. There is evidence that suggests this ATP release occurs through connexin 43 hemichannels [84]. This release of ATP has been shown to efficiently activate the purinergic nucleotide receptor (P2X7), an ATP-gated ion channel, in osteocytes[92]. It has recently been suggested that this is the main mechanism of osteocyte calcium influx in response to fluid flow shear stress. However, deletion of P2X7 in mice only resulted in about a 70% reduction in the anabolic response to mechanical loading, suggesting that while a major contributor to the osteocyte mechanically induced calcium influx, it is not the only contributor[92,94]. Many groups have explored the role of stretch activated calcium channels as a potential source

of calcium influx in response to mechanical stimuli in osteocytes as well. One group has made a case for transient receptor potential vanilloid 4 (TRPV4) as a major contributor to calcium influx[73]. However, it was shown to only play a role in the primary cilia and other studies have suggested that the primary cilium is not involved in the initial calcium increase observed in osteocytes[73].

Here we provide evidence for a more important role for TRPV4 as previously thought. We show that not only is TRPV4 a major contributor to FSS induced Ca^{2+} influx in osteocytes, but that the generation of ROS is upstream of this Ca^{2+} response. Further, we show that FSS in osteocytes activates the mechano-sensitive ROS generating enzyme NADPH Oxidase 2 (Nox2).

Results

Ocy454 FSS-induced calcium influx is mediated by TRPV4.

While pathways for Ca^{2+} entry have been described in osteocytes [82,94,311], we interrogated the calcium channel(s) responsible for the MT-dependent, FSS-induced Ca^{2+} influx that drive sclerostin downregulation. By qRT-PCR, we determined the expression profile of various Ca^{2+} channels implicated in osteocyte Ca^{2+} signaling. Among the most abundantly expressed channels in Ocy454 cells was TRPV4 (Figure 19); an attractive candidate given recent evidence that this channel may be directly modulated by MT-dependent mechanotransduction in other cell types [312-314]. Consistent with the abundance of TRPV4 transcript, immunofluorescence staining of Ocy454 cells and paraffin embedded murine cortical bone sections showed the presence of TRPV4 in osteocytes and western blot analysis of Ocy454 cells and murine long bone extracts confirmed the presence of TRPV4 protein (Figure 20A,B).

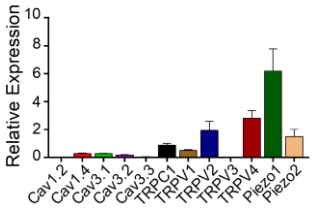

Figure 19. TRPV4 is an abundantly expressed Ca^{2+} channel in Ocy454 cells.
Ca^{2+} channel expression was analyzed in Ocy454 cells by qRT-PCR.

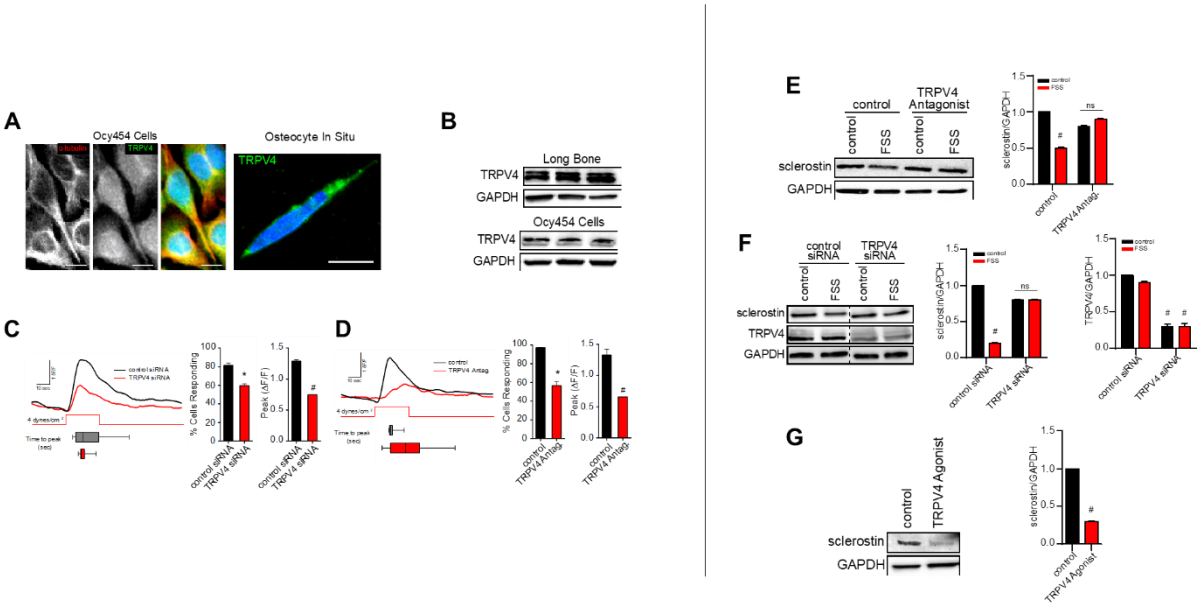

Figure 20. TRPV4 is a major contributor to osteocyte FSS-induced Ca^{2+} response and is necessary and sufficient for the FSS-induced downregulation of sclerostin.
(**A**) Ocy454 cells (left) and sections of murine long bones (right) were immunostained with TRPV4, showing positive labeling of osteocytes. Scale bar, 100µm. (**B**) Immunoblotting was performed on Ocy454 whole cell lysates and murine long bone extracts for TRPV4. GAPDH served as a loading control. (**C**) FSS-induced Ca^{2+} response of Fluo-4 loaded Ocy454 cells in the presence or absence (control) of TRPV4 antagonist (GSK-2193874) and subjected to 4 dynes/cm^2 FSS. The calcium trace (left) indicates the average Fluo-4 fluorescence changes over time, % Cells Responding (middle) indicates number of cells which elicit more than 25% increase fluorescence, and Peak (ΔF/F) indicates peak magnitude of Ca^{2+} response in those cells that responded (right). Ca^{2+} are aggregated data from >200 cells imaged in n=3 independent experiments. (**D**) FSS-induced Ca^{2+} response of Fluo-4 loaded Ocy454 cells transfected with control or TRPV4 siRNA and subjected to 4 dynes/cm^2 FSS. Ca^{2+} are aggregated data from >200 cells imaged in n=3 independent experiments. (**E**) Ocy454 cells treated with or without (control) TRPV4 antagonist (GSK-2193874) were subjected to 4 dynes/cm^2 FSS followed by immunoblotting for sclerostin. GAPDH served as a loading control. Sclerostin to GAPDH ratio is indicated (n=3 independent experiments). (**F**) Ocy454 cells transfected with control or TRPV4 siRNA were subjected to 4 dynes/cm^2 FSS followed by immunoblotting for sclerostin and TRPV4. GAPDH served as a loading control. Sclerostin to GAPDH and TRPV4 to GAPDH ratios are indicated (n=3 independent experiments). The image is from a single exposure of a contiguous membrane. The vertical dotted line indicates the removal of irrelevant lanes. (**G**) Ocy454 cells were treated with or without (control) TRPV4 agonist (GSK-1016790A) followed by immunoblotting for sclerostin. GAPDH served as a loading control. Sclerostin to GAPDH ratio is indicated (n=3 independent experiments). Graphs depict mean ± sem. * indicates $p<0.001$ versus control; # indicates $p<0.0001$ versus control by student's unpaired two tailed *t*-test or one-way ANOVA with Dunnet's post hoc test. ns indicates not statistically significant.

To determine the impact of TRPV4 on FSS-triggered mechanotransduction, Ocy454 cells were treated with GSK2193874, a TRPV4 antagonist. Our data revealed a significant decrease in mechano-sensitivity (i.e., % cells responding) and mechano-responsiveness (i.e., peak Ca^{2+} response) in GSK2193874 (10μM, 15min) treated Ocy454 cells (Figure 20C). Additionally, transfection of Ocy454 cells with TRPV4 targeting siRNA (Figure 20D) yielded quantitatively similar results to the pharmacological antagonist, supporting the conclusion that TRPV4 was a major contributor to Ca^{2+} influx pathway acutely activated by FSS.

Consistent with TRPV4 as the source of FSS induced Ca^{2+} influx, Ocy454 cells treated with the TRPV4 antagonist or transfected with siRNA specific to TRPV4 showed a blunted FSS-induced downregulation of sclerostin (Figure 20E,F). Conversely, treating Ocy454 cells with a TRPV4 agonist, GSK-1016790A (10μM, 15min), recapitulated the sclerostin protein reduction, independent of FSS (Figure 20G), demonstrating that TRPV4 activation was sufficient to regulate sclerostin.

TRPV4 opens in response to FSS-induced ROS.

Reports have implicated either direct mechano-activation [312] or ROS-dependent oxidation [315,316] as mechanisms for TRPV4 activation. To assess the impact of ROS-mediated activation, Ocy454 cells were simultaneously loaded with Fluo-4 Ca^{2+} indicator and CellROX ROS indicator, and treated with H_2O_2 to induce ROS (Figure 21A). Further, Ocy454 cells loaded with these indicators were pre-treated with the TRPV4 Antagonist, and then treated with H_2O_2. Interestingly, while we observed a rapid increase in CellROX fluorescence, which was not affected by the TRPV4 Antagonist, we see a

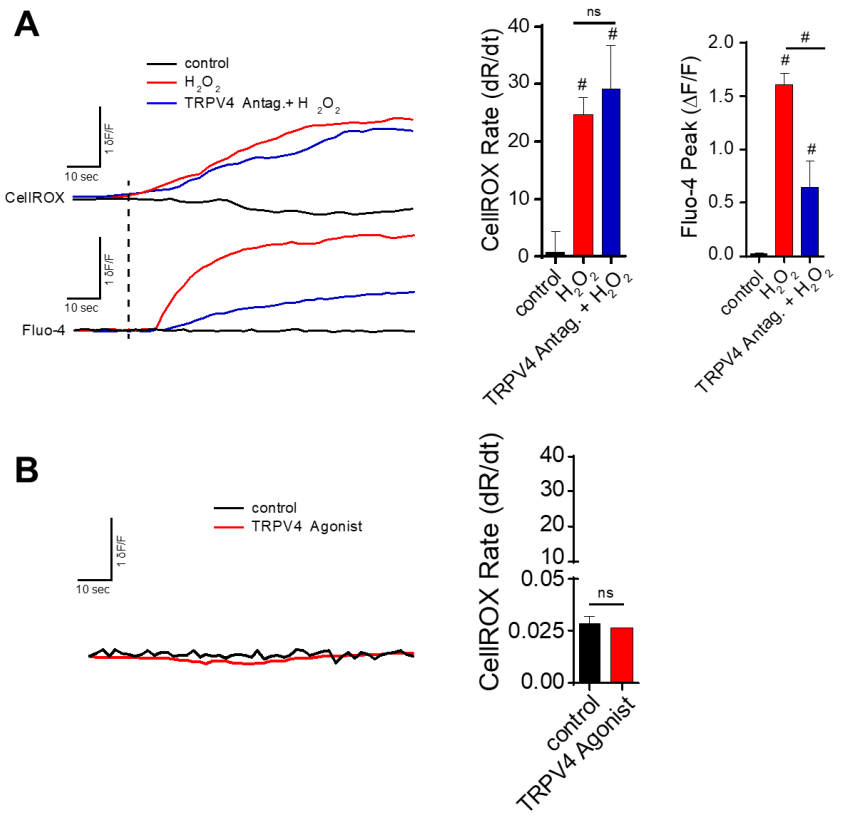

Figure 21. TRV4 is activated by the production of ROS.

(**A**) ROS and Ca^{2+} response in control Ocy454 cells and Ocy454 cells treated with H_2O_2 alone or pretreated with TRPV4 Antagonist before H_2O_2 treatment, and loaded simultaneously with CellROX ROS indicator and Fluo-4 Ca^{2+} indicator. Traces (left) indicate CellROX and Flou-4 fluorescence changes over time. Dotted line indicates H_2O_2 treatment. CellROX Rate (d*R*/d*t*) indicates the rate of change in CellROX fluorescence (middle), and the Fluo-4 Peak (ΔF/F) indicates peak magnitude of Ca^{2+} response in those cells that responded (right). All traces are aggregated data from >50 cells imaged in n=2 independent experimetns. (**B**) ROS response in Ocy454 cells treated with or without (control) TRPV4 agonist. Traces (left) indicate CellROX fluorescence changes over time, CellROX Rate (d*R*/d*t*) indicates the rate of change in CellROX fluorescence (right). Graphs depict mean ± sem. # indicates $p<0.0001$ versus control by student's unpaired two tailed *t*-test or one-way ANOVA with Dunnet's post hoc test. ns indicates not statistically significant.

significantly blunted Fluo-4 Ca^{2+} response in the TRPV4 Antagonist pre-treated cells (Figure 21A). Importantly, activation of TRPV4 with the TRPV4 Agonist, does not affect ROS production (Figure 21B).

To assess the effects of ROS on the FSS induced response of osteocytes, Ocy454 cells were treated with the ROS scavenger N-acetylcysteine (NAC; 10mM 20 min). Real-time, live cell Ca^{2+} imaging showed that NAC treatment abrogated the FSS-induced response at both 4 and 16 dynes/cm^2 (Figure 22A,B). Likewise, we observed a blunting of the FSS-induced decrease in sclerostin protein in NAC treated cells (Figure 22C). Evidence that a hydrogen peroxide (100μM, 30min) challenge to Ocy454 cells reduced sclerostin protein independent of FSS (Figure 22D) supports ROS as the signal downstream of mechano-activation.

FSS-induced ROS signaling is mediated by the mechano-sensitive ROS generating enzyme Nox2.

Nox2 is a mechano-sensitive ROS generating enzyme implicated in MT-dependent ROS signaling [141,157,248,317]. Western blot confirmed the expression of Nox2 in Ocy454 cells (Figure 23A). To evaluate the impact of Nox2 on the FSS-induced mechanical response, Ocy454 cells were treated with the Nox2 inhibitor, GP91ds-TAT (10μM, 30min). GP91ds-TAT significantly reduced the FSS-induced ROS production in Ocy454 cells. Interestingly, to further support Glu-tubulin dependent regulation of the osteocyte resposne to FSS, PTL also significantly blunted the FSS-induced ROS production in Ocy454 cells subjected to 4 dynes/cm^2 (Figure 23B). When GP91ds-TAT treated Ocy454 cells were subjected to FSS, the mechano-sensitivity (% cells responding), mechano-responsiveness (peak Ca^{2+} response), and sclerostin downregulation were attenuated

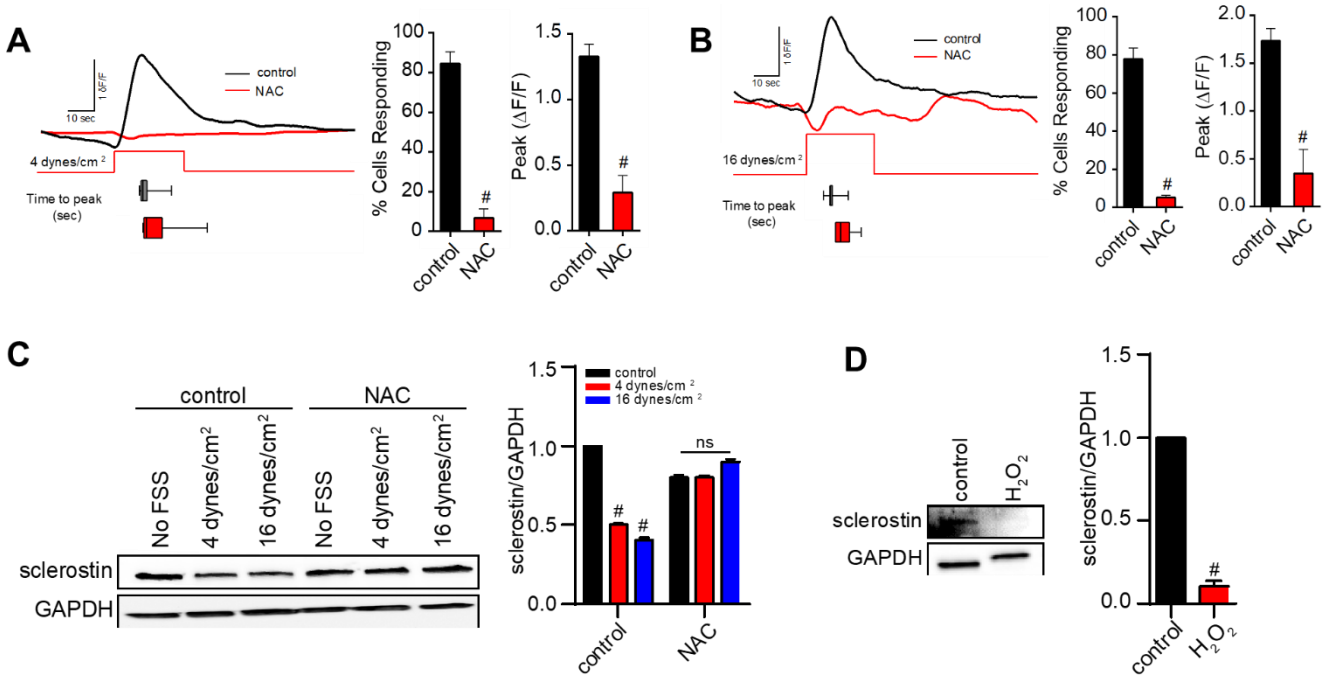

Figure 22. Blocking ROS inhibits the FSS-induced Ca^{2+} influx and sclerostin down regulation and ROS is sufficient to drive sclerostin downregulation independent of FSS.
(**A**) FSS-induced Ca^{2+} response of Fluo-4 loaded Ocy454 cells treated with α-N-acetyl cysteine (NAC) and subjected to 4 dynes/cm^2 FSS. The calcium trace (left) indicates the average Fluo-4 fluorescence changes over time, % Cells Responding (middle) indicates number of cells which elicit more than 25% increase fluorescence, and Peak (ΔF/F) indicates peak magnitude of Ca^{2+} response in those cells that responded (right). All Ca^{2+} traces are aggregated data from >200 cells imaged in n=3 independent experiments across all conditions. (**B**) FSS-induced Ca^{2+} response of Fluo-4 loaded Ocy454 cells treated with α-N-acetyl cysteine (NAC) and subjected to 16 dynes/cm^2 FSS. The calcium trace (left) indicates the average Fluo-4 fluorescence changes over time, % Cells Responding (middle) indicates number of cells which elicit more than 25% increase fluorescence, and Peak (ΔF/F) indicates peak magnitude of Ca^{2+} response in those cells that responded (right). All Ca^{2+} traces are aggregated data from >200 cells imaged in n=3 independent experiments across all conditions. (**C**) Ocy454 cells treated with or without (control) NAC were subjected to FSS as indicated followed by immunoblotting for sclerostin. GAPDH served as a loading control. Sclerostin to GAPDH ratio is indicated (n=3 independent experiments). (**D**) Ocy454 cells were treated with H_2O_2 followed by immunoblotting for sclerostin. GAPDH served as a loading control. Sclerostin to GAPDH ratio is indicated (n=3 independent experiments).

(Figure 23C,D,E). Unlike stiffening the MT network with Taxol, which can be overcome with increased FSS, the Nox2 inhibition persisted at higher flow rates, confirming Nox2 as a convergence point in this mechanotransduction cascade. These data implicate Nox2 as the source of ROS that activates TRPV4-dependent Ca^{2+} influx during FSS.

Discussion

We found that TPV4 is a major pathway for the initial and rapid FSS-induced Ca^{2+} influx that drives sclerostin downregulation in osteocytes. Unlike modifications of the MT network which fully abrogated mechanosensitivity (i.e., Ca^{2+} influx and sclerostin downregulation), we still observed residual FSS-induced Ca^{2+} influx with pharmacologic or molecular inhibition of TRPV4. While several other Ca^{2+} influx pathways have been identified in osteocytes, our results suggest that these pathways are likely activated in response to sustained FSS or via its induction of ligands that further promote Ca^{2+} influx, perhaps downstream of the initial Ca^{2+} influx through TRPV4. Indeed, numerous studies have demonstrated oscillating Ca^{2+} waves driven by ATP release and purinergic receptor activation in mechano-activated osteocytes [84,89,318] as well as Ca^{2+} influx through T-type voltage gated calcium channels [68,311].

The involvement of TRPV4 in osteocyte mechano-sensing is wholly consistent with the demonstration of TRPV4 as a mediator of mechanically-induced Ca^{2+} influx in the primary cilia of bone cells [73]. Likewise, TRPV4 plays an important role in chondrocyte mechanotransduction, as blocking TRPV4 prevents an anabolic response to load, while activating the receptor mimics load [319]. In contrast to our prediction, global TRPV4 knockout mice have increased bone mass; however, the interpretation is complicated by a severe osteoclast defect that contributes to the skeletal phenotype [320].

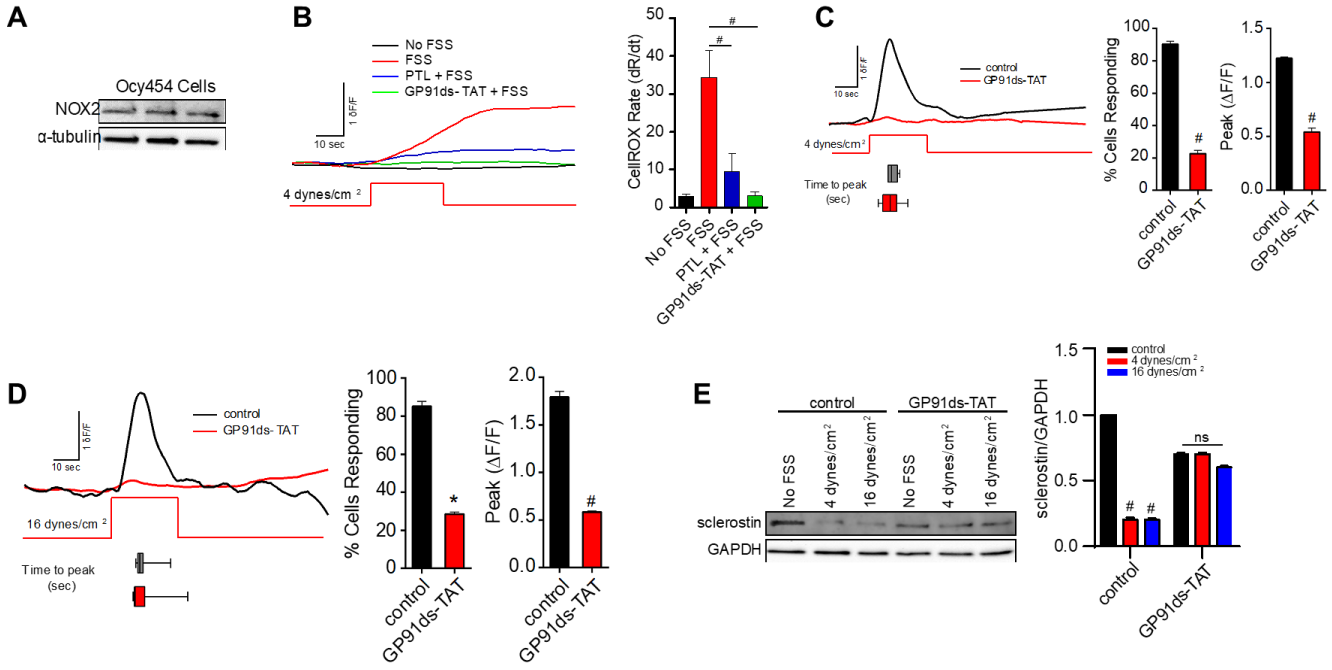

Figure 23. Nox2-dependent ROS is required for the FSS-induced Ca^{2+} response and downregulation of sclerostin

(**A**) Immunoblotting was performed on Ocy454 whole cell lysates for NOX2. α-tubulin served as a loading control. (**B**) FSS-induced ROS response in Ocy454 cells treated with or without (control) PTL or GP91ds-TAT and subjected to 4 dynes/cm^2 FSS. Traces (left) indicate CellROX fluorescence changes over time, CellROX Rate (d*R*/d*t*) indicates the rate of change in CellROX fluorescence (right). (**C**) FSS-induced Ca^{2+} response of Fluo4-loaded Ocy454 cells treated with GP91ds-TAT and subjected to 4 dynes/cm^2 FSS. The calcium trace (left) indicates the average Fluo-4 fluorescence changes over time, % Cells Responding (middle) indicates number of cells which elicit more than 25% increase fluorescence, and Peak (ΔF/F) indicates peak magnitude of Ca^{2+} response in those cells that responded (right). All Ca^{2+} traces are aggregated data from >200 cells imaged in n=3 independent experiments across all conditions. (**D**) FSS-induced Ca^{2+} response of Fluo4-loaded Ocy454 cells treated with GP91ds-TAT and subjected to 16 dynes/cm^2 FSS. The calcium trace (left) indicates the average Fluo-4 fluorescence changes over time, % Cells Responding (middle) indicates number of cells which elicit more than 25% increase fluorescence, and Peak (ΔF/F) indicates peak magnitude of Ca^{2+} response in those cells that responded (right). All Ca^{2+} traces are aggregated data from >200 cells imaged in n=3 independent experiments across all conditions. (**E**) Ocy454 cells treated with or without (control) GP91ds-TAT were subjected to FSS as indicated followed by immunoblotting for sclerostin. GAPDH served as a loading control. Sclerostin to GAPDH ratio is indicated (n=3 independent experiments). Graphs depict mean ± sem. * indicates $p<0.001$ versus control; # indicates $P<0.0001$ versus control by student's unpaired two tailed *t*-test or one-way ANOVA with Dunnet's post hoc test. ns indicates not statistically significant.

Despite higher trabecular and cortical bone mass, male TRPV4 knockout mice have reduced bone matrix mineralization, increased cortical porosity, a lower ultimate stress and reduced elastic modulus [321]. While these reports do not preclude a role of TRPV4 in osteocyte mechano-responsiveness, they also do not definitively support our hypothesis. Regardless, TRPV4 plays a role in the skeleton as numerous gain of function TRPV4 mutations cause skeletal dysplasias with a breadth of severity [322]. Intriguingly, a SNP in the human TRPV4 locus was associated with a 30% increase risk of non-vertebral fractures in males in the Rotterdam study and was confirmed in subsequent meta-analysis [321].

Consistent with reports in striated muscle [141,157,248], our data show an important role for mechano-activated, Nox2-dependent ROS in the osteocyte response to FSS. To our knowledge, this is the first implication of Nox2 in osteocyte mechano-responsiveness. Interestingly, $p47^{phox}$ global knockout mice, a subunit of the Nox2 enzyme, have decreased bone mass and strength in aged adult mice, due to deficits in osteoblast differentiation, osteoblast number, and accelerated cell senescence [323]. Interestingly, this phenotype is not observed in 6-week-old mice, which have increased bone mass. Whether or not changes in mechano-sensing or sclerostin bioavailability contribute to the worsening skeletal phenotype have not been assessed nor have these mice been studied in the context of mechanical loading.

In summary, we have defined a major contributor to the FSS induced Ca^{2+} influx observed in osteocytes. These findings call into question to long standing notion that the first response to FSS is Ca^{2+} influx. Our data suggests that the first response in actually Nox2 derived ROS which leads to this Ca^{2+} influx. Further, it is important to note that

TRPV4 dependent Ca^{2+} influx signals drive the downregulation of sclerostin protein in osteocytes. Given the importance of osteocyte FSS induced Ca^{2+} influx and sclerostin bioavailability, these new mechanistic details of the osteocyte mechano-response and sclerostin regulation may further provide a better understanding of skeletal diseases and conditions which are characterized by altered bone structure and properties. Thus, we propose this TRPV4 and Nox2 dependent mechanotransduction pathway as a novel target for manipulating the osteocyte response to mechanical cues for therapeutic interventions in bone.

Chapter 6: Fluid shear stress induces calcium/calmodulin-dependent kinase II signaling resulting in sclerostin degradation

Introduction

Sclerostin is widely accepted as one of the most important regulators of bone formation[263]. It has even been targeted for potential therapeutic use to combat diseases of skeletal fragility[116]. However, our knowledge of sclerostin and its role in the skeletal response to mechanical load is still lacking.

Gene regulation of *SOST*, the gene that encodes sclerostin, has been widely studied. Two essential transcription factors for osteoblast differentiation, RUNX2 and osterix (OSX) bind to the *SOST* proximal promoter and contribute to *SOST* expression[122,132]. There is evidence that both of these factors play a role in activation of *SOST* expression. Also, a distal enhancer region with an ECR5 site in the *SOST* gene plays a vital role in regulating *SOST* gene expression[120]. Deletion of just the ECR5 enhancer is sufficient to drive significant decreases in *SOST* gene expression independent of changes in the proximal promoter. The ECR5 enhancer contains a myocyte enhancer factor-2 (MEF2) response element. This response element is responsible for binding to the MEF2 family of transcription factors. Deletion of just the MEF2 response element is sufficient to drive reductions in *SOST* gene expression similar to what is observed when the entire ECR5 region is deleted[136]. TGFβ-1, -2, and -3, and ActivinA increase *SOST* expression in an ECR5-dependent manner[131]. Further, PTH suppresses *SOST* expression through the ECR5 enhancer. PTH binding to its receptor activates cAMP/PKA signaling which results in a decrease is *SOST* expression[136].

Finally, mechanical loading is a major regulator of sclerostin. It has been shown in several models that mechanical loading reduces *SOST*/sclerostin both *in vitro* and *in vivo*[110,115,138,289,290]. However, the exact mechanisms by which mechanical loading regulates *SOST* expression has not been fully detailed. It is likely that there is a combination of any number of the above mentioned signaling pathways that are activated by mechanical loading in osteocytes. For example, the IGF-1 and cAMP/PKA pathways have both been implicated to be involved[137,139]. Further, detailed mechanisms of sclerostin protein regulation in response to mechanical loading are completely unknown.

Here, we define a novel regulatory pathway for sclerostin protein in response to FSS. We observed rapid activation of calcium/calmodulin dependent kinase II (CamKII) in response to FSS. Further, this CamKII signaling lead to rapid degradation of sclerostin protein by the lysosome.

Results

CamKII is rapidly activated in response to FSS in Ocy454 cells.

While it has been well documented that sclerostin is down regulated in response to mechanical stimuli in osteocytes, a mechanistic link between FSS induced Ca^{2+} influx and sclerostin protein regulation has yet to be established[139]. We observe a rapid increase in phosphorylated CamKII in response to FSS in Ocy454 cells (Figure 24A). Further, when Ocy454 cells were loaded with BAPTA AM-ester and subjected to 4 dynes/cm^2 FSS using a Ca^{2+} free fluid flow buffer, this increase in phosphorylated CamKII is attenuated (Figure 24A). Interestingly, we observed activation of CamKII independent of FSS when Ocy454 cells were treated with a TRPV4 agonist (GSK-1016790A - 15 μM, 30 min) (Figure 24B). This indicates that Ca^{2+} influx through

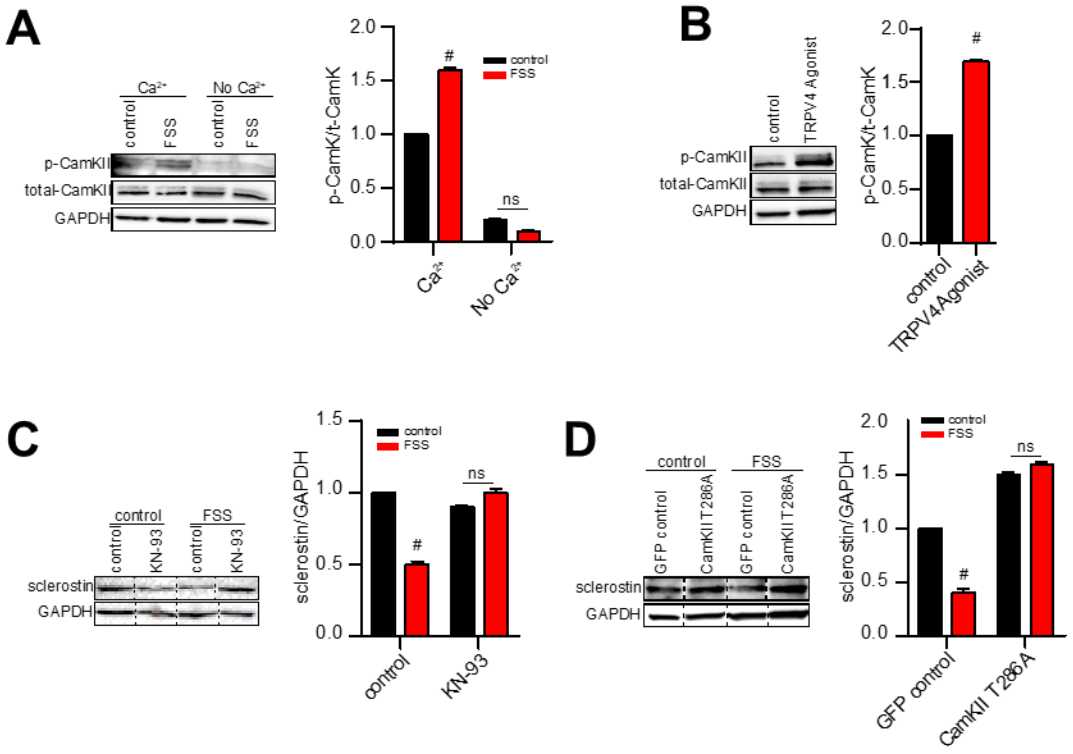

Figure 24. FSS induces a rapid activation of CamKII, which is required for the downregulation of sclerostin.

(**A**) Untreated Ocy454 cells and BAPTA-AM ester loaded Ocy454 cells were subjected to 4 dynes/cm^2 FSS with Ca^{2+} containing or Ca^{2+} free flow buffer, respectively. Immunoblotting was performed for indicated proteins (n=3 independent experiments). GAPDH served as a loading control. Densitometric quantitation of the p-CamKII to total-CamKII ratio is shown. (**B**) Control or TRPV4 Agonist treated Ocy454 cells were immunoblotted for indicated proteins. GAPDH served as a loading control. P-CamKII to total-CamKII ratio is indicated (n=3 independent experiments). (**C**) Control Ocy454 cells or Ocy454cells treated with CamKII inhibitor KN-93 were subjected to 4 dynes/cm^2 FSS followed by immunoblotting for sclerostin. GAPDH served as a loading control. Sclerostin to GAPDH ratio is indicated (n=3 independent experiments). (**D**) GFP control or CamKII T286A dominate negative transfected Ocy454 cells were subjected to 4 dynes/cm^2 FSS followed by immunoblotting for sclerostin. GAPDH served as a loading control. Sclerostin to GAPDH ratio is indicated (n=3 independent experiments). Graphs depict mean ± sem. Statistical significance determined using one-way ANOVA with Dunnet's post hoc test. # indicates p <.0001 versus control, ns indicates not statistically significant.

TRPV4 is sufficient to drive activation of CamKII in Ocy454 cells independent of FSS. While these data do not show a cause and effect relationship between CamKII and sclerostin, it does reveal a previously unknown signaling pathway involved in the osteocyte mechanical load response.

CamKII is required for the FSS induced downregulation in sclerostin protein.
In order to determine if the activation of CamKII was in fact required for the observed decrease in sclerostin protein, we utilized two approaches of interrupting CamKII signaling. First, we treated Ocy454 cells with KN-93, a selective inhibitor of CamKII activation. In KN-93 treated cells subjected to 4 dynes/cm2 of FSS, we see an attenuation of the FSS induced downregulation of sclerostin (Figure 24C). Second, we transfected Ocy454 cells with a dominate negative form of CamKII. In Oc454 cells transfected with a dominate negative CamKII, the FSS induced downregulation of sclerostin is inhibited (Figure 24D). Interestingly, we noted an enhanced decrease in sclerostin when Ocy454 cells transfected with a constitutively active CamKII were subjected to 4 dynes/cm2 (data not shown). These data indicate that the FSS induced downregulation of sclerostin protein is dependent on CamKII signaling.

Alterations to the MT network also regulate the FSS-induced activation of CamKII.
Since we observed significant regulation of the FSS-induced down regulation of sclerostin by alerations in the MT network, we decided to explore whether the same is true for the FSS-induced activation of CamKII. When Ocy454 cells are treated with colchicine and subjected to 4 dynes/cm2, we see a significant blunting in the FSS-induced activation of CamKII (Figure 25A). Similarly, the FSS-induced activation of

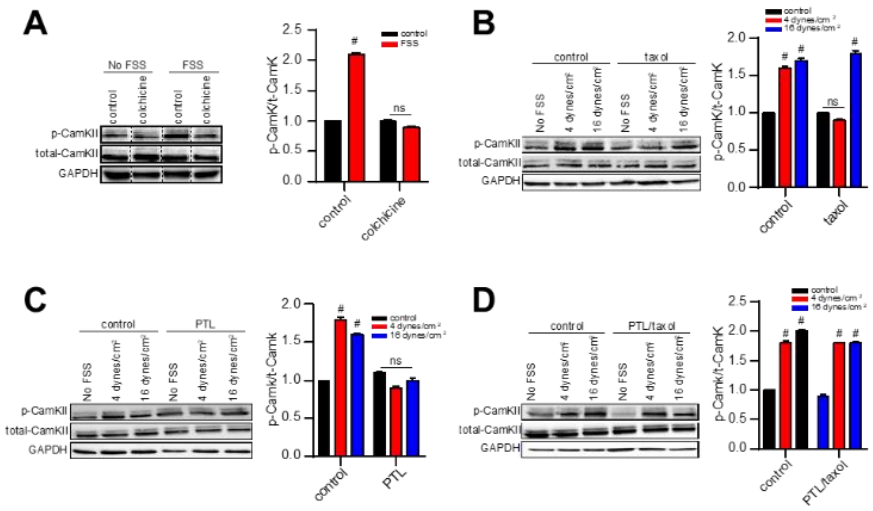

Figure 25. Alterations in the MT network affect FSS-induced activation of CamKII.
(**A**) Ocy454 cells treated with colchicine were subjected to 4 dynes/cm^2 FSS followed by immunoblotting for indicated proteins. GAPDH served as a loading control. P-CamKII to total-CamKII ratio is indicated (n=3 independent experiments). (**B**) Control or Taxol treated Ocy454 cells were subjected to FSS as indicated followed by immunoblotting for indicated proteins. GAPDH served as a loading control. P-CamKII to total-CamKII ratio is indicated (n=3 independent experiments). (**C**) Control or PTL treated Ocy454 cells were subjected to FSS as indicated followed by immunoblotting for indicated proteins. GAPDH served as a loading control. P-CamKII to total-CamKII ratio is indicated (n=3 independent experiments). (**D**) Control Ocy454 cells or Ocy454cells treated with combination of PTL and Taxol were subjected to FSS as indicated followed by immunoblotting for indicated proteins. GAPDH served as a loading control. P-CamKII to total-CamKII ratio is indicated (n=3 independent experiments). Graphs depict mean ± sem., # indicates $p<0.0001$ by one-way ANOVA with Dunnet's post hoc test. ns indicates not statistically significant.

CamKII mimics what is seen with sclerostin downregulation when Ocy454 cells are treated with taxol. When taxol treated cells are subjected to 4 dynes/cm2 the FSS-induced activation of CamKII is attenuated, however this is overcome by 16 dynes/cm2 (Figure 25B). Further, the same regulation observed by changes in Glu-tubulin are conserved when examining the FSS-induced activation of CamKII. PTL blocks the activation of CamKII, while a combination of PTL and taxol restores the activation (Figure 25C,D).

FSS-induced Ca^{2+} through TRPV4 is required for the FSS-induced activation of CamKII.
To examine if TRPV4 dependent Ca^{2+} influx was the source of the FSS-induced CamKII activation, Ocy454 cells were treated with the TRPV4 antagonist and transfected with TRPV4 specific siRNA. As expected, inhibition or knockdown of TRPV4 attenuated the FSS-induced activation of CamKII (Figure 26A,B). Likewise, if we block the upstream activator of TRPV4, ROS, using either NAC or GP91ds-TAT, we also attenuate the FSS-induced activation of CamKII (Figure 27A,B). Interestingly, Ocy454 cells treated with H_2O_2 showed activation of CamKII independent of FSS (Figure 27C). This suggests that ROS dependent Ca^{2+} influx is sufficient to drive activation of CamKII.

Sclerostin protein is degraded by the lysosome in response to FSS.
Since the response being observed is very rapid, it was necessary to determine the fate of the sclerostin protein and to rule out the possibility that the protein was being rapid secreted. Therefore, we treated Ocy454 cells with Bafilomyocin A1 (BafA1), a potent lysosomal inhibitor. Cells treated with BafA1 and subjected to 4 dynes/cm^2 the downregulation of sclerostin was blunted (Figure 28). However, it is important to note that when these cells are subjected to FSS, we observed normal activation of CamKII

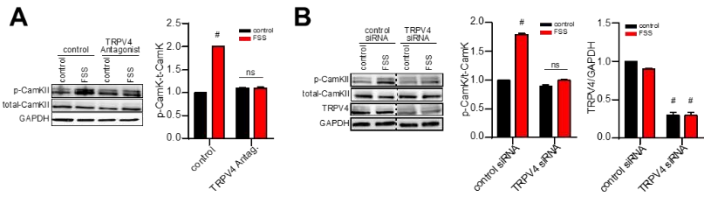

Figure 26. TRPV4 dependent Ca^{2+} influx is required and sufficient for CamKII activation.
(A) Ocy454 cells treated with the TRPV4 Antagonist were subjected to 4 dynes/cm^2 FSS followed by immunoblotting for indicated proteins. GAPDH served as a loading control. P-CamKII to total-CamKII ratio is indicated (n=3 independent experiments). (**B**) Control siRNA or TRPV4 specific siRNA transfected Ocy454 cells were subjected to 4 dynes/cm^2 FSS followed by immunoblotting for indicated proteins. GAPDH served as a loading control. P-CamKII to total-CamKII and TRPV4 to GAPDH ratios are indicated (n=3 independent experiments).

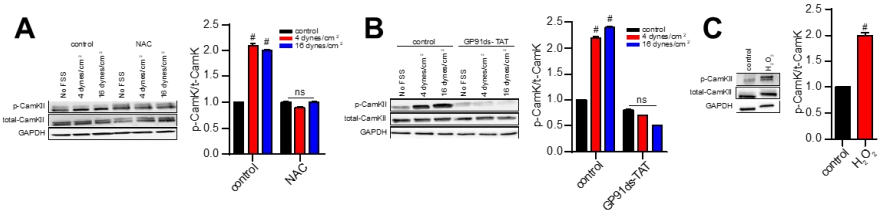

Figure 27. ROS is required and sufficient for activation of CamKII.
(**A**) Ocy454 cells treated with NAC were subjected to FSS as indicated followed by immunoblotting for indicated proteins. GAPDH served as a loading control. P-CamKII to total-CamKII ratio is indicated (n=3 independent experiments). (**B**) Control or GP91ds-TAT treated Ocy454 cells were subjected to FSS as indicated followed by immunoblotting for indicated proteins. GAPDH served as a loading control. P-CamKII to total-CamKII ratio is indicated (n=3 independent experiments). (**C**) Control or H_2O_2 treated Ocy454 cells were immunoblotted for indicated proteins. GAPDH served as a loading control. P-CamKII to total-CamKII ratio is indicated (n=3 independent experiments).

consistent with a normal response to the stimuli despite the lack of a decrease in sclerostin levels (Figure 28). These data suggest that in response to FSS, sclerostin protein is rapidly degraded by the lysosome.

CamKII signaling also regulates osteocytes specific gene expression.

In most cases, the osteocyte response to mechanical stimuli has been studied at the level of gene expression[57]. It has been widely shown that changes in osteocyte gene expression is an important response to FSS in osteocytes[264]. In order to examine the role of CamKII signaling in osteocyte gene expression regulation, we transfected Ocy454 cells with a constitutively active CamKII construct and performed qRT-PCR for osteocyte specific markers. Interestingly, independent of FSS, activated CamKII was sufficient to drive a decrease in *SOST* gene expression (Figure 29). Further, we observed significant increases in the genes encoding RANKL and OPG, important regulatory factors for osteoclast activation (Figure 29). Interestingly, we also observed a significant increase in Cox2, which is responsible for the production of PGE_2 (Figure 29). Taken together, this data suggests an important role for CamKII signaling in the osteocyte response to FSS not only in the regulation of sclerostin protein but throughout the osteocyte mechanical load response.

Discussion

Here we report a mechanically activated signaling pathway that involves CamKII signaling leading to sclerostin degradation by the lysosome.

Our data show that mechanical stimuli induces a rapid increase in phosphorylated CamKII in Ocy454 cells. Blocking this activation of CamKII using a pharmacologic

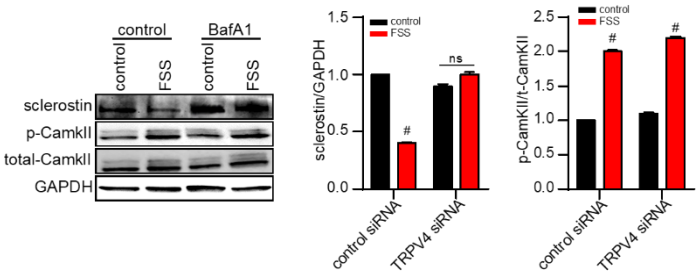

Figure 28. Sclerostin is rapidly degraded by the lysosome in response to FSS.

Ocy454 cells treated with or without (control) Bafilomyocin A1 were subjected to 4 dynes/cm^2 FSS followed by immunoblotting for indicated proteins. GAPDH served as a loading control. Sclerostin to GAPDH and p-CamKII to total-CamKII ratios are indicated (n=3 independent experiments). Graphs depict mean ± sem. # indicates P<0.0001 versus control by one-way ANOVA with Dunnet's post hoc test. ns indicates not statistically significant.

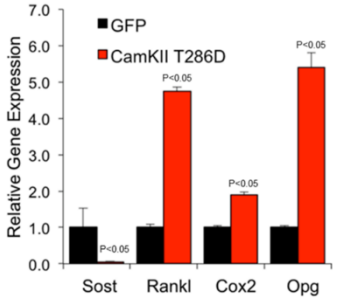

Figure 29. Activation of CamKII affects osteocyte specific gene expression.

Ocy454 cells transfected with either GFP control or CamKII T286D constitutively active constructs were analyzed by qRT-PCR for indicated proteins. Statistical significance was determined using student's unpaired two tailed *t*-test. p values are indicated.

inhibitor or a dominate negative CamKII construct results in an abrogation of the FSS induced downregulation of sclerostin protein. Further, a constitutively active form of CamKII seems to enhance the FSS induced downregulation of sclerostin protein. This is the first report of activation of CamKII signaling in osteocytes in response to FSS.

Due to the nature of sclerostin being a secreted glycoprotein, it was important to show that the observed response was not simply secretion. Our data indicates that the rapid decrease in sclerostin levels are indeed not due to secretion, but instead are due to sclerostin degradation by the lysosome. It has been observed in other systems that CamKII signaling can lead to protein degradation, thus lysosomal degradation of sclerostin was a viable option for the results we obverse[324-326] . Indeed, inhibition of lysosomal degradation using a pharmacologic blocker results in a loss of the FSS induced down regulation of sclerostin. This result reveals two important concepts. First, this data shows that the Ocy454 cell line is a viable model to study and better understand sclerostin protein regulation than previous models[115]. This system more accurately mimics osteocytes *in situ* and can be an important model as we build a better understanding of osteocyte biology. Second, this data reveals an important regulatory factor with regards to sclerostin. It had been previously understood that sclerostin was glycosylated and secreted, however the mechanisms and regulation of these events had yet to be elucidated[117]. These results provide insight into some of these potential mechanisms.

Important to note is that CamKII signaling also seems to play a role in osteocyte gene expression. This suggests that CamKII signaling may play a much wider role in osteocyte mechanotransduction than shown here. For example, the reduction in *SOST* gene

expression when Ocy454 cells are transfected with a constitutively active CamKII construct suggests that the well-established decreases in *SOST* in response to mechanical stimuli could be partly controlled by CamKII signaling[290]. It is possible that this occurs through regulation of MEF2C as it has been shown in neurons and muscle that CamKII signaling can regulate the MEF family of transcription factors[327-330]. Also, changes in *RANKL* and *OPG* suggest that CamKII signaling not only could regulate factors of bone growth, but also factors of bone resorption. Therefore, it is possible that CamKII signaling may be a major regulator of the bone remodeling process as a whole. While it is widely accepted that osteocytes respond to mechanical stimuli by producing a releasing PGE_2, our data shows that CamKII signaling may also be involved[74].

In conclusion, this data reveals several previously unreported mechanisms of the osteocyte mechanical load response. It is safe to speculate that some of these mechanisms may also be involved in other aspects of osteocyte biology, including CamKII singling being involved in the osteocyte response to hormones like PTH and testosterone. Ultimately, this data reveal potential new targets for modulation of the osteocyte response to mechanical stimuli and possible new therapeutic interventions for treatment of diseases of skeletal fragility.

Chapter 7: Further Discussion and Future Directions

Further Discussion

Summary

Despite years of research into the adaptive nature of the skeleton, the molecular mechanisms of the osteocyte mechanical load response still remains poorly understood. Here we have presented compelling data that fills some of the previously unknown mechanisms of this process. While there have been many hypotheses and reports of different mechanisms being involved, there was still substantial gaps in our understanding of the osteocyte response to mechanical stimuli.

We have developed a cheap high-throughput alternative to commercially available systems for studying cellular mechanotransduction[250]. Many labs utilize FSS as a means to subject their tissue or cells to a mechanical stimuli[66,83,98,270,273,281,282,308,331,332]. Our newly developed device for introducing FSS to cells in culture overcome many of the shortcomings of available models including the ability to achieve truly independent replicate samples[250]. Of upmost importance, our device eliminates any variability in the results that may be introduced by using different devices for different outcome measures. With our device we can image live cells and collect protein, RNA, or DNA for biochemical and molecular analysis all using one device. Finally, the simplicity of our device allows for any lab to explore mechanotransduction without the cost of the necessary equipment being a barrier to entry into this field[250].

With this work, we have presented a mechanism of how the osteocyte senses and responds to FSS[333]. The osteocyte MT network alters the overall cytoskeletal stiffness of the cells through the abundance of the α-tubulin PTM, detyrosination/Glu-tubulin. The

relative abundance of Glu-tubulin and measured cytoskeletal stiffness directly impact how the osteocyte responds to FSS. Our data support a model of the osteocyte containing a "goldilocks zone" of Glu-tubulin levels and cytoskeletal stiffness. In short, high levels of Glu-tubulin and increased cytoskeletal stiffness resist FSS induced deformation of the osteocyte cytoskeleton, thus reducing the response, however low levels of Glu-tubulin and decreased cytoskeletal stiffness cause an inability for the osteocyte to transduce the force produced by FSS to the appropriate effector molecules[333]. Thus, osteocytes must maintain an intermediate level of Glu-tubulin and cytoskeletal stiffness. We hypothesize that this is an active process that can be readily altered to meet changing demands and precisely regulate the bone remodeling process.

Second, our data have revealed a major contributor to the well-established FSS induced Ca^{2+} influx observed in osteocytes, TRPV4[333]. TRPV4 was previously shown to play an important role in the Ca^{2+} influx in the primary cilia of osteocytes, however its overall role in the osteocyte mechanical load response was still disputed[73]. Here we have shown a definitive role for TRPV4 in the FSS induced Ca^{2+} influx observed in osteocytes[333].

Next, we have mechanistically linked two hallmark readouts of studying osteocyte mechanotransduction. Our data shows that the FSS induced Ca^{2+} influx is absolutely required for the downregulation of sclerostin protein[333]. Decreases in sclerostin of *SOST* gene expression have traditionally been used to indicate a response to mechanical stimuli by osteocytes, however the exact mechanisms of this have remained elusive due to the lack of an appropriate *in vitro* model for studying sclerostin[115].

Also, we have revealed a previously unreported signaling cascade that is involved in the osteocyte response to FSS, CamKII signaling[333]. CamKII signaling is ubiquitous in a

number of other tissues, however it has not been widely explored in osteocyte biology[327]. Our data shows a rapid increase in phosphorylated CamKII indicating activation of CamKII signaling in response to FSS. Further, we have shown that this CamKII signaling is required for the rapid downregulation of sclerostin observed[250]. Finally, CamKII signaling also appears to alter osteocyte specific gene expression changes which could indicate a broad role for CamKII signaling in osteocyte biology. Finally, we have discovered a novel mechanism of sclerostin protein regulation, degradation. Our data demonstrates that in response to FSS sclerostin protein is rapidly degraded by the lysosome. This taken together with the decrease in *SOST* gene expression suggest a two tiered response to mechanical stimuli. The first tier is the rapid degradation of sclerostin protein. We postulate that this is a safety mechanism. The osteocyte feels an anabolic load, however in order to refrain from building unnecessary bone, it simply degrades the available pool of sclerostin and then waits to sense if the anabolic load persists. If this load does persist, than the osteocyte feels it necessary to begin the remodeling process and thus proceeds to reduce *SOST* gene expression as well. This sort of two tier mechanism makes sense in terms of a cellular system. It takes much more energy and resources to build bone than it does to reinitiate production of a single protein.

This work has brought to light many new avenues of research to be explored in the future. Many of these mechanisms also have varying degrees of implication for not only basic osteocyte biology but also diseases of skeletal fragility and therapeutic interventions.

Implications for Osteocyte Biology

Great strides have been made in the field of osteocyte biology using a variety of *in vitro* models of mechanical stimulation[57]. These range from simply placing the cell culture vessel on a rocking platform to complex systems offered by commercial companies like the FlexCell Streamer. However, due to the limits of these systems, it was not possible to accurately connect the FSS induced Ca^{2+} influx observed in osteocytes to the downstream signaling and gene expression changes[250,333]. While most groups used multiple techniques for introducing FSS to cells and then extrapolated their results, there was always one lingering question. Does the differences in the technique used have differing effects on the cellular response? It has been shown in the literature that the mechanism of FSS, whether the flow is laminar or turbulent, can affect the cellular response[308]. Further, it has even been shown that different mechanical stimuli can have different outcomes[240]. For example, mechanical stretching of osteocytes causes a different response than FSS application[240]. Our new device allows for the accurate comparison and connection of these mechanisms by eliminating the need for different systems. This allows us to compare the cellular response to mechanical stimuli using the exact same conditions for every outcome measure[250]. This could open new avenues of research into studying the underlying mechanisms of osteocyte mechanotransduction.

Further, our research has proved that the Ocy454 osteocyte cell line is indeed an appropriate model for exploring osteocyte biology. Much of the work has been traditionally done using MLO-Y4 cells, however these cells have been characterized as osteocytes mainly by their morphology[114]. While they are in fact very similar to osteocytes in morphology, they lack key characteristics of osteocytes including a lack of detectible levels of sclerostin protein[115]. With the Ocy454 cell line, our work further

enforces the notion that this novel cell line is a better model for studying osteocytes *in vitro* and could lead to many new revelations in osteocyte biology[333].

We have revealed a few new mechanisms of osteocyte mechanotransduction that challenge long standing notions in this field. For example, it was previously thought that the osteocyte cell process were mainly actin rich elements[239]. However, our work regarding the MT network shows that in fact the osteocyte cell processes are also rich in MTs[333]. This could lead to further investigation into the role of the MT network in osteocyte mechanotransduction and proposes the concept that the MT network actually plays a more functional role in osteocytes that previously considered. Further, our work has introduced the idea that MT detyrosination plays an important role in osteocyte mechanotransduction. It is also likely that other MT PTMs could play an important functional role in osteocyte biology.

The broader role of TRPV4 in the osteocyte FSS induced Ca^{2+} influx further expands our knowledge of this phenomenon. While many other mechanisms have been shown to be involved including t-type Ca^{2+} channels and P2X channels, it is clear from our data that these are not the only contributors to the response[92,311]. In fact we postulate that the initial Ca^{2+} bolus is mediated by TRPV4 and the downstream Ca^{2+} oscillations are mediated by these previously described mechanisms. However, this distinction would require further investigation to conclude.

CamKII signaling is a ubiquitous Ca^{2+} dependent singling pathway throughout many tissues[324-330]. However, the idea that this is a major signaling pathway involved in osteocyte biology could have significant impacts on the field. Many of the mechanisms that have been previously outline in osteocytes, including the singling response to

hormones, osteocyte mechanotransduction, and osteocyte gene expression regulation, could all in some part involve CamKII signaling. This data open many new avenues of investigation into the details of these biochemical and molecular pathways. We hypothesize that CamKII will become a major player in osteocyte biology and have long standing implications on future research.

Sclerostin protein has been exceedingly difficult to study, mainly due to the lack of an appropriate *in vitro* model[115]. However, our data has revealed that post translational regulation of sclerostin protein could be very important to osteocyte biology. Understanding these mechanisms could lead to novel therapeutic targets and interventions for treating diseases of skeletal fragility. We have shown that Ocy454 cells are an appropriate model for exploring these mechanisms and open a string a new opportunities for further research.

Implications for Osteoporosis

While all of the work we have presented thus far has been *in vitro*, there are still many implication for diseases of skeletal fragility like osteoporosis. Skeletal fragility is a substantial and growing problem. In 2006, >200 million people worldwide suffered from osteoporosis, contributing to ~9 million factures annually. The disability due to osteoporosis is greater than that caused by many cancers and many other chronic diseases[334]. Thus, preventing or restoring bone loss is of vital importance to limiting the personal and economic impact of skeletal fragility. Currently, there is no cure for osteoporosis and the current treatment only work to slow the progression of bone loss[291]. While a humanized anti-sclerostin antibody has shown great promise in clinical trials, there are still issues with the route of intervention. First, bone remodeling is a process

that couple bone resorption with bone formation. Therefore, simply increasing bone formation helps to increase bone mass, but does not build good quality bone because bone resorption is not equally increased. Further, there were recent reports of patients in this clinical trial began to show severe heart related side effects[335]. With these new revelations regarding the safety of sclerostin humanized monoclonal antibodies, there remains a great need to stimulate the bone remodeling process in total.

Some of the mechanisms we have outlined here have the potential to do this. For example, if we can modulate the osteocyte MT network and adjust the threshold of what load is considered anabolic, we could stimulate the skeleton's natural ability to adapt to load and maintain peak bone mass. Imagine a healthy individual who exercises regularly. This person's osteocytes will respond to the load generated by exercise and build and maintain bone mass. Now imagine an elderly person who cannot exercise this way. If we could tune the cytoskeletal stiffness of their osteocytes down just slightly, this could decrease the limit at which the osteocytes sense mechanical stimuli. Therefore, light mechanical load which was previously not sensed, like day to day walking or even just gravity, would now become anabolic. This would allow the elderly person to build and maintain bone mass in the same manner as the healthy individual despite experiencing much less load. Further, this brings to mind the notion that astronauts who spend extended time in zero gravity could also benefit from these findings for the same reason. We could tune their MT network while they are experiencing the reduced load and potentially limit the progression of bone loss that is observed in astronauts[336].

Also, our work has revealed potential new therapeutic targets for the treatment of osteoporosis. Activators of TRPV4, independent of mechanical stimulation was sufficient

to decrease sclerostin[333]. Thus, activators of TRPV4 could be potential candidates for the treatment of osteoporosis. This could be useful in combating resistance that may build up from long term use of humanized anti-sclerostin antibodies or even be used independently for therapeutic intervention. Further, CamKII signaling lead to the reduction of sclerostin and other osteocyte specific genes. Therefore, activation of CamKII signaling independent of mechanical load could also serve as a possible therapeutic target for the treatment of low bone mass. Similarly, activating Nox2 could be a potential route for stimulating the osteocyte mechanical load response independent of actual load. Unfortunately, all of these potential targets are ubiquitously expressed throughout the body. Thus, while these implications have great potential, it would still take significant investigation before any of these options became viable targets for therapeutic intervention. In the next section, the future directions of this research will be discussed in more detail.

Future Directions

Future research

While we showed that sclerostin degradation is dependent on CamKII signaling, we did not outline the molecular mechanism linking these two events. It is possible that CamKII is acting as a switch that determines whether sclerostin gets secreted or sclerostin gets trafficked to the lysosome, however this still remains to be determined.

A major concern for this work is the mechanism of action of the drug Taxol. Many new reports are indicating that the activity of Taxol is due to increases in oxidative stress. Since our work showed that ROS is required for the FSS induced Ca^{2+} influx observed in

osteocytes, it will be important in the future to separate the FSS induced ROS and any oxidative stress generated by our interventions. This will likely be resolved by using different methods of increasing Glu-tubulin levels independent of Taxol.

Further, it would be important to explore the mechanisms of CamKII dependent changes in osteocyte gene expression. Since CamKII is such a ubiquitous signaling molecule, there are quite a few options that could account for the changes observed. However, it will also be important to explore the role of CamKII in FSS induced changes in osteocyte gene expression as our work only showed changes independent of mechanical stimulation. By outlining this pathway in more detail, it will not only further enhance our understanding of osteocyte biology, but could also potentially reveal novel targets for therapeutic intervention in osteoporosis.

As mentioned above, all of this work to this point has been *in vitro* work in cells in culture. This is a major shortcoming of this work. However, we do have some preliminary results *in vivo* that suggest these mechanisms are conserved. We used an ulna load model to explore the signaling events we observed *in vitro*. Indeed when we subject mice to repeated ulnar loading of 2.5N for 90sec at 2Hz, we see a decrease in sclerostin protein and activation of CamKII signaling within 1 hour post load (Figure 30). Further, when we treat mice with colchicine or a TRPV4 antagonist *in vivo*, and then subject them to the same ulnar loading protocol, we abrogate the downregulation of sclerostin and activation of CamKII signaling compared to vehicle treated controls (Figure 30). While this preliminary data is promising there is still substantial work that needs to be done to prove these mechanisms are in fact conserved *in vivo*. All of these mechanisms, including

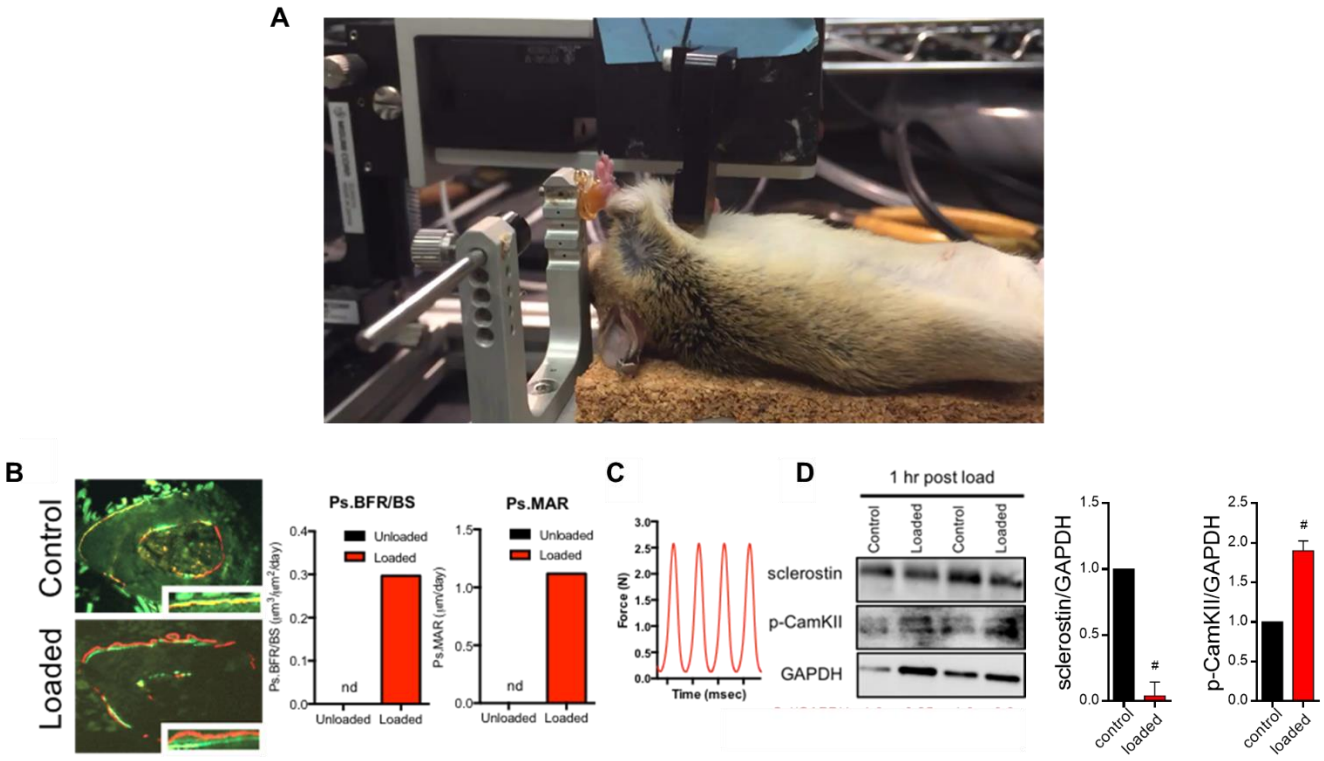

Figure 30. Acute mechanical loading causes rapid sclerostin downregulation and CamKII activation in a murine unlar load model.

(**A**) 12 week old mixed background mice were anesthetized and loaded into a modified Aurora Scientific 305B muscle lever system. The volar flexed carpus was placed into a small cup on a fixed substrate while the elbow was placed into a small cup on the lever arm of the force transducer. Contralateral ulnas which experienced no mechanical load used as controls. (**B**) **Dynamic histomorphometry** was performed on loaded mice to validate the model of ulnar loading. Representative fluorescence images of murine ulna showing dual labeling of Alizerin Red (red) and Calcein (green) (left). Ps. BFR/BS ($\mu m^3/\mu m^2$/day) indicates the periosteal bone formation rate (middle). Ps. MAR (μm/day) indicates the periosteal mineral apposition rate (right). (**C**) Graphical representation of ulnar loading protocol. Limbs were preloaded at 0.3 N and then subjected to repeated loading of 2.5 N at a frequency of 2 Hz for 90 secs, daily for 3 days. (**D**) Ulna extracts from loaded ulnas were immunoblotted for the indicated proteins. The contralateral limbs were used as control and GAPDH served as a loading control. Sclerostin to GAPDH and p-CamKII to GAPDH ratios are indicated. Graphs depict mean ± sem. # indicates P<0.0001 versus control by one-way ANOVA with Dunnet's post hoc test.

changes in cytoskeletal stiffness and activation of Nox2 must be translated to *in vivo* models for confirmation. Interestingly, acute treatment with Taxol altered the skeletal morphology of 8 week old mice (Figure 31). However, this data is complicated due to the fact that the mice were not at skeletal maturity. It is impossible to conclude whether the observed changes in bone mass is caused by the loss of the ability of the osteocytes to sense mechanical stimuli. In reality, it is much more likely that the observed effects are caused by an inability of the osteoblasts to divide and proliferate due to the Taxol treatment. However, while complicated and difficult to interpret, this data does provide some promise that these interventions can be utilized to alter bone mass. Thus, the ability of these inhibitor to increase bone mass in osteoporosis models or in patients with diseases of skeletal fragility is something that should be explored in greater detail.

More importantly, the notion that regulation of cytoskeletal stiffness is indeed an active process, needs to be explored. This could be done by performing adaptation experiments. For example, subjecting the cells or the mice to repeated bouts of supra-physiologic loading and then subjecting them to a decreased load to show that the cells or mice no longer respond. Also, we have not explored if repeated bouts of mechanical load alter the abundance of Glu-tubulin in a meaningful way. Both of these would be important parameters to explore in the future.

Lastly, it would be important to show that alterations of these pathways can be used as a therapeutic intervention for osteoporosis. Using some of these inhibitors or similar pharmacologic agents to treat animal models of osteoporosis is a logical final step for this work. While this work has made great strides in the field of osteocyte mechanotransduction, much remains to be done.

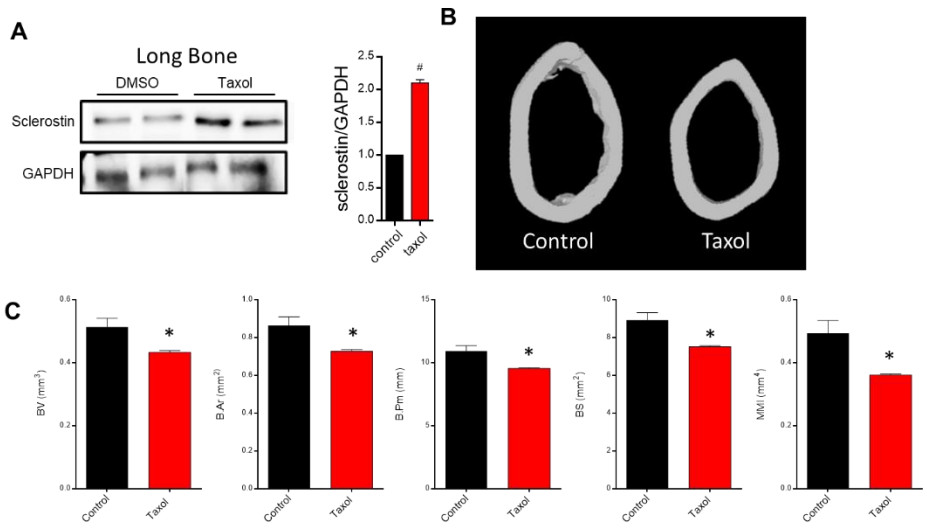

Figure 31. Acute Taxol treatment alters bone quality *in vivo*.
(**A**) Long bone extracts from mice treated acutely with Taxol were immunoblotted from sclerostin. GAPDH served as a loading control. Sclerostin to GAPDH ratio is indicated. (**B**) Representative 3D reconstitution of murine femurs from mice treated with and without (control) Taxol and scanned using µCT. (**C**) µCT analysis of murine femurs from mice treated with and without (control) Taxol. Graphs depict mean ± sem. * indicates $p<0.05$ versus control by student's unpaired two tailed *t*-test

Conclusion

The great personal and economic burden of diseases of skeletal fragility highlight the necessity to better understand osteocyte biology and how the skeleton senses and responds to mechanical stimulation. This data presented here help to delineate some of the molecular mechanisms involved in this fundamental aspect of skeletal physiology. With the increasing life expectancy of humans and the increased interest in space travel, these vital concepts are going to continue to have a greater impact on society. In the future, there will be even greater importance in further expanding our understanding of the skeleton.

References

1. Taichman RS. Blood and bone: two tissues whose fates are intertwined to create the hematopoietic stem-cell niche. Blood. Apr 01 2005;105(7):2631-9.

2. Mammal Anatomy: An Illustrated Guide. New York: Marshall Cavendish; 2010.

3. Cooper RR, Milgram JW, Robinson RA. Morphology of the osteon. An electron microscopic study. The Journal of bone and joint surgery American volume. Oct 1966;48(7):1239-71.

4. Carter DR, Hayes WC. Bone compressive strength: the influence of density and strain rate. Science. Dec 10 1976;194(4270):1174-6.

5. Parkinson IH. Characterisation of Trabecular Bone Structure. In: Silva MJ, editor. Skeletal Aging and Osteoporosis: Springer; 2013. p. 31-51.

6. Usha Kini BNN. Physiology of Bone Formation, Remodeling, and Metabolism. In: Fogelman I, editor. Radionuclide and Hybrid Bone Imaging: Springer; 2012. p. 29-57.

7. Richard Parker FHN. Musculoskeletal System: Anatomy, Physiology, and Metabolic Disorders: Elsevier - Health Sciences Division; 1988.

8. Field RA, Riley ML, Mello FC, Corbridge MH, Kotula AW. Bone composition in cattle, pigs, sheep and poultry. Journal of animal science. Sep 1974;39(3):493-9.

9. Vaananen HK, Zhao H, Mulari M, Halleen JM. The cell biology of osteoclast function. Journal of cell science. Feb 2000;113 (Pt 3):377-81.

10. Mackie EJ. Osteoblasts: novel roles in orchestration of skeletal architecture. The international journal of biochemistry & cell biology. Sep 2003;35(9):1301-5.

11. Bonewald LF. The amazing osteocyte. J Bone Miner Res. Feb 2011;26(2):229-38.

12. Franz-Odendaal TA, Hall BK, Witten PE. Buried alive: how osteoblasts become osteocytes. Developmental dynamics : an official publication of the American Association of Anatomists. Jan 2006;235(1):176-90.

13. Winkler DG, Sutherland MK, Geoghegan JC, Yu C, Hayes T, Skonier JE, et al. Osteocyte control of bone formation via sclerostin, a novel BMP antagonist. The EMBO journal. Dec 01 2003;22(23):6267-76.

14. Palumbo C. A three-dimensional ultrastructural study of osteoid-osteocytes in the tibia of chick embryos. Cell and tissue research. 1986;246(1):125-31.

15. Tanaka-Kamioka K, Kamioka H, Ris H, Lim SS. Osteocyte shape is dependent on actin filaments and osteocyte processes are unique actin-rich projections. Journal

of bone and mineral research : the official journal of the American Society for Bone and Mineral Research. Oct 1998;13(10):1555-68.

16. Dudley HR, Spiro D. The Fine Structure of Bone Cells. The Journal of biophysical and biochemical cytology. Dec 01 1961;11(3):627-49.

17. Dallas SL, Prideaux M, Bonewald LF. The osteocyte: an endocrine cell ... and more. Endocrine reviews. Oct 2013;34(5):658-90.

18. Liu S, Tang W, Zhou J, Vierthaler L, Quarles LD. Distinct roles for intrinsic osteocyte abnormalities and systemic factors in regulation of FGF23 and bone mineralization in Hyp mice. American journal of physiology Endocrinology and metabolism. Dec 2007;293(6):E1636-44.

19. Shimada T, Kakitani M, Yamazaki Y, Hasegawa H, Takeuchi Y, Fujita T, et al. Targeted ablation of Fgf23 demonstrates an essential physiological role of FGF23 in phosphate and vitamin D metabolism. The Journal of clinical investigation. Feb 2004;113(4):561-8.

20. Miyamoto K, Ito M, Kuwahata M, Kato S, Segawa H. Inhibition of intestinal sodium-dependent inorganic phosphate transport by fibroblast growth factor 23. Therapeutic apheresis and dialysis : official peer-reviewed journal of the International Society for Apheresis, the Japanese Society for Apheresis, the Japanese Society for Dialysis Therapy. Aug 2005;9(4):331-5.

21. Vezeridis PS, Semeins CM, Chen Q, Klein-Nulend J. Osteocytes subjected to pulsating fluid flow regulate osteoblast proliferation and differentiation. Biochemical and biophysical research communications. Sep 29 2006;348(3):1082-8.

22. Yellowley CE, Li Z, Zhou Z, Jacobs CR, Donahue HJ. Functional gap junctions between osteocytic and osteoblastic cells. Journal of bone and mineral research : the official journal of the American Society for Bone and Mineral Research. Feb 2000;15(2):209-17.

23. Bodine PV, Vernon SK, Komm BS. Establishment and hormonal regulation of a conditionally transformed preosteocytic cell line from adult human bone. Endocrinology. Nov 1996;137(11):4592-604.

24. Burr DB. Targeted and nontargeted remodeling. Bone. Jan 2002;30(1):2-4.

25. Brighton CT, Hunt RM. Early histological and ultrastructural changes in medullary fracture callus. The Journal of bone and joint surgery American volume. Jul 1991;73(6):832-47.

26. Roodman GD. Cell biology of the osteoclast. Experimental hematology. Aug 1999;27(8):1229-41.

27. Bruzzaniti A, Baron R. Molecular regulation of osteoclast activity. Reviews in endocrine & metabolic disorders. Jun 2006;7(1-2):123-39.

28. Locklin RM, Oreffo RO, Triffitt JT. Effects of TGFbeta and bFGF on the differentiation of human bone marrow stromal fibroblasts. Cell biology international. 1999;23(3):185-94.

29. Siris ES. Paget's disease of bone. Journal of bone and mineral research : the official journal of the American Society for Bone and Mineral Research. Jul 1998;13(7):1061-5.

30. Emerton KB, Hu B, Woo AA, Sinofsky A, Hernandez C, Majeska RJ, et al. Osteocyte apoptosis and control of bone resorption following ovariectomy in mice. Bone. Mar 2010;46(3):577-83.

31. Mundy GR, Bonewald LF. Role of TGF beta in bone remodeling. Annals of the New York Academy of Sciences. 1990;593:91-7.

32. Lind M, Deleuran B, Thestrup-Pedersen K, Soballe K, Eriksen EF, Bunger C. Chemotaxis of human osteoblasts. Effects of osteotropic growth factors. APMIS : acta pathologica, microbiologica, et immunologica Scandinavica. Feb 1995;103(2):140-6.

33. Hessle L, Johnson KA, Anderson HC, Narisawa S, Sali A, Goding JW, et al. Tissue-nonspecific alkaline phosphatase and plasma cell membrane glycoprotein-1 are central antagonistic regulators of bone mineralization. Proceedings of the National Academy of Sciences of the United States of America. Jul 09 2002;99(14):9445-9.

34. Raisz LG. Physiology and pathophysiology of bone remodeling. Clinical chemistry. Aug 1999;45(8 Pt 2):1353-8.

35. Pocock NA, Eisman JA, Hopper JL, Yeates MG, Sambrook PN, Eberl S. Genetic determinants of bone mass in adults. A twin study. The Journal of clinical investigation. Sep 1987;80(3):706-10.

36. Grant SF, Ralston SH. Genes and osteoporosis. Trends in endocrinology and metabolism: TEM. Aug 1997;8(6):232-6.

37. Trueta J, Buhr AJ. The Vascular Contribution to Osteogenesis. V. The Vasculature Supplying the Epiphysial Cartilage in Rachitic Rats. The Journal of bone and joint surgery British volume. Aug 1963;45:572-81.

38. Jones KB, Mollano AV, Morcuende JA, Cooper RR, Saltzman CL. Bone and brain: a review of neural, hormonal, and musculoskeletal connections. The Iowa orthopaedic journal. 2004;24:123-32.

39. Shaker JL, Deftos L. Calcium and Phosphate Homeostasis. In: De Groot LJ, Chrousos G, Dungan K, Feingold KR, Grossman A, Hershman JM, et al., editors. Endotext. South Dartmouth (MA)2000.

40. Martin TJ. Parathyroid Hormone-Related Protein, Its Regulation of Cartilage and Bone Development, and Role in Treating Bone Diseases. Physiological reviews. Jul 2016;96(3):831-71.

41. Sapir-Koren R, Livshits G. Bone mineralization is regulated by signaling cross talk between molecular factors of local and systemic origin: the role of fibroblast growth factor 23. BioFactors. Nov-Dec 2014;40(6):555-68.

42. Sharan K, Yadav VK. Hypothalamic control of bone metabolism. Best practice & research Clinical endocrinology & metabolism. Oct 2014;28(5):713-23.

43. Manolagas SC, O'Brien CA, Almeida M. The role of estrogen and androgen receptors in bone health and disease. Nature reviews Endocrinology. Dec 2013;9(12):699-712.

44. Kawaguchi H, Pilbeam CC, Raisz LG. Anabolic effects of 3,3',5-triiodothyronine and triiodothyroacetic acid in cultured neonatal mouse parietal bones. Endocrinology. Sep 1994;135(3):971-6.

45. Dempster DW, Cosman F, Parisien M, Shen V, Lindsay R. Anabolic actions of parathyroid hormone on bone. Endocrine reviews. Dec 1993;14(6):690-709.

46. Raisz LG. Bone cell biology: new approaches and unanswered questions. Journal of bone and mineral research : the official journal of the American Society for Bone and Mineral Research. Dec 1993;8 Suppl 2:S457-65.

47. Hofbauer LC, Khosla S. Androgen effects on bone metabolism: recent progress and controversies. European journal of endocrinology. Apr 1999;140(4):271-86.

48. Hofbauer LC, Khosla S, Dunstan CR, Lacey DL, Spelsberg TC, Riggs BL. Estrogen stimulates gene expression and protein production of osteoprotegerin in human osteoblastic cells. Endocrinology. Sep 1999;140(9):4367-70.

49. Caplan A, Fett N, Rosenbach M, Werth VP, Micheletti RG. Prevention and management of glucocorticoid-induced side effects: A comprehensive review: A review of glucocorticoid pharmacology and bone health. Journal of the American Academy of Dermatology. Jan 2017;76(1):1-9.

50. Manolagas SC. Birth and death of bone cells: basic regulatory mechanisms and implications for the pathogenesis and treatment of osteoporosis. Endocrine reviews. Apr 2000;21(2):115-37.

51. Rosen CJ, Donahue LR. Insulin-like growth factors and bone: the osteoporosis connection revisited. Proceedings of the Society for Experimental Biology and Medicine Society for Experimental Biology and Medicine. Oct 1998;219(1):1-7.

52. Wolff J. Das Gesetz der Transformation der Knochen. 1892.

53. Cowin SC, Moss-Salentijn L, Moss ML. Candidates for the mechanosensory system in bone. Journal of biomechanical engineering. May 1991;113(2):191-7.

54. Tatsumi S, Ishii K, Amizuka N, Li M, Kobayashi T, Kohno K, et al. Targeted ablation of osteocytes induces osteoporosis with defective mechanotransduction. Cell metabolism. Jun 2007;5(6):464-75.

55. Piekarski K, Munro M. Transport mechanism operating between blood supply and osteocytes in long bones. Nature. Sep 01 1977;269(5623):80-2.

56. Zhang D, Weinbaum S, Cowin SC. Electrical signal transmission in a bone cell network: the influence of a discrete gap junction. Annals of biomedical engineering. Jul-Aug 1998;26(4):644-59.

57. Klein-Nulend J, Bakker AD, Bacabac RG, Vatsa A, Weinbaum S. Mechanosensation and transduction in osteocytes. Bone. Jun 2013;54(2):182-90.

58. Price C, Zhou X, Li W, Wang L. Real-time measurement of solute transport within the lacunar-canalicular system of mechanically loaded bone: direct evidence for load-induced fluid flow. Journal of bone and mineral research : the official journal of the American Society for Bone and Mineral Research. Feb 2011;26(2):277-85.

59. Knothe Tate ML, Knothe U, Niederer P. Experimental elucidation of mechanical load-induced fluid flow and its potential role in bone metabolism and functional adaptation. The American journal of the medical sciences. Sep 1998;316(3):189-95.

60. Gardinier JD, Townend CW, Jen KP, Wu Q, Duncan RL, Wang L. In situ permeability measurement of the mammalian lacunar-canalicular system. Bone. Apr 2010;46(4):1075-81.

61. Bacabac RG, Mizuno D, Schmidt CF, MacKintosh FC, Van Loon JJ, Klein-Nulend J, et al. Round versus flat: bone cell morphology, elasticity, and mechanosensing. Journal of biomechanics. 2008;41(7):1590-8.

62. Klein-Nulend J, van der Plas A, Semeins CM, Ajubi NE, Frangos JA, Nijweide PJ, et al. Sensitivity of osteocytes to biomechanical stress in vitro. FASEB journal : official publication of the Federation of American Societies for Experimental Biology. Mar 1995;9(5):441-5.

63. Wang L, Wang Y, Han Y, Henderson SC, Majeska RJ, Weinbaum S, et al. In situ measurement of solute transport in the bone lacunar-canalicular system. Proceedings of the National Academy of Sciences of the United States of America. Aug 16 2005;102(33):11911-6.

64. Kufahl RH, Saha S. A theoretical model for stress-generated fluid flow in the canaliculi-lacunae network in bone tissue. Journal of biomechanics. 1990;23(2):171-80.

65. Weinbaum S, Cowin SC, Zeng Y. A model for the excitation of osteocytes by mechanical loading-induced bone fluid shear stresses. Journal of biomechanics. Mar 1994;27(3):339-60.

66. Kamel MA, Picconi JL, Lara-Castillo N, Johnson ML. Activation of beta-catenin signaling in MLO-Y4 osteocytic cells versus 2T3 osteoblastic cells by fluid flow shear stress and PGE2: Implications for the study of mechanosensation in bone. Bone. Nov 2010;47(5):872-81.

67. Kalogeropoulos M, Varanasi SS, Olstad OK, Sanderson P, Gautvik VT, Reppe S, et al. Zic1 transcription factor in bone: neural developmental protein regulates mechanotransduction in osteocytes. FASEB journal : official publication of the Federation of American Societies for Experimental Biology. Aug 2010;24(8):2893-903.

68. Lu XL, Huo B, Chiang V, Guo XE. Osteocytic network is more responsive in calcium signaling than osteoblastic network under fluid flow. Journal of bone and mineral research : the official journal of the American Society for Bone and Mineral Research. Mar 2012;27(3):563-74.

69. Thi MM, Suadicani SO, Schaffler MB, Weinbaum S, Spray DC. Mechanosensory responses of osteocytes to physiological forces occur along processes and not cell body and require alphaVbeta3 integrin. Proc Natl Acad Sci U S A. Dec 24 2013;110(52):21012-7.

70. Anderson EJ, Kaliyamoorthy S, Iwan J, Alexander D, Knothe Tate ML. Nano-microscale models of periosteocytic flow show differences in stresses imparted to cell body and processes. Annals of biomedical engineering. Jan 2005;33(1):52-62.

71. Nguyen AM, Jacobs CR. Emerging role of primary cilia as mechanosensors in osteocytes. Bone. Jun 2013;54(2):196-204.

72. Espinha LC, Hoey DA, Fernandes PR, Rodrigues HC, Jacobs CR. Oscillatory fluid flow influences primary cilia and microtubule mechanics. Cytoskeleton. Jul 2014;71(7):435-45.

73. Lee KL, Guevarra MD, Nguyen AM, Chua MC, Wang Y, Jacobs CR. The primary cilium functions as a mechanical and calcium signaling nexus. Cilia. 2015;4:7.

74. Ajubi NE, Klein-Nulend J, Alblas MJ, Burger EH, Nijweide PJ. Signal transduction pathways involved in fluid flow-induced PGE2 production by cultured osteocytes. The American journal of physiology. Jan 1999;276(1 Pt 1):E171-8.

75. Lean JM, Jagger CJ, Chambers TJ, Chow JW. Increased insulin-like growth factor I mRNA expression in rat osteocytes in response to mechanical stimulation. The American journal of physiology. Feb 1995;268(2 Pt 1):E318-27.

76. Zaman G, Pitsillides AA, Rawlinson SC, Suswillo RF, Mosley JR, Cheng MZ, et al. Mechanical strain stimulates nitric oxide production by rapid activation of endothelial nitric oxide synthase in osteocytes. Journal of bone and mineral research : the official journal of the American Society for Bone and Mineral Research. Jul 1999;14(7):1123-31.

77. Forwood MR. Inducible cyclo-oxygenase (COX-2) mediates the induction of bone formation by mechanical loading in vivo. Journal of bone and mineral research : the official journal of the American Society for Bone and Mineral Research. Nov 1996;11(11):1688-93.

78. Bakker AD, Klein-Nulend J, Burger EH. Mechanotransduction in bone cells proceeds via activation of COX-2, but not COX-1. Biochemical and biophysical research communications. Jun 06 2003;305(3):677-83.

79. Hung CT, Pollack SR, Reilly TM, Brighton CT. Real-time calcium response of cultured bone cells to fluid flow. Clinical orthopaedics and related research. Apr 1995(313):256-69.

80. Hung CT, Allen FD, Pollack SR, Brighton CT. Intracellular Ca2+ stores and extracellular Ca2+ are required in the real-time Ca2+ response of bone cells experiencing fluid flow. Journal of biomechanics. Nov 1996;29(11):1411-7.

81. Gu Y, Preston MR, El Haj AJ, Howl JD, Publicover SJ. Three types of K(+) currents in murine osteocyte-like cells (MLO-Y4). Bone. Jan 2001;28(1):29-37.

82. Thompson WR, Majid AS, Czymmek KJ, Ruff AL, Garcia J, Duncan RL, et al. Association of the alpha(2)delta(1) subunit with Ca(v)3.2 enhances membrane expression and regulates mechanically induced ATP release in MLO-Y4 osteocytes. Journal of bone and mineral research : the official journal of the American Society for Bone and Mineral Research. Sep 2011;26(9):2125-39.

83. Genetos DC, Geist DJ, Liu D, Donahue HJ, Duncan RL. Fluid shear-induced ATP secretion mediates prostaglandin release in MC3T3-E1 osteoblasts. Journal of bone and mineral research : the official journal of the American Society for Bone and Mineral Research. Jan 2005;20(1):41-9.

84. Genetos DC, Kephart CJ, Zhang Y, Yellowley CE, Donahue HJ. Oscillating fluid flow activation of gap junction hemichannels induces ATP release from MLO-Y4 osteocytes. J Cell Physiol. Research Support, N.I.H., Extramural

Research Support, U.S. Gov't, Non-P.H.S. Jul 2007;212(1):207-14. Epub 2007/02/16.

85. Turner CH, Takano Y, Owan I, Murrell GA. Nitric oxide inhibitor L-NAME suppresses mechanically induced bone formation in rats. The American journal of physiology. Apr 1996;270(4 Pt 1):E634-9.

86. Fox SW, Chambers TJ, Chow JW. Nitric oxide is an early mediator of the increase in bone formation by mechanical stimulation. The American journal of physiology. Jun 1996;270(6 Pt 1):E955-60.

87. Robinson JA, Chatterjee-Kishore M, Yaworsky PJ, Cullen DM, Zhao W, Li C, et al. Wnt/beta-catenin signaling is a normal physiological response to mechanical loading in bone. The Journal of biological chemistry. Oct 20 2006;281(42):31720-8.

88. Burra S, Jiang JX. Connexin 43 hemichannel opening associated with Prostaglandin E(2) release is adaptively regulated by mechanical stimulation. Communicative & integrative biology. May 2009;2(3):239-40.

89. Kringelbach TM, Aslan D, Novak I, Ellegaard M, Syberg S, Andersen CK, et al. Fine-tuned ATP signals are acute mediators in osteocyte mechanotransduction. Cell Signal. Dec 2015;27(12):2401-9.

90. Cherian PP, Cheng B, Gu S, Sprague E, Bonewald LF, Jiang JX. Effects of mechanical strain on the function of Gap junctions in osteocytes are mediated through the prostaglandin EP2 receptor. The Journal of biological chemistry. Oct 31 2003;278(44):43146-56.

91. Cherian PP, Siller-Jackson AJ, Gu S, Wang X, Bonewald LF, Sprague E, et al. Mechanical strain opens connexin 43 hemichannels in osteocytes: a novel mechanism for the release of prostaglandin. Molecular biology of the cell. Jul 2005;16(7):3100-6.

92. Li J, Liu D, Ke HZ, Duncan RL, Turner CH. The P2X7 nucleotide receptor mediates skeletal mechanotransduction. The Journal of biological chemistry. Dec 30 2005;280(52):42952-9.

93. Wang N, Rumney RM, Yang L, Robaye B, Boeynaems JM, Skerry TM, et al. The P2Y13 receptor regulates extracellular ATP metabolism and the osteogenic response to mechanical loading. Journal of bone and mineral research : the official journal of the American Society for Bone and Mineral Research. Jun 2013;28(6):1446-56.

94. Seref-Ferlengez Z, Maung S, Schaffler MB, Spray DC, Suadicani SO, Thi MM. P2X7R-Panx1 Complex Impairs Bone Mechanosignaling under High Glucose Levels Associated with Type-1 Diabetes. PLoS One. 2016;11(5):e0155107.

95. Wang Y, McNamara LM, Schaffler MB, Weinbaum S. A model for the role of integrins in flow induced mechanotransduction in osteocytes. Proceedings of the National Academy of Sciences of the United States of America. Oct 02 2007;104(40):15941-6.

96. Plotkin LI, Stains JP. Connexins and pannexins in the skeleton: gap junctions, hemichannels and more. Cellular and molecular life sciences : CMLS. Aug 2015;72(15):2853-67.

97. Moorer MC, Stains JP. Connexin43 and the Intercellular Signaling Network Regulating Skeletal Remodeling. Current osteoporosis reports. Feb 2017;15(1):24-31.

98. Litzenberger JB, Kim JB, Tummala P, Jacobs CR. Beta1 integrins mediate mechanosensitive signaling pathways in osteocytes. Calcified tissue international. Apr 2010;86(4):325-32.

99. Maniotis AJ, Chen CS, Ingber DE. Demonstration of mechanical connections between integrins, cytoskeletal filaments, and nucleoplasm that stabilize nuclear structure. Proceedings of the National Academy of Sciences of the United States of America. Feb 04 1997;94(3):849-54.

100. Cabahug-Zuckerman P, Frikha-Benayed D, Majeska RJ, Tuthill A, Yakar S, Judex S, et al. Osteocyte Apoptosis Caused by Hindlimb Unloading is Required to Trigger Osteocyte RANKL Production and Subsequent Resorption of Cortical and Trabecular Bone in Mice Femurs. Journal of bone and mineral research : the official journal of the American Society for Bone and Mineral Research. Jul 2016;31(7):1356-65.

101. Liedert A, Kaspar D, Blakytny R, Claes L, Ignatius A. Signal transduction pathways involved in mechanotransduction in bone cells. Biochemical and biophysical research communications. Oct 13 2006;349(1):1-5.

102. Iqbal J, Zaidi M. Molecular regulation of mechanotransduction. Biochemical and biophysical research communications. Mar 18 2005;328(3):751-5.

103. Franceschi RT, Xiao G, Jiang D, Gopalakrishnan R, Yang S, Reith E. Multiple signaling pathways converge on the Cbfa1/Runx2 transcription factor to regulate osteoblast differentiation. Connective tissue research. 2003;44 Suppl 1:109-16.

104. Mikuni-Takagaki Y. Mechanical responses and signal transduction pathways in stretched osteocytes. Journal of bone and mineral metabolism. 1999;17(1):57-60.

105. Hughes-Fulford M. Signal transduction and mechanical stress. Science's STKE : signal transduction knowledge environment. Aug 31 2004;2004(249):RE12.

106. Ogasawara A, Arakawa T, Kaneda T, Takuma T, Sato T, Kaneko H, et al. Fluid shear stress-induced cyclooxygenase-2 expression is mediated by C/EBP beta, cAMP-response element-binding protein, and AP-1 in osteoblastic MC3T3-E1 cells. The Journal of biological chemistry. Mar 09 2001;276(10):7048-54.

107. Fitzgerald J, Hughes-Fulford M. Mechanically induced c-fos expression is mediated by cAMP in MC3T3-E1 osteoblasts. FASEB journal : official publication of the Federation of American Societies for Experimental Biology. Mar 1999;13(3):553-7.

108. Slusarski DC, Corces VG, Moon RT. Interaction of Wnt and a Frizzled homologue triggers G-protein-linked phosphatidylinositol signalling. Nature. Nov 27 1997;390(6658):410-3.

109. Cui Y, Niziolek PJ, MacDonald BT, Zylstra CR, Alenina N, Robinson DR, et al. Lrp5 functions in bone to regulate bone mass. Nature medicine. Jun 2011;17(6):684-91.

110. Robling AG, Bellido T, Turner CH. Mechanical stimulation in vivo reduces osteocyte expression of sclerostin. Journal of musculoskeletal & neuronal interactions. Oct-Dec 2006;6(4):354.

111. Ray S, Khassawna TE, Sommer U, Thormann U, Wijekoon ND, Lips K, et al. Differences in expression of Wnt antagonist Dkk1 in healthy versus pathological bone samples. Journal of microscopy. Jan 2017;265(1):111-20.

112. Thompson WR, Rubin CT, Rubin J. Mechanical regulation of signaling pathways in bone. Gene. Jul 25 2012;503(2):179-93.

113. Honasoge M, Rao AD, Rao SD. Sclerostin: recent advances and clinical implications. Current opinion in endocrinology, diabetes, and obesity. Dec 2014;21(6):437-46.

114. Kato Y, Windle JJ, Koop BA, Mundy GR, Bonewald LF. Establishment of an osteocyte-like cell line, MLO-Y4. Journal of bone and mineral research : the official journal of the American Society for Bone and Mineral Research. Dec 1997;12(12):2014-23.

115. Spatz JM, Wein MN, Gooi JH, Qu Y, Garr JL, Liu S, et al. The Wnt Inhibitor Sclerostin Is Up-regulated by Mechanical Unloading in Osteocytes in Vitro. J Biol Chem. Jul 3 2015;290(27):16744-58.

116. Ominsky MS, Li C, Li X, Tan HL, Lee E, Barrero M, et al. Inhibition of sclerostin by monoclonal antibody enhances bone healing and improves bone density and strength of nonfractured bones. Journal of bone and mineral research :

the official journal of the American Society for Bone and Mineral Research. May 2011;26(5):1012-21.

117. Poole KE, van Bezooijen RL, Loveridge N, Hamersma H, Papapoulos SE, Lowik CW, et al. Sclerostin is a delayed secreted product of osteocytes that inhibits bone formation. FASEB journal : official publication of the Federation of American Societies for Experimental Biology. Nov 2005;19(13):1842-4.

118. Hernandez P, Whitty C, John Wardale R, Henson FM. New insights into the location and form of sclerostin. Biochemical and biophysical research communications. Apr 18 2014;446(4):1108-13.

119. Li X, Ominsky MS, Niu QT, Sun N, Daugherty B, D'Agostin D, et al. Targeted deletion of the sclerostin gene in mice results in increased bone formation and bone strength. Journal of bone and mineral research : the official journal of the American Society for Bone and Mineral Research. Jun 2008;23(6):860-9.

120. Balemans W, Patel N, Ebeling M, Van Hul E, Wuyts W, Lacza C, et al. Identification of a 52 kb deletion downstream of the SOST gene in patients with van Buchem disease. Journal of medical genetics. Feb 2002;39(2):91-7.

121. Balemans W, Ebeling M, Patel N, Van Hul E, Olson P, Dioszegi M, et al. Increased bone density in sclerosteosis is due to the deficiency of a novel secreted protein (SOST). Human molecular genetics. Mar 01 2001;10(5):537-43.

122. Ohyama Y, Nifuji A, Maeda Y, Amagasa T, Noda M. Spaciotemporal association and bone morphogenetic protein regulation of sclerostin and osterix expression during embryonic osteogenesis. Endocrinology. Oct 2004;145(10):4685-92.

123. Balemans W, Van Hul W. Extracellular regulation of BMP signaling in vertebrates: a cocktail of modulators. Developmental biology. Oct 15 2002;250(2):231-50.

124. Weidauer SE, Schmieder P, Beerbaum M, Schmitz W, Oschkinat H, Mueller TD. NMR structure of the Wnt modulator protein Sclerostin. Biochemical and biophysical research communications. Feb 27 2009;380(1):160-5.

125. van Bezooijen RL, Roelen BA, Visser A, van der Wee-Pals L, de Wilt E, Karperien M, et al. Sclerostin is an osteocyte-expressed negative regulator of bone formation, but not a classical BMP antagonist. The Journal of experimental medicine. Mar 15 2004;199(6):805-14.

126. Ellies DL, Viviano B, McCarthy J, Rey JP, Itasaki N, Saunders S, et al. Bone density ligand, Sclerostin, directly interacts with LRP5 but not LRP5G171V to modulate Wnt activity. Journal of bone and mineral research : the official journal of the American Society for Bone and Mineral Research. Nov 2006;21(11):1738-49.

127. Veverka V, Henry AJ, Slocombe PM, Ventom A, Mulloy B, Muskett FW, et al. Characterization of the structural features and interactions of sclerostin: molecular insight into a key regulator of Wnt-mediated bone formation. The Journal of biological chemistry. Apr 17 2009;284(16):10890-900.

128. Li X, Zhang Y, Kang H, Liu W, Liu P, Zhang J, et al. Sclerostin binds to LRP5/6 and antagonizes canonical Wnt signaling. The Journal of biological chemistry. May 20 2005;280(20):19883-7.

129. Krishnan V, Bryant HU, Macdougald OA. Regulation of bone mass by Wnt signaling. The Journal of clinical investigation. May 2006;116(5):1202-9.

130. Sawakami K, Robling AG, Ai M, Pitner ND, Liu D, Warden SJ, et al. The Wnt co-receptor LRP5 is essential for skeletal mechanotransduction but not for the anabolic bone response to parathyroid hormone treatment. The Journal of biological chemistry. Aug 18 2006;281(33):23698-711.

131. Loots GG, Keller H, Leupin O, Murugesh D, Collette NM, Genetos DC. TGF-beta regulates sclerostin expression via the ECR5 enhancer. Bone. Mar 2012;50(3):663-9.

132. Sevetson B, Taylor S, Pan Y. Cbfa1/RUNX2 directs specific expression of the sclerosteosis gene (SOST). The Journal of biological chemistry. Apr 02 2004;279(14):13849-58.

133. Delgado-Calle J, Sanudo C, Bolado A, Fernandez AF, Arozamena J, Pascual-Carra MA, et al. DNA methylation contributes to the regulation of sclerostin expression in human osteocytes. Journal of bone and mineral research : the official journal of the American Society for Bone and Mineral Research. Apr 2012;27(4):926-37.

134. Papathanasiou I, Kostopoulou F, Malizos KN, Tsezou A. DNA methylation regulates sclerostin (SOST) expression in osteoarthritic chondrocytes by bone morphogenetic protein 2 (BMP-2) induced changes in Smads binding affinity to the CpG region of SOST promoter. Arthritis research & therapy. Jun 12 2015;17:160.

135. Delgado-Calle J, Arozamena J, Perez-Lopez J, Bolado-Carrancio A, Sanudo C, Agudo G, et al. Role of BMPs in the regulation of sclerostin as revealed by an epigenetic modifier of human bone cells. Molecular and cellular endocrinology. Apr 30 2013;369(1-2):27-34.

136. Leupin O, Kramer I, Collette NM, Loots GG, Natt F, Kneissel M, et al. Control of the SOST bone enhancer by PTH using MEF2 transcription factors. Journal of bone and mineral research : the official journal of the American Society for Bone and Mineral Research. Dec 2007;22(12):1957-67.

137. Genetos DC, Yellowley CE, Loots GG. Prostaglandin E2 signals through PTGER2 to regulate sclerostin expression. PloS one. Mar 16 2011;6(3):e17772.

138. Robling AG, Niziolek PJ, Baldridge LA, Condon KW, Allen MR, Alam I, et al. Mechanical stimulation of bone in vivo reduces osteocyte expression of Sost/sclerostin. The Journal of biological chemistry. Feb 29 2008;283(9):5866-75.

139. Moester MJ, Papapoulos SE, Lowik CW, van Bezooijen RL. Sclerostin: current knowledge and future perspectives. Calcified tissue international. Aug 2010;87(2):99-107.

140. Jeff Hardin GB, Lewis J. Kleinsmith. Becker's World of the Cell. 8th ed. ed. New York: Pearson; 2015.

141. Kerr JP, Robison P, Shi G, Bogush AI, Kempema AM, Hexum JK, et al. Detyrosinated microtubules modulate mechanotransduction in heart and skeletal muscle. Nature communications. 2015;6:8526.

142. Weisenberg RC. Microtubule formation in vitro in solutions containing low calcium concentrations. Science. Sep 22 1972;177(4054):1104-5.

143. Desai A, Mitchison TJ. Microtubule polymerization dynamics. Annual review of cell and developmental biology. 1997;13:83-117.

144. Chretien D, Metoz F, Verde F, Karsenti E, Wade RH. Lattice defects in microtubules: protofilament numbers vary within individual microtubules. The Journal of cell biology. Jun 1992;117(5):1031-40.

145. Walker RA, O'Brien ET, Pryer NK, Soboeiro MF, Voter WA, Erickson HP, et al. Dynamic instability of individual microtubules analyzed by video light microscopy: rate constants and transition frequencies. The Journal of cell biology. Oct 1988;107(4):1437-48.

146. Weisenberg RC, Deery WJ, Dickinson PJ. Tubulin-nucleotide interactions during the polymerization and depolymerization of microtubules. Biochemistry. Sep 21 1976;15(19):4248-54.

147. Weisenberg RC, Deery WJ. Role of nucleotide hydrolysis in microtubule assembly. Nature. Oct 28 1976;263(5580):792-3.

148. Mikhailov A, Gundersen GG. Relationship between microtubule dynamics and lamellipodium formation revealed by direct imaging of microtubules in cells treated with nocodazole or taxol. Cell motility and the cytoskeleton. 1998;41(4):325-40.

149. Ren XD, Kiosses WB, Schwartz MA. Regulation of the small GTP-binding protein Rho by cell adhesion and the cytoskeleton. The EMBO journal. Feb 01 1999;18(3):578-85.

150. Waterman-Storer CM, Worthylake RA, Liu BP, Burridge K, Salmon ED. Microtubule growth activates Rac1 to promote lamellipodial protrusion in fibroblasts. Nature cell biology. May 1999;1(1):45-50.

151. Ganguly A, Yang H, Sharma R, Patel KD, Cabral F. The role of microtubules and their dynamics in cell migration. The Journal of biological chemistry. Dec 21 2012;287(52):43359-69.

152. Vale RD. The molecular motor toolbox for intracellular transport. Cell. Feb 21 2003;112(4):467-80.

153. Yang H, Ganguly A, Cabral F. Inhibition of cell migration and cell division correlates with distinct effects of microtubule inhibiting drugs. The Journal of biological chemistry. Oct 15 2010;285(42):32242-50.

154. Beddington RS, Robertson EJ. Axis development and early asymmetry in mammals. Cell. Jan 22 1999;96(2):195-209.

155. Tucker RP. The roles of microtubule-associated proteins in brain morphogenesis: a review. Brain research Brain research reviews. May-Aug 1990;15(2):101-20.

156. Ott C, Iwanciw D, Graness A, Giehl K, Goppelt-Struebe M. Modulation of the expression of connective tissue growth factor by alterations of the cytoskeleton. The Journal of biological chemistry. Nov 07 2003;278(45):44305-11.

157. Khairallah RJ, Shi G, Sbrana F, Prosser BL, Borroto C, Mazaitis MJ, et al. Microtubules underlie dysfunction in duchenne muscular dystrophy. Science signaling. Aug 7 2012;5(236):ra56.

158. Brangwynne CP, MacKintosh FC, Kumar S, Geisse NA, Talbot J, Mahadevan L, et al. Microtubules can bear enhanced compressive loads in living cells because of lateral reinforcement. The Journal of cell biology. Jun 05 2006;173(5):733-41.

159. Mandelkow E, Mandelkow EM. Microtubules and microtubule-associated proteins. Current opinion in cell biology. Feb 1995;7(1):72-81.

160. Billingsley ML, Kincaid RL. Regulated phosphorylation and dephosphorylation of tau protein: effects on microtubule interaction, intracellular trafficking and neurodegeneration. The Biochemical journal. May 01 1997;323 (Pt 3):577-91.

161. Akhmanova A, Hoogenraad CC. Microtubule plus-end-tracking proteins: mechanisms and functions. Current opinion in cell biology. Feb 2005;17(1):47-54.

162. Hirokawa N, Noda Y, Tanaka Y, Niwa S. Kinesin superfamily motor proteins and intracellular transport. Nature reviews Molecular cell biology. Oct 2009;10(10):682-96.

163. Gelfand VI, Bershadsky AD. Microtubule dynamics: mechanism, regulation, and function. Annual review of cell biology. 1991;7:93-116.

164. Song Y, Brady ST. Post-translational modifications of tubulin: pathways to functional diversity of microtubules. Trends in cell biology. Mar 2015;25(3):125-36.

165. Gundersen GG, Khawaja S, Bulinski JC. Postpolymerization detyrosination of alpha-tubulin: a mechanism for subcellular differentiation of microtubules. The Journal of cell biology. Jul 1987;105(1):251-64.

166. Magiera MM, Janke C. Post-translational modifications of tubulin. Current biology : CB. May 05 2014;24(9):R351-4.

167. Prota AE, Magiera MM, Kuijpers M, Bargsten K, Frey D, Wieser M, et al. Structural basis of tubulin tyrosination by tubulin tyrosine ligase. The Journal of cell biology. Feb 04 2013;200(3):259-70.

168. Szyk A, Piszczek G, Roll-Mecak A. Tubulin tyrosine ligase and stathmin compete for tubulin binding in vitro. Journal of molecular biology. Jul 24 2013;425(14):2412-4.

169. Webster DR, Wehland J, Weber K, Borisy GG. Detyrosination of alpha tubulin does not stabilize microtubules in vivo. The Journal of cell biology. Jul 1990;111(1):113-22.

170. Bieling P, Kandels-Lewis S, Telley IA, van Dijk J, Janke C, Surrey T. CLIP-170 tracks growing microtubule ends by dynamically recognizing composite EB1/tubulin-binding sites. The Journal of cell biology. Dec 29 2008;183(7):1223-33.

171. Ghosh-Roy A, Goncharov A, Jin Y, Chisholm AD. Kinesin-13 and tubulin posttranslational modifications regulate microtubule growth in axon regeneration. Developmental cell. Oct 16 2012;23(4):716-28.

172. Konishi Y, Setou M. Tubulin tyrosination navigates the kinesin-1 motor domain to axons. Nature neuroscience. May 2009;12(5):559-67.

173. Sirajuddin M, Rice LM, Vale RD. Regulation of microtubule motors by tubulin isotypes and post-translational modifications. Nature cell biology. Apr 2014;16(4):335-44.

174. Robison P, Caporizzo MA, Ahmadzadeh H, Bogush AI, Chen CY, Margulies KB, et al. Detyrosinated microtubules buckle and bear load in contracting cardiomyocytes. Science. Apr 22 2016;352(6284):aaf0659.

175. Janke C, Kneussel M. Tubulin post-translational modifications: encoding functions on the neuronal microtubule cytoskeleton. Trends in neurosciences. Aug 2010;33(8):362-72.

176. Berezniuk I, Vu HT, Lyons PJ, Sironi JJ, Xiao H, Burd B, et al. Cytosolic carboxypeptidase 1 is involved in processing alpha- and beta-tubulin. The Journal of biological chemistry. Feb 24 2012;287(9):6503-17.

177. Tort O, Tanco S, Rocha C, Bieche I, Seixas C, Bosc C, et al. The cytosolic carboxypeptidases CCP2 and CCP3 catalyze posttranslational removal of acidic amino acids. Molecular biology of the cell. Oct 01 2014;25(19):3017-27.

178. Berezniuk I, Lyons PJ, Sironi JJ, Xiao H, Setou M, Angeletti RH, et al. Cytosolic carboxypeptidase 5 removes alpha- and gamma-linked glutamates from tubulin. The Journal of biological chemistry. Oct 18 2013;288(42):30445-53.

179. Paturle-Lafanechere L, Manier M, Trigault N, Pirollet F, Mazarguil H, Job D. Accumulation of delta 2-tubulin, a major tubulin variant that cannot be tyrosinated, in neuronal tissues and in stable microtubule assemblies. Journal of cell science. Jun 1994;107 (Pt 6):1529-43.

180. Audebert S, Koulakoff A, Berwald-Netter Y, Gros F, Denoulet P, Edde B. Developmental regulation of polyglutamylated alpha- and beta-tubulin in mouse brain neurons. Journal of cell science. Aug 1994;107 (Pt 8):2313-22.

181. Sloboda RD. Posttranslational protein modifications in cilia and flagella. Methods in cell biology. 2009;94:347-63.

182. Gaertig J, Wloga D. Ciliary tubulin and its post-translational modifications. Current topics in developmental biology. 2008;85:83-113.

183. !!! INVALID CITATION !!!

184. van Dijk J, Miro J, Strub JM, Lacroix B, van Dorsselaer A, Edde B, et al. Polyglutamylation is a post-translational modification with a broad range of substrates. The Journal of biological chemistry. Feb 15 2008;283(7):3915-22.

185. Ikegami K, Heier RL, Taruishi M, Takagi H, Mukai M, Shimma S, et al. Loss of alpha-tubulin polyglutamylation in ROSA22 mice is associated with abnormal targeting of KIF1A and modulated synaptic function. Proceedings of the National Academy of Sciences of the United States of America. Feb 27 2007;104(9):3213-8.

186. Bonnet C, Boucher D, Lazereg S, Pedrotti B, Islam K, Denoulet P, et al. Differential binding regulation of microtubule-associated proteins MAP1A, MAP1B, and MAP2 by tubulin polyglutamylation. The Journal of biological chemistry. Apr 20 2001;276(16):12839-48.

187. Maas C, Belgardt D, Lee HK, Heisler FF, Lappe-Siefke C, Magiera MM, et al. Synaptic activation modifies microtubules underlying transport of postsynaptic cargo. Proceedings of the National Academy of Sciences of the United States of America. May 26 2009;106(21):8731-6.

188. Wloga D, Gaertig J. Post-translational modifications of microtubules. Journal of cell science. Oct 15 2010;123(Pt 20):3447-55.

189. Rogowski K, Juge F, van Dijk J, Wloga D, Strub JM, Levilliers N, et al. Evolutionary divergence of enzymatic mechanisms for posttranslational polyglycylation. Cell. Jun 12 2009;137(6):1076-87.

190. Perdiz D, Mackeh R, Pous C, Baillet A. The ins and outs of tubulin acetylation: more than just a post-translational modification? Cellular signalling. May 2011;23(5):763-71.

191. L'Hernault SW, Rosenbaum JL. Chlamydomonas alpha-tubulin is posttranslationally modified by acetylation on the epsilon-amino group of a lysine. Biochemistry. Jan 15 1985;24(2):473-8.

192. Soppina V, Herbstman JF, Skiniotis G, Verhey KJ. Luminal localization of alpha-tubulin K40 acetylation by cryo-EM analysis of fab-labeled microtubules. PloS one. 2012;7(10):e48204.

193. Szyk A, Deaconescu AM, Spector J, Goodman B, Valenstein ML, Ziolkowska NE, et al. Molecular basis for age-dependent microtubule acetylation by tubulin acetyltransferase. Cell. Jun 05 2014;157(6):1405-15.

194. Maruta H, Greer K, Rosenbaum JL. The acetylation of alpha-tubulin and its relationship to the assembly and disassembly of microtubules. The Journal of cell biology. Aug 1986;103(2):571-9.

195. Kalebic N, Sorrentino S, Perlas E, Bolasco G, Martinez C, Heppenstall PA. alphaTAT1 is the major alpha-tubulin acetyltransferase in mice. Nature communications. 2013;4:1962.

196. Kalebic N, Martinez C, Perlas E, Hublitz P, Bilbao-Cortes D, Fiedorczuk K, et al. Tubulin acetyltransferase alphaTAT1 destabilizes microtubules independently of its acetylation activity. Molecular and cellular biology. Mar 2013;33(6):1114-23.

197. Zhang Y, Kwon S, Yamaguchi T, Cubizolles F, Rousseaux S, Kneissel M, et al. Mice lacking histone deacetylase 6 have hyperacetylated tubulin but are viable and develop normally. Molecular and cellular biology. Mar 2008;28(5):1688-701.

198. North BJ, Marshall BL, Borra MT, Denu JM, Verdin E. The human Sir2 ortholog, SIRT2, is an NAD+-dependent tubulin deacetylase. Molecular cell. Feb 2003;11(2):437-44.

199. Giustiniani J, Daire V, Cantaloube I, Durand G, Pous C, Perdiz D, et al. Tubulin acetylation favors Hsp90 recruitment to microtubules and stimulates the signaling function of the Hsp90 clients Akt/PKB and p53. Cellular signalling. Apr 2009;21(4):529-39.

200. Sudo H, Baas PW. Acetylation of microtubules influences their sensitivity to severing by katanin in neurons and fibroblasts. The Journal of neuroscience : the official journal of the Society for Neuroscience. May 26 2010;30(21):7215-26.

201. Reed NA, Cai D, Blasius TL, Jih GT, Meyhofer E, Gaertig J, et al. Microtubule acetylation promotes kinesin-1 binding and transport. Current biology : CB. Nov 07 2006;16(21):2166-72.

202. Walter WJ, Beranek V, Fischermeier E, Diez S. Tubulin acetylation alone does not affect kinesin-1 velocity and run length in vitro. PloS one. 2012;7(8):e42218.

203. Otterbein LR, Graceffa P, Dominguez R. The crystal structure of uncomplexed actin in the ADP state. Science. Jul 27 2001;293(5530):708-11.

204. Reisler E. Actin molecular structure and function. Current opinion in cell biology. Feb 1993;5(1):41-7.

205. Graceffa P, Dominguez R. Crystal structure of monomeric actin in the ATP state. Structural basis of nucleotide-dependent actin dynamics. The Journal of biological chemistry. Sep 05 2003;278(36):34172-80.

206. Collins JH, Elzinga M. The primary structure of actin from rabbit skeletal muscle. Completion and analysis of the amino acid sequence. The Journal of biological chemistry. Aug 10 1975;250(15):5915-20.

207. Brackley KI, Grantham J. Activities of the chaperonin containing TCP-1 (CCT): implications for cell cycle progression and cytoskeletal organisation. Cell stress & chaperones. Jan 2009;14(1):23-31.

208. Vandamme D, Lambert E, Waterschoot D, Cognard C, Vandekerckhove J, Ampe C, et al. alpha-Skeletal muscle actin nemaline myopathy mutants cause cell death in cultured muscle cells. Biochimica et biophysica acta. Jul 2009;1793(7):1259-71.

209. Oda T, Iwasa M, Aihara T, Maeda Y, Narita A. The nature of the globular- to fibrous-actin transition. Nature. Jan 22 2009;457(7228):441-5.

210. Begg DA, Rodewald R, Rebhun LI. The visualization of actin filament polarity in thin sections. Evidence for the uniform polarity of membrane-associated filaments. The Journal of cell biology. Dec 1978;79(3):846-52.

211. Mullins RD, Pollard TD. Structure and function of the Arp2/3 complex. Current opinion in structural biology. Apr 1999;9(2):244-9.

212. Machesky LM, Gould KL. The Arp2/3 complex: a multifunctional actin organizer. Current opinion in cell biology. Feb 1999;11(1):117-21.

213. Vavylonis D, Yang Q, O'Shaughnessy B. Actin polymerization kinetics, cap structure, and fluctuations. Proceedings of the National Academy of Sciences of the United States of America. Jun 14 2005;102(24):8543-8.

214. Pollard TD, Blanchoin L, Mullins RD. Molecular mechanisms controlling actin filament dynamics in nonmuscle cells. Annual review of biophysics and biomolecular structure. 2000;29:545-76.

215. Goldschmidt-Clermont PJ, Furman MI, Wachsstock D, Safer D, Nachmias VT, Pollard TD. The control of actin nucleotide exchange by thymosin beta 4 and profilin. A potential regulatory mechanism for actin polymerization in cells. Molecular biology of the cell. Sep 1992;3(9):1015-24.

216. Carlsson L, Nystrom LE, Sundkvist I, Markey F, Lindberg U. Actin polymerizability is influenced by profilin, a low molecular weight protein in non-muscle cells. Journal of molecular biology. Sep 25 1977;115(3):465-83.

217. Dominguez R. Actin-binding proteins--a unifying hypothesis. Trends in biochemical sciences. Nov 2004;29(11):572-8.

218. Southwick FS. Gelsolin and ADF/cofilin enhance the actin dynamics of motile cells. Proceedings of the National Academy of Sciences of the United States of America. Jun 20 2000;97(13):6936-8.

219. Caldwell JE, Heiss SG, Mermall V, Cooper JA. Effects of CapZ, an actin capping protein of muscle, on the polymerization of actin. Biochemistry. Oct 17 1989;28(21):8506-14.

220. Pollard TD. Actin and Actin-Binding Proteins. Cold Spring Harbor perspectives in biology. Aug 01 2016;8(8).

221. Aberle H. Redox switch for actin. Nature cell biology. Dec 2013;15(12):1403-4.

222. Huber F, Schnauss J, Ronicke S, Rauch P, Muller K, Futterer C, et al. Emergent complexity of the cytoskeleton: from single filaments to tissue. Advances in physics. Jan 2013;62(1):1-112.

223. Mitchison TJ, Cramer LP. Actin-based cell motility and cell locomotion. Cell. Feb 09 1996;84(3):371-9.

224. Zaidel-Bar R, Cohen M, Addadi L, Geiger B. Hierarchical assembly of cell-matrix adhesion complexes. Biochemical Society transactions. Jun 2004;32(Pt3):416-20.

225. Riveline D, Zamir E, Balaban NQ, Schwarz US, Ishizaki T, Narumiya S, et al. Focal contacts as mechanosensors: externally applied local mechanical force induces growth of focal contacts by an mDia1-dependent and ROCK-independent mechanism. The Journal of cell biology. Jun 11 2001;153(6):1175-86.

226. Pelham RJ, Chang F. Actin dynamics in the contractile ring during cytokinesis in fission yeast. Nature. Sep 05 2002;419(6902):82-6.

227. Hofmann WA. Cell and molecular biology of nuclear actin. International review of cell and molecular biology. 2009;273:219-63.

228. Ohashi K, Fujiwara S, Mizuno K. Roles of the cytoskeleton, cell adhesion and rho signalling in mechanosensing and mechanotransduction. Journal of biochemistry. Mar 01 2017;161(3):245-54.

229. Finch-Edmondson M, Sudol M. Framework to function: mechanosensitive regulators of gene transcription. Cellular & molecular biology letters. 2016;21:28.

230. Herrmann H, Bar H, Kreplak L, Strelkov SV, Aebi U. Intermediate filaments: from cell architecture to nanomechanics. Nature reviews Molecular cell biology. Jul 2007;8(7):562-73.

231. Quinlan R, Hutchison C, Lane B. Intermediate filament proteins. Protein profile. 1995;2(8):795-952.

232. Lee CH, Kim MS, Chung BM, Leahy DJ, Coulombe PA. Structural basis for heteromeric assembly and perinuclear organization of keratin filaments. Nature structural & molecular biology. Jun 17 2012;19(7):707-15.

233. Kreplak L, Fudge D. Biomechanical properties of intermediate filaments: from tissues to single filaments and back. BioEssays : news and reviews in molecular, cellular and developmental biology. Jan 2007;29(1):26-35.

234. Herrmann H, Aebi U. Intermediate Filaments: Structure and Assembly. Cold Spring Harbor perspectives in biology. Nov 01 2016;8(11).

235. Kim S, Coulombe PA. Intermediate filament scaffolds fulfill mechanical, organizational, and signaling functions in the cytoplasm. Genes & development. Jul 01 2007;21(13):1581-97.

236. Snider NT, Omary MB. Post-translational modifications of intermediate filament proteins: mechanisms and functions. Nature reviews Molecular cell biology. Mar 2014;15(3):163-77.

237. Yusko EC, Asbury CL. Force is a signal that cells cannot ignore. Molecular biology of the cell. Nov 15 2014;25(23):3717-25.

238. Kamioka H, Sugawara Y, Honjo T, Yamashiro T, Takano-Yamamoto T. Terminal differentiation of osteoblasts to osteocytes is accompanied by dramatic changes in the distribution of actin-binding proteins. Journal of bone and mineral research : the official journal of the American Society for Bone and Mineral Research. Mar 2004;19(3):471-8.

239. Murshid SA, Kamioka H, Ishihara Y, Ando R, Sugawara Y, Takano-Yamamoto T. Actin and microtubule cytoskeletons of the processes of 3D-cultured MC3T3-E1 cells and osteocytes. Journal of bone and mineral metabolism. 2007;25(3):151-8.

240. Plotkin LI, Mathov I, Aguirre JI, Parfitt AM, Manolagas SC, Bellido T. Mechanical stimulation prevents osteocyte apoptosis: requirement of integrins, Src kinases, and ERKs. Am J Physiol Cell Physiol. Sep 2005;289(3):C633-43.

241. Lombardi ML, Lammerding J. Keeping the LINC: the importance of nucleocytoskeletal coupling in intracellular force transmission and cellular function. Biochemical Society transactions. Dec 2011;39(6):1729-34.

242. Kardas D, Nackenhorst U, Balzani D. Computational model for the cell-mechanical response of the osteocyte cytoskeleton based on self-stabilizing tensegrity structures. Biomechanics and modeling in mechanobiology. Jan 2013;12(1):167-83.

243. Bacabac RG, Smit TH, Van Loon JJ, Doulabi BZ, Helder M, Klein-Nulend J. Bone cell responses to high-frequency vibration stress: does the nucleus oscillate within the cytoplasm? FASEB journal : official publication of the Federation of American Societies for Experimental Biology. May 2006;20(7):858-64.

244. Davies PF. Flow-mediated endothelial mechanotransduction. Physiological reviews. Jul 1995;75(3):519-60.

245. Ingber DE. Tensegrity: the architectural basis of cellular mechanotransduction. Annual review of physiology. 1997;59:575-99.

246. Janmey PA. The cytoskeleton and cell signaling: component localization and mechanical coupling. Physiological reviews. Jul 1998;78(3):763-81.

247. Klein-Nulend J, Bacabac RG, Bakker AD. Mechanical loading and how it affects bone cells: the role of the osteocyte cytoskeleton in maintaining our skeleton. European cells & materials. Sep 24 2012;24:278-91.

248. Prosser BL, Ward CW, Lederer WJ. X-ROS signaling: rapid mechano-chemo transduction in heart. Science. Sep 9 2011;333(6048):1440-5.

249. Prosser BL, Khairallah RJ, Ziman AP, Ward CW, Lederer WJ. X-ROS signaling in the heart and skeletal muscle: stretch-dependent local ROS regulates [Ca(2)(+)]i. Journal of molecular and cellular cardiology. May 2013;58:172-81.

250. Lyons J.S. ISR, Lovering R.M., Ward C.W., Stains J.P. Novel multi-functional fluid flow device for studying cellular mechanotransduction. Journal of biomechanics. 2016. Epub Under Review.

251. James S. Lyons HCJ, Robert A. Law, Katrina M. Williams, Jaclyn P. Kerr, Guoli Shi, Ramzi J. Khairallah, Stuart S. Martin, Konstantinos Konstantopoulos, Christopher W. Ward, Joseph P. Stains. Microtubules tune mechanotransduction through Nox2 and TRPV4 to decrease sclerostin abundance in osteocytes. Science signaling. 2017.

252. Gupta A, Anderson H, Buo AM, Moorer MC, Ren M, Stains JP. Communication of cAMP by connexin43 gap junctions regulates osteoblast signaling and gene expression. Cellular signalling. Aug 2016;28(8):1048-57.

253. Hanley WD, Wirtz D, Konstantopoulos K. Distinct kinetic and mechanical properties govern selectin-leukocyte interactions. Journal of cell science. May 15 2004;117(Pt 12):2503-11.

254. Raman PS, Alves CS, Wirtz D, Konstantopoulos K. Single-molecule binding of CD44 to fibrin versus P-selectin predicts their distinct shear-dependent interactions in cancer. Journal of cell science. Jun 01 2011;124(Pt 11):1903-10.

255. Hung WC, Yang JR, Yankaskas CL, Wong BS, Wu PH, Pardo-Pastor C, et al. Confinement Sensing and Signal Optimization via Piezo1/PKA and Myosin II Pathways. Cell reports. May 17 2016;15(7):1430-41.

256. Hebert C, Stains JP. An intact connexin43 is required to enhance signaling and gene expression in osteoblast-like cells. Journal of cellular biochemistry. Nov 2013;114(11):2542-50.

257. Niger C, Hebert C, Stains JP. Interaction of connexin43 and protein kinase C-delta during FGF2 signaling. BMC biochemistry. Mar 25 2010;11:14.

258. Niger C, Buo AM, Hebert C, Duggan BT, Williams MS, Stains JP. ERK acts in parallel to PKCdelta to mediate the connexin43-dependent potentiation of Runx2 activity by FGF2 in MC3T3 osteoblasts. American journal of physiology Cell physiology. Apr 1 2012;302(7):C1035-44.

259. Liu S, Niger C, Koh EY, Stains JP. Connexin43 Mediated Delivery of ADAMTS5 Targeting siRNAs from Mesenchymal Stem Cells to Synovial Fibroblasts. PloS one. 2015;10(6):e0129999.

260. Liedert A, Mattausch L, Rontgen V, Blakytny R, Vogele D, Pahl M, et al. Midkine-deficiency increases the anabolic response of cortical bone to mechanical loading. Bone. Apr 01 2011;48(4):945-51.

261. Jaalouk DE, Lammerding J. Mechanotransduction gone awry. Nature reviews Molecular cell biology. Jan 2009;10(1):63-73.

262. Oftadeh R, Perez-Viloria M, Villa-Camacho JC, Vaziri A, Nazarian A. Biomechanics and mechanobiology of trabecular bone: a review. Journal of biomechanical engineering. Jan 2015;137(1).

263. Turner CH, Warden SJ, Bellido T, Plotkin LI, Kumar N, Jasiuk I, et al. Mechanobiology of the skeleton. Science signaling. 2009;2(68):pt3.

264. Bonewald LF, Johnson ML. Osteocytes, mechanosensing and Wnt signaling. Bone. Apr 2008;42(4):606-15.

265. Rubin J, Rubin C, Jacobs CR. Molecular pathways mediating mechanical signaling in bone. Gene. Feb 15 2006;367:1-16.

266. de Castro LF, Maycas M, Bravo B, Esbrit P, Gortazar A. VEGF Receptor 2 (VEGFR2) Activation Is Essential for Osteocyte Survival Induced by Mechanotransduction. Journal of cellular physiology. Feb 2015;230(2):278-85.

267. Michael Delaine-Smith R, Javaheri B, Helen Edwards J, Vazquez M, Rumney RM. Preclinical models for in vitro mechanical loading of bone-derived cells. BoneKEy reports. 2015;4:728.

268. Burra S, Nicolella DP, Francis WL, Freitas CJ, Mueschke NJ, Poole K, et al. Dendritic processes of osteocytes are mechanotransducers that induce the opening of hemichannels. Proceedings of the National Academy of Sciences of the United States of America. Aug 3 2010;107(31):13648-53.

269. Aryaei A, Jayasuriya AC. The effect of oscillatory mechanical stimulation on osteoblast attachment and proliferation. Materials science & engineering C, Materials for biological applications. 2015;52:129-34.

270. Shemesh J, Jalilian I, Shi A, Heng Yeoh G, Knothe Tate ML, Ebrahimi Warkiani M. Flow-induced stress on adherent cells in microfluidic devices. Lab on a chip. Nov 7 2015;15(21):4114-27.

271. Cardoso L, Fritton SP, Gailani G, Benalla M, Cowin SC. Advances in assessment of bone porosity, permeability and interstitial fluid flow. Journal of biomechanics. Jan 18 2013;46(2):253-65.

272. Ban Y, Wu YY, Yu T, Geng N, Wang YY, Liu XG, et al. Response of osteoblasts to low fluid shear stress is time dependent. Tissue & cell. Oct 2011;43(5):311-7.

273. Ishihara Y, Sugawara Y, Kamioka H, Kawanabe N, Hayano S, Balam TA, et al. Ex vivo real-time observation of Ca(2+) signaling in living bone in response to shear stress applied on the bone surface. Bone. Mar 2013;53(1):204-15.

274. Jing D, Lu XL, Luo E, Sajda P, Leong PL, Guo XE. Spatiotemporal properties of intracellular calcium signaling in osteocytic and osteoblastic cell networks under fluid flow. Bone. Apr 2013;53(2):531-40.

275. Su JH, Xu F, Lu XL, Lu TJ. Fluid flow induced calcium response in osteoblasts: mathematical modeling. Journal of biomechanics. Jul 28 2011;44(11):2040-6.

276. Suzuki T, Notomi T, Miyajima D, Mizoguchi F, Hayata T, Nakamoto T, et al. Osteoblastic differentiation enhances expression of TRPV4 that is required for calcium oscillation induced by mechanical force. Bone. May 2013;54(1):172-8.

277. Xing Y, Gu Y, Xu LC, Siedlecki CA, Donahue HJ, You J. Effects of membrane cholesterol depletion and GPI-anchored protein reduction on osteoblastic mechanotransduction. Journal of cellular physiology. Sep 2011;226(9):2350-9.

278. You J, Reilly GC, Zhen X, Yellowley CE, Chen Q, Donahue HJ, et al. Osteopontin gene regulation by oscillatory fluid flow via intracellular calcium mobilization and activation of mitogen-activated protein kinase in MC3T3-E1 osteoblasts. The Journal of biological chemistry. Apr 20 2001;276(16):13365-71.

279. Zhang J, Ryder KD, Bethel JA, Ramirez R, Duncan RL. PTH-induced actin depolymerization increases mechanosensitive channel activity to enhance mechanically stimulated Ca2+ signaling in osteoblasts. Journal of bone and mineral research : the official journal of the American Society for Bone and Mineral Research. Nov 2006;21(11):1729-37.

280. Weyts FA, Li YS, van Leeuwen J, Weinans H, Chien S. ERK activation and alpha v beta 3 integrin signaling through Shc recruitment in response to mechanical stimulation in human osteoblasts. Journal of cellular biochemistry. 2002;87(1):85-92.

281. Kapur S, Chen ST, Baylink DJ, Lau KH. Extracellular signal-regulated kinase-1 and -2 are both essential for the shear stress-induced human osteoblast proliferation. Bone. Aug 2004;35(2):525-34.

282. Wadhwa S, Godwin SL, Peterson DR, Epstein MA, Raisz LG, Pilbeam CC. Fluid flow induction of cyclo-oxygenase 2 gene expression in osteoblasts is dependent on an extracellular signal-regulated kinase signaling pathway. Journal of bone and mineral research : the official journal of the American Society for Bone and Mineral Research. Feb 2002;17(2):266-74.

283. Triplett JW, O'Riley R, Tekulve K, Norvell SM, Pavalko FM. Mechanical loading by fluid shear stress enhances IGF-1 receptor signaling in osteoblasts in a PKCzeta-dependent manner. Molecular & cellular biomechanics : MCB. Mar 2007;4(1):13-25.

284. Huang LW, Ren L, Yang PF, Shang P. Response of Osteoblasts to the Stimulus of Fluid Flow. Critical reviews in eukaryotic gene expression. 2015;25(2):153-62.

285. Roy B, Das T, Mishra D, Maiti TK, Chakraborty S. Oscillatory shear stress induced calcium flickers in osteoblast cells. Integrative biology : quantitative biosciences from nano to macro. Mar 2014;6(3):289-99.

286. Anderson EJ, Falls TD, Sorkin AM, Knothe Tate ML. The imperative for controlled mechanical stresses in unraveling cellular mechanisms of mechanotransduction. Biomedical engineering online. 2006;5:27.

287. Sorkin AM, Dee KC, Knothe Tate ML. "Culture shock" from the bone cell's perspective: emulating physiological conditions for mechanobiological investigations. American journal of physiology Cell physiology. Dec 2004;287(6):C1527-36.

288. Schaffler MB, Cheung WY, Majeska R, Kennedy O. Osteocytes: master orchestrators of bone. Calcified tissue international. Jan 2014;94(1):5-24.

289. Lin C, Jiang X, Dai Z, Guo X, Weng T, Wang J, et al. Sclerostin mediates bone response to mechanical unloading through antagonizing Wnt/beta-catenin signaling. Journal of bone and mineral research : the official journal of the American Society for Bone and Mineral Research. Oct 2009;24(10):1651-61.

290. Tu X, Rhee Y, Condon KW, Bivi N, Allen MR, Dwyer D, et al. Sost downregulation and local Wnt signaling are required for the osteogenic response to mechanical loading. Bone. Jan 2012;50(1):209-17.

291. McClung MR, Grauer A, Boonen S, Bolognese MA, Brown JP, Diez-Perez A, et al. Romosozumab in postmenopausal women with low bone mineral density. The New England journal of medicine. Jan 30 2014;370(5):412-20.

292. Compton JT, Lee FY. A review of osteocyte function and the emerging importance of sclerostin. The Journal of bone and joint surgery American volume. Oct 01 2014;96(19):1659-68.

293. Pavalko FM, Chen NX, Turner CH, Burr DB, Atkinson S, Hsieh YF, et al. Fluid shear-induced mechanical signaling in MC3T3-E1 osteoblasts requires cytoskeleton-integrin interactions. Am J Physiol. Dec 1998;275(6 Pt 1):C1591-601.

294. Batra N, Burra S, Siller-Jackson AJ, Gu S, Xia X, Weber GF, et al. Mechanical stress-activated integrin alpha5beta1 induces opening of connexin 43 hemichannels. Proc Natl Acad Sci U S A. Research Support, N.I.H., Extramural

Research Support, Non-U.S. Gov't Feb 28 2012;109(9):3359-64. Epub 2012/02/15.

295. Wu D, Schaffler MB, Weinbaum S, Spray DC. Matrix-dependent adhesion mediates network responses to physiological stimulation of the osteocyte cell process. Proc Natl Acad Sci U S A. Jul 16 2013;110(29):12096-101.

296. Pavalko FM, Norvell SM, Burr DB, Turner CH, Duncan RL, Bidwell JP. A model for mechanotransduction in bone cells: the load-bearing mechanosomes. Journal of cellular biochemistry. Jan 01 2003;88(1):104-12.

297. Vignaud T, Blanchoin L, Thery M. Directed cytoskeleton self-organization. Trends in cell biology. Dec 2012;22(12):671-82.

298. Lopez BJ, Valentine MT. Molecular control of stress transmission in the microtubule cytoskeleton. Biochimica et biophysica acta. Nov 2015;1853(11 Pt B):3015-24.

299. Wloga D, Joachimiak E, Louka P, Gaertig J. Posttranslational Modifications of Tubulin and Cilia. Cold Spring Harbor perspectives in biology. Jun 01 2017;9(6).

300. Kreitzer G, Liao G, Gundersen GG. Detyrosination of tubulin regulates the interaction of intermediate filaments with microtubules in vivo via a kinesin-dependent mechanism. Mol Biol Cell. Apr 1999;10(4):1105-18.

301. Liao G, Gundersen GG. Kinesin is a candidate for cross-bridging microtubules and intermediate filaments. Selective binding of kinesin to detyrosinated tubulin and vimentin. J Biol Chem. Apr 17 1998;273(16):9797-803.

302. Babich A, Burkhardt JK. Coordinate control of cytoskeletal remodeling and calcium mobilization during T-cell activation. Immunol Rev. Nov 2013;256(1):80-94.

303. Oka T, Hori M, Ozaki H. Microtubule disruption suppresses allergic response through the inhibition of calcium influx in the mast cell degranulation pathway. J Immunol. Apr 15 2005;174(8):4584-9.

304. Ward CW, Prosser BL, Lederer WJ. Mechanical stretch-induced activation of ROS/RNS signaling in striated muscle. Antioxid Redox Signal. Feb 20 2014;20(6):929-36.

305. Toma CD, Ashkar S, Gray ML, Schaffer JL, Gerstenfeld LC. Signal transduction of mechanical stimuli is dependent on microfilament integrity: identification of osteopontin as a mechanically induced gene in osteoblasts. J Bone Miner Res. Oct 1997;12(10):1626-36.

306. Rosenberg N. The role of the cytoskeleton in mechanotransduction in human osteoblast-like cells. Hum Exp Toxicol. May 2003;22(5):271-4.

307. Myers KA, Rattner JB, Shrive NG, Hart DA. Osteoblast-like cells and fluid flow: cytoskeleton-dependent shear sensitivity. Biochem Biophys Res Commun. Dec 14 2007;364(2):214-9.

308. Gardinier JD, Majumdar S, Duncan RL, Wang L. Cyclic Hydraulic Pressure and Fluid Flow Differentially Modulate Cytoskeleton Re-Organization in MC3T3 Osteoblasts. Cell Mol Bioeng. Mar 01 2009;2(1):133-43.

309. Janke C, Bulinski JC. Post-translational regulation of the microtubule cytoskeleton: mechanisms and functions. Nat Rev Mol Cell Biol. Nov 16 2011;12(12):773-86.

310. Fonrose X, Ausseil F, Soleilhac E, Masson V, David B, Pouny I, et al. Parthenolide inhibits tubulin carboxypeptidase activity. Cancer research. Apr 1 2007;67(7):3371-8.

311. Brown GN, Leong PL, Guo XE. T-Type voltage-sensitive calcium channels mediate mechanically-induced intracellular calcium oscillations in osteocytes by regulating endoplasmic reticulum calcium dynamics. Bone. Jul 2016;88:56-63.

312. Suzuki M, Hirao A, Mizuno A. Microtubule-associated [corrected] protein 7 increases the membrane expression of transient receptor potential vanilloid 4 (TRPV4). J Biol Chem. Dec 19 2003;278(51):51448-53.

313. Wei H, Zhang Y, Fan ZZ, Ge HY, Arendt-Nielsen L, Jiang H, et al. Effects of colchicine-induced microtubule depolymerization on TRPV4 in rats with chronic compression of the dorsal root ganglion. Neurosci Lett. Feb 8 2013;534:344-50.

314. Goswami C, Kuhn J, Heppenstall PA, Hucho T. Importance of non-selective cation channel TRPV4 interaction with cytoskeleton and their reciprocal regulations in cultured cells. PLoS One. 2010;5(7):e11654.

315. Suresh K, Servinsky L, Reyes J, Baksh S, Undem C, Caterina M, et al. Hydrogen peroxide-induced calcium influx in lung microvascular endothelial cells involves TRPV4. American journal of physiology Lung cellular and molecular physiology. Dec 15 2015;309(12):L1467-77.

316. Wegierski T, Lewandrowski U, Muller B, Sickmann A, Walz G. Tyrosine phosphorylation modulates the activity of TRPV4 in response to defined stimuli. J Biol Chem. Jan 30 2009;284(5):2923-33.

317. Browning EA, Chatterjee S, Fisher AB. Stop the flow: a paradigm for cell signaling mediated by reactive oxygen species in the pulmonary endothelium. Annu Rev Physiol. 2012;74:403-24.

318. Jing D, Baik AD, Lu XL, Zhou B, Lai X, Wang L, et al. In situ intracellular calcium oscillations in osteocytes in intact mouse long bones under dynamic mechanical loading. FASEB J. Apr 2014;28(4):1582-92.

319. O'Conor CJ, Leddy HA, Benefield HC, Liedtke WB, Guilak F. TRPV4-mediated mechanotransduction regulates the metabolic response of chondrocytes to dynamic loading. Proc Natl Acad Sci U S A. Jan 28 2014;111(4):1316-21.

320. Masuyama R, Vriens J, Voets T, Karashima Y, Owsianik G, Vennekens R, et al. TRPV4-mediated calcium influx regulates terminal differentiation of osteoclasts. Cell Metab. Sep 2008;8(3):257-65.

321. van der Eerden BC, Oei L, Roschger P, Fratzl-Zelman N, Hoenderop JG, van Schoor NM, et al. TRPV4 deficiency causes sexual dimorphism in bone metabolism and osteoporotic fracture risk. Bone. Dec 2013;57(2):443-54.

322. Leddy HA, McNulty AL, Guilak F, Liedtke W. Unraveling the mechanism by which TRPV4 mutations cause skeletal dysplasias. Rare Dis. 2014;2(1):e962971.

323. Chen JR, Lazarenko OP, Blackburn ML, Mercer KE, Badger TM, Ronis MJ. p47phox-Nox2-dependent ROS Signaling Inhibits Early Bone Development in Mice but Protects against Skeletal Aging. J Biol Chem. Jun 05 2015;290(23):14692-704.

324. Herrmann TL, Agrawal RS, Connolly SF, McCaffrey RL, Schlomann J, Kusner DJ. MHC Class II levels and intracellular localization in human dendritic cells are regulated by calmodulin kinase II. Journal of leukocyte biology. Sep 2007;82(3):686-99.

325. Jarome TJ, Ferrara NC, Kwapis JL, Helmstetter FJ. CaMKII regulates proteasome phosphorylation and activity and promotes memory destabilization following retrieval. Neurobiology of learning and memory. Feb 2016;128:103-9.

326. Cid-Diaz T, Santos-Zas I, Gonzalez-Sanchez J, Gurriaran-Rodriguez U, Mosteiro CS, Casabiell X, et al. Obestatin controls the ubiquitin-proteasome and autophagy-lysosome systems in glucocorticoid-induced muscle cell atrophy. Journal of cachexia, sarcopenia and muscle. Jul 03 2017.

327. Zhang M, Hagenmueller M, Riffel JH, Kreusser MM, Bernhold E, Fan J, et al. Calcium/calmodulin-dependent protein kinase II couples Wnt signaling with histone deacetylase 4 and mediates dishevelled-induced cardiomyopathy. Hypertension. Feb 2015;65(2):335-44.

328. Ojuka EO, Goyaram V, Smith JA. The role of CaMKII in regulating GLUT4 expression in skeletal muscle. American journal of physiology Endocrinology and metabolism. Aug 01 2012;303(3):E322-31.

329. Ginnan R, Sun LY, Schwarz JJ, Singer HA. MEF2 is regulated by CaMKIIdelta2 and a HDAC4-HDAC5 heterodimer in vascular smooth muscle cells. The Biochemical journal. May 15 2012;444(1):105-14.

330. Linseman DA, Bartley CM, Le SS, Laessig TA, Bouchard RJ, Meintzer MK, et al. Inactivation of the myocyte enhancer factor-2 repressor histone deacetylase-5 by endogenous Ca(2+) //calmodulin-dependent kinase II promotes depolarization-mediated cerebellar granule neuron survival. The Journal of biological chemistry. Oct 17 2003;278(42):41472-81.

331. Mehrotra M, Saegusa M, Wadhwa S, Voznesensky O, Peterson D, Pilbeam C. Fluid flow induces Rankl expression in primary murine calvarial osteoblasts. Journal of cellular biochemistry. Aug 1 2006;98(5):1271-83.

332. Kapur S, Baylink DJ, Lau KH. Fluid flow shear stress stimulates human osteoblast proliferation and differentiation through multiple interacting and competing signal transduction pathways. Bone. Mar 2003;32(3):241-51.

333. James Lyons HJ, Robert Law, Jaclyn Kerr, Guoli Shi, Ramzi Khairallah, Stuart Martin, Konstantinos Konstantopoulos, Christopher Ward, Joseph Stains. Microtubule-dependent regulation of a signaling pathway tunes the osteocyte mechanical load response. Science signaling. 2017.

334. Johnell O, Kanis JA. An estimate of the worldwide prevalence and disability associated with osteoporotic fractures. Osteoporosis international : a journal established as result of cooperation between the European Foundation for Osteoporosis and the National Osteoporosis Foundation of the USA. Dec 2006;17(12):1726-33.

335. Amgen. Amgen And UCB Announce Top-Line Phase 3 Data From Active-Comparator Study Of EVENITY™ (Romosozumab) In Postmenopausal Women With Osteoporosis. PRNewswire2017.

336. Cavanagh PR, Licata AA, Rice AJ. Exercise and pharmacological countermeasures for bone loss during long-duration space flight. Gravitational and space biology bulletin : publication of the American Society for Gravitational and Space Biology. Jun 2005;18(2):39-58.